



**HAL**  
open science

## Nouvelle strategies en Protéomique

Giovanni Chiappetta

► **To cite this version:**

Giovanni Chiappetta. Nouvelle strategies en Protéomique. Ingénierie biomédicale. Université Pierre et Marie Curie - Paris VI, 2009. Français. NNT: . pastel-00558455

**HAL Id: pastel-00558455**

**<https://pastel.hal.science/pastel-00558455>**

Submitted on 21 Jan 2011

**HAL** is a multi-disciplinary open access archive for the deposit and dissemination of scientific research documents, whether they are published or not. The documents may come from teaching and research institutions in France or abroad, or from public or private research centers.

L'archive ouverte pluridisciplinaire **HAL**, est destinée au dépôt et à la diffusion de documents scientifiques de niveau recherche, publiés ou non, émanant des établissements d'enseignement et de recherche français ou étrangers, des laboratoires publics ou privés.



**THESE DE DOCTORAT DE  
L'UNIVERSITE PIERRE ET MARIE CURIE  
ET DE  
L'UNIVERSITÉ FEDERICO II**

Spécialité

Ecole Doctorale Inter///Bio (ED387)  
Interfaces de la Chimie, de la Physique et de l'Informatique avec la Biologie

Ecole Doctorale de Biotechnologies

Présentée par

M. Giovanni Chiappetta

Pour obtenir le grade de

**DOCTEUR de l'UNIVERSITÉ PIERRE ET MARIE CURIE  
ET  
DOCTEUR de L'UNIVERSITÉ FEDERICO II**

Sujet de la thèse :

Nouvelle strategies en Protéomique

soutenu le 08/01/2009

devant le jury composé de :

Prof. Jean Rossier Directeur de thèse  
Prof. Marino Gennaro Directeur de thèse

Prof. Giovanni Sanna Rapporteur  
Dr. Ariane, Jalila Simaan Rapporteur

Dr. Joelle Vinh Examineur  
Prof. Germain Trugnan Examineur  
Prof. Pasquale De Santis Examineur  
Prof. Claudio Palleschi Examineur  
Prof. Vincenzo Scarlato Examineur



*A' Giugno fann' turnà cu' te....*



<b>Riassunto</b>	pag.	1
<b>Résumé</b>	pag.	8
<b>1 INTRODUCTION</b>	pag.	9
1.1 Proteomics impact on modern Biotechnologies	pag.	9
1.2 Proteomics analysis	pag	10
1.2.1 Mass spectrometry tools for Proteomics analysis	pag	11
1.2.2 The first generation of the Proteomic analysis	pag	17
1.2.3 The second generation of the Proteomic analysis	pag	18
1.2.4 Quantitative Proteomics	pag	19
1.3 Oxidative stress	pag	20
1.4 Oxidative stress related PTMs	pag	22
1.4.1 Protein nitration	pag	22
1.4.2 Thiol oxydation	pag	24
1.6 References	pag	26
<b>2 BIDIMENSIONAL TANDEM MASS SPECTROMETRY FOR SELECTIVE IDENTIFICATION OF NITRATION SITES IN PROTEIN</b>	pag	30
2.1 Introduction	pag	30
2.1.1 Proteomic identification of nitrated proteins: the state of the art	pag	30
2.1.2 The hybrid Triple Quadrupole/ Linear Ion Trap mass spectrometer	pag	33
2.1.3 Dansyl-Chloride: the RIGhT reagent	pag	35
2.2 Materials and methods	pag	37
2.3 Results and discussions	pag	38
2.4 Conclusion	pag	44
2.5 References	pag	47
<b>3. QUANTITATIVE IDENTIFICATION OF PROTEIN NITRATION SITES BY USING iTRAQ REAGENTS</b>	pag	49
3.1 Introduction	pag	49
3.1.1 Protein nitration quantification: state of the art	pag	49
3.1.2 iTRAQ strategy	pag	51
3.2 Materials and methods	pag	52
3.3 Results and discussions	pag	54
3.4 Conclusion	pag	63
3.5 References	pag	66
<b>4. IMPROVED LC-MALDI-MS<sup>2</sup> ANALYSIS BY PEPTIDES DANSYLATION</b>	pag	69
4.1 Introduction	pag	69
4.1.1 MALDI-TOF/TOF mass spectrometer	pag	69

4.1.2 Enhanced MALDI-MS analysis by peptide modification: state of the art	pag	70
4.2 Materials and methods	pag	71
4.3 Results and discussions	pag	72
4.4 Conclusion	pag	83
4.5 References	pag	85
<b>5 A NEW METHOD TO SELECTIVELY EVALUATE PROTEIN THIOLS OXIDATION STATE.</b>	pag	86
5.1 Introduction	pag	86
5.1.1 Proteomic analysis of oxidation related cysteine: state of the art	pag	86
5.2 Materials and methods	pag	87
5.3 Results and discussions	pag	90
5.4 Conclusion	pag	99
5.4.1 Perspective	pag	99
5.5 References	pag	101
<b>INDEX A: table of the abbreviations</b>	pag	A
<b>INDEX B</b>	pag	B



## Riassunto

### Nuove metodologie per l'analisi Proteomica

Le "Biotecnologie Moderne" sono l'insieme delle tecniche rivolte alla produzione di prodotti e servizi mediante l'utilizzo di sistemi biologici e moderne tecniche di biologia molecolare. Tipicamente i prodotti finali delle produzioni biotecnologiche sono proteine che trovano largo impiego in campo medico, industriale e agrario. La maggioranza dei prodotti biotecnologici sono ottenuti mediante l'utilizzo di tecniche di DNA ricombinante basate su cellule "ospite" geneticamente modificate in sistemi biologici come batteri, lieviti ed anche cellule mammifere. Per l'ottimizzazione di un sistema di produzione biotecnologico, oltre alla messa a punto dei sistemi di fermentazione e crescita cellulare "a monte" del processo, è altrettanto necessario realizzare "a valle" efficienti procedure di estrazione e purificazione dei bio-prodotti dalle matrici impiegate. Tradizionalmente lo sviluppo di un processo prevedeva la progettazione e l'ottimizzazione delle procedure "a monte" e "a valle" mediante l'utilizzo di dati empirici e con un'incompleta o limitata conoscenza dei meccanismi cellulari a livello molecolare. I recenti progressi nel campo della Genomica e Proteomica, tecnologie che permettono di ottenere informazioni sui meccanismi cellulari a livello molecolare, hanno fornito nuovi strumenti e conoscenze utili per la progettazione dei processi biotecnologici. La Genomica è una branca della biologia molecolare che si occupa dello studio della composizione, delle funzioni e dell'evoluzione del patrimonio genetico negli organismi viventi. Tuttavia, è apparso subito evidente che la staticità dei dati genomici non era in grado di spiegare la dinamicità del corrispondente comparto proteico, caratterizzato da eventi di *splicing* alternativo, modifiche post-traduzionali e formazioni di complessi funzionali proteina-proteina. Per questo motivo negli ultimi anni l'attenzione è stata focalizzata maggiormente sui prodotti del genoma: le proteine. L'analisi Proteomica si occupa proprio della definizione del comparto proteico di un organismo mediante studi di caratterizzazione, variazione dei profili d'espressione, definizione di modifiche post-traduzionali e ricostruzione delle interazioni funzionali tra proteine. L'approccio proteomico ha avuto un forte impatto nel campo delle moderne biotecnologie. Oggi, tali metodologie sono comunemente applicate nelle produzioni biotecnologiche alimentari, nel controllo qualità e anche nel campo delle fermentazioni, per l'ottimizzazione dei bio-processi. La grande innovazione dell'analisi Proteomica è lo studio dell'intero comparto proteico come un unico analita. Differentemente dagli approcci classici di biochimica, le proteine non sono più separate dall'originale contesto di complessità che caratterizza i sistemi cellulari, ma sono piuttosto analizzate contemporaneamente, cercando di mantenere invariata la rete d'interazioni che esse formano *in vivo*. Attualmente l'analisi proteomica si avvale di numerose tecniche analitiche capaci di fornire una visione globale del comparto proteico di un organismo, tra queste sicuramente le più importanti sono l'elettroforesi bidimensionale (2DE) e la spettrometria di massa (MS) accoppiata a sistemi cromatografici nano-HPLC (LC-MSMS). La versatilità e la sinergia di queste tecnologie hanno permesso di raggiungere innumerevoli risultati in tempi brevi, rendendo oggi l'analisi Proteomica una tappa obbligatoria di qualsiasi studio biochimico. Tuttavia, il vasto campo di applicabilità di tale approccio porta inevitabilmente ad incontrare diversi limiti connessi sia alle caratteristiche dei campioni in analisi sia alle peculiarità delle tecniche analitiche utilizzate. Per esempio l'analisi delle proteine di membrana può essere problematica a causa della scarsa

solubilità di questa classe di analiti nei tamponi utilizzati per la separazione elettroforetica. Inoltre l'ampia gamma dinamica di concentrazione in esame rende difficile l'analisi di modifiche post traduzionali sub-stechiometriche anche mediante l'utilizzo di tecniche *gel-free*. Negli ultimi anni sono stati diversi i lavori metodologici rivolti a superare questi limiti costituzionali dell'analisi proteomica, permettendo di estendere il campo d'analisi perseguibile. Seguendo questa tendenza, lo scopo di questo progetto di tesi è l'ottimizzazione di nuove procedure d'analisi per migliorare l'analisi Proteomica di importanti modifiche post-traduzionali. Ciò è stato realizzato mediante la manipolazione chimica di peptidi e proteine combinata all'impiego di avanzate tecniche di spettrometria di massa.

Il primo studio affrontato in questo lavoro di tesi è dedicato alla ottimizzazione di una procedura di analisi per migliorare l'identificazione dei siti di nitrurazione nelle proteine. La nitrurazione dei residui di tirosina è un'importante modifica post-traduzionale che può verificarsi *in vivo* durante fenomeni di stress ossidativo associati alla iperproduzione di ossido nitrico (1). Essa consiste nella sostituzione di un idrogeno in posizione *orto* nel gruppo fenolico dei residui di tirosina con un gruppo nitro (NO<sub>2</sub>). L'importanza biologica di questa modifica è globalmente accettata sia per le sue funzioni di mediatore della trasduzione dei segnali cellulari sia come *bio-marker* di diverse patologie (2). Quest'ultima caratteristica è oggetto di numerosi studi, infatti la nitrurazione delle proteine sembra essere implicata in numerose patologie riguardanti il sistema nervoso come il morbo di Parkinson, il morbo di Alzheimer e l'ischemia (3). Tuttavia, l'approccio classico di Proteomica presenta numerosi limiti nella rivelazione dei fenomeni di nitrurazione *in vivo*. Infatti, anche se l'analisi mediante anticorpi specifici permette di identificare la presenza di proteine nitate frazionate con tecniche di 2DE (4), il carattere sub-stechiometrico della reazione di nitrurazione *in vivo* rende molto difficile l'identificazione dei siti di modifica. Inoltre, è stato anche dimostrato che l'analisi di spettrometria di massa risente enormemente dell'incorporazione del gruppo nitro nell'anello fenolico dei residui di tirosina (5). Per superare questi limiti sono state realizzate diverse metodologie alternative rivolte ad arricchire proteine o peptidi contenenti residui di nitro-tirosina. Questo è stato realizzato mediante tecniche di immuno-precipitazione (6) o anche di derivatizzazione chimica con reagenti che permettono la purificazione specifica dei residui marcati (7). Mediante quest'ultimo tipo di approccio è anche possibile migliorare l'analisi di spettrometria di massa, in quanto il gruppo nitro è convertito in una specie che favorisce la ionizzazione. Tuttavia le tecniche appena citate consistono di molteplici passaggi cromatografici che possono risultare dispersivi in termini di materiale, tempo e campione. In questo lavoro di tesi è stata ottimizzata una metodologia innovativa che, basandosi sulla modifica chimica dei residui di nitro-tyrosina, permette di identificare proteine nitate in miscele complesse evitando preventive separazioni cromatografiche. La strategia prevede la riduzione dei gruppi nitro ad ammina e la successiva sulfonazione di quest'ultimi con il reagente cloruro di dansile (DNS-Cl). Le condizioni di reazione e analisi di spettrometria di massa sono state inizialmente ottimizzate utilizzando una proteina modello. A questo scopo è stata scelta l'albumina siero bovina (BSA), costituita da 20 tirosine, che è stata nitrata *in vitro*. La selettività della reazione di marcatura è stata controllata dal pH della soluzione che è stato mantenuto a 5,0, sfruttando in questo modo il peculiare pKa delle ammine aromatiche che è 4,7. L'utilizzo del cloruro di dansile permette di effettuare analisi di spettrometria di massa estremamente selettive con strumenti dotati di analizzatori ibridi triplo quadrupolo-trappola ionica lineare. Infatti, in precedenti studi è stato dimostrato che i peptidi modificati con il dansile generano in

esperimenti di massa tandem frammenti peculiari con rapporto massa carica ( $m/z$ ) 234 e 170 (8). Inoltre, quest'ultimo frammento può essere anche generato in esperimenti di tipo MS3 dal precursore a  $m/z$  234. Tali caratteristiche di frammentazione sono state utilizzate per ottimizzare una procedura d'analisi LC-MSMS in modalità *Precursor Ion Scan* (PIS) e MS3. In pratica la miscela peptidica ottenuta dall'idrolisi delle proteine in esame è frazionata mediante cromatografia a fase inversa e analizzata direttamente mediante spettrometria di massa in modalità PIS. Questa modalità permette di ridurre l'analisi ad un numero molto ridotto di specie poiché sono rivelate solo le specie ioniche che generano frammenti a  $m/z$  170 a seguito di collisione con gas neutro (CID), peculiarità tipica dei peptidi modificati con dansile. È stato stimato che in questa modalità operativa, per la BSA nitrata il 73% dei peptidi non nitrati non è stato rivelato. Combinando all'analisi PIS anche esperimenti di tipo MS3, che permettono di determinare quali ioni possono generare frammenti  $m/z$  170 da frammenti  $m/z$  234, è possibile definitivamente ridurre l'analisi alle sole specie marcate, con delezione del 100% delle specie di non interesse. La riduzione della complessità analitica permette di guadagnare enormemente in sensibilità, in quanto è incrementato considerevolmente il *duty cycle* del sistema. Il frazionamento in fase gassosa, realizzato dalla metodica di spettrometria di massa, può considerarsi dunque equivalente ad un passaggio di arricchimento dei peptidi nitrati, senza tuttavia aggiungere ulteriori sistemi cromatografici. L'applicabilità della tecnica è stata verificata in miscele complesse come estratti proteici di *E.coli* e di latte bovino, confermando la possibilità di individuare proteine ntrate e i corrispondenti siti di modifica anche in campioni di origine biologica. Infine i dati ottenuti da questo lavoro sono stati pubblicati da un'importante rivista di Chimica Analitica (9).

La strategia appena proposta tuttavia non permette di effettuare stime quantitative per valutare variazioni di concentrazione di proteine ntrate in differenti campioni. L'analisi quantitativa di questa modifica post-traduzionale rappresenta un vero limite della Proteomica, al punto che attualmente non ci sono procedure che permettono di identificare e quantificare allo stesso tempo i siti di ntrazione nelle proteine. Le uniche metodologie attualmente disponibili sono il saggio ELISA (10) e il dosaggio mediante gas cromatografia della nitrotirosina in forma aminoacidica ottenuta dall'idrolisi in HCl delle proteine (11). Tale problematica è stata affrontata in questo progetto di dottorato. In particolare sulla base dell'esperienza pregressa è stato ipotizzato che l'utilizzo di un criterio di elevata selettività in spettrometria di massa, accoppiato ad una marcatura altrettanto selettiva dei residui di interesse con un reagente arricchito nella componente isotopica, potesse permettere l'identificazione e quantificazione dei siti di ntrazione. Per questo scopo, non essendo disponibili in commercio isotopi del cloruro di dansile, è stato scelto come reagente la N-metilpiperazina-acetato N-idrossisuccinimide estere che è la molecola utilizzata nella più nota strategia di analisi quantitativa in Proteomica: iTRAQ (12). Il successo di questa metodica è dovuto alla peculiare struttura del reagente iTRAQ che permette l'acilazione delle ammine primarie. Esso è commercializzato in 4 forme isobare che differiscono tra loro per la composizione e distribuzione degli atomi pesanti del C, N, e O, consentendo di modificare i peptidi sempre con lo stesso incremento di massa. La strategia prevede la marcatura di fino a 4 profili d'espressione differenti e successivamente le miscele peptidiche sono unificate prima dell'analisi LC-MSMS. La grande innovazione di iTRAQ è l'indistinguibilità in modalità MS dei peptidi provenienti dai differenti campioni di origine, aumentando di fatto l'intensità del segnale rivelato e soprattutto non introducendo ulteriori segnali nello spettro di

massa. Nei relativi spettri di frammentazione MS/MS sono distinguibili i segnali peculiari del reagente iTRAQ utilizzato, rispettivamente a valori di  $m/z$  114, 115, 116, 117 dalla cui misura dell'intensità è possibile realizzare stime quantitative relative. Differentemente dal cloruro di dansile, la chimica degli esteri della N-idrossisuccinimide non permette di utilizzare il tipico  $pK_a$  delle ammine aromatiche per realizzare acilazioni selettive dei residui di nitrotirosina a pH 5,0. Per questo motivo, prima della riduzione del gruppo nitro e della marcatura, le ammine primarie delle lisine e dei residui N-terminali dei peptidi devono essere acetilati. In questo modo è possibile successivamente condurre la marcatura a pH 8,0 senza reazioni aspecifiche. Anche in questo caso le condizioni di reazione sono state ottimizzate utilizzando come proteina modello la BSA. L'analisi di LC-MSMS è stata ancora una volta effettuata mediante uno spettrometro ibrido triplo quadrupolo trappola ionica lineare realizzando esperimenti in modalità PIS, usando come criterio di selettività uno degli ioni frammento peculiari del reagente iTRAQ (114, 115, 116, 117). Mediante questo tipo di analisi è stato possibile per la BSA eliminare il 96% dei peptidi di non interesse. Da un confronto con i risultati ottenuti mediante l'utilizzo del cloruro di dansile, risulta che l'analisi in PIS dei peptidi marcati con iTRAQ è molto più selettiva. Questo perché la regione dello spettro MSMS dei peptidi compreso tra 114 e 117 è più libera di segnali rispetto a alla regione intorno al valore 170. Tuttavia non è stato possibile realizzare la completa rimozione dei peptidi non nitrati mediante analisi MS3, in quanto non sono state trovate transizioni efficaci. Basandosi solo sull'elevata selettività della PIS la procedura è stata quindi verificata su scala proteomica analizzando miscele complesse di estratti proteici di *E.coli* e di latte bovino, caratterizzati da differenti concentrazioni di proteine ntrate. E' stato in questo modo possibile in una singola analisi identificare ed effettuare stime quantitative dei siti di nitrificazione anche per proteine poco rappresentate. I dati ottenuti sono stati accettati e pubblicati da un'importante rivista di Proteomica (13).

Un altro aspetto affrontato in questo progetto di tesi riguarda il miglioramento dell'analisi MALDI-MSMS mediante la modifica chimica delle miscele peptidiche in esame. Questa problematica è stata largamente affrontata in altri lavori, dove è stato dimostrato che la frammentazione dei peptidi triptici in sorgenti MALDI generalmente non permette di ottenere una distribuzione omogenea dei segnali per consentire un corretto sequenziamento della regione N-terminale (14). Questo effetto è dovuto alla caratteristiche della ionizzazione MALDI che genera ioni mono-carica nella forma di addotti  $MH^+$ . La presenza costante di un residuo fortemente basico di arginina o lisina in posizione C-Terminale, ha un effetto di localizzazione della carica in questa regione, favorendo la generazione di ioni frammento appartenenti alla serie  $y$ . Inoltre l'effetto di localizzazione sopra citato, sfavorisce la frammentazione dei legami peptidici nella regione N-Terminale come predetto dalla teoria del protone mobile (15). Per superare questo limite sono state realizzate diverse strategie che prevedono la marcatura chimica dell'ammina N-Terminale inserendo un ulteriore "protone mobile" o una carica fissa, capaci di favorire la frammentazione dei legami e la ritenzione della carica nella regione N-Terminale dei peptidi (14). Queste strategie hanno permesso di migliorare la qualità degli spettri di frammentazione ottenuti con spettrometri di massa MALDI, tuttavia diminuendo l'intensità dei segnali in modalità MS. Inoltre tali strategie non sono mai state applicate su scala proteomica. In questo progetto di tesi è stato valutato l'utilizzo del cloruro di dansile per la marcatura del residuo N-Terminale dei peptidi con lo scopo di migliorare l'analisi MS e MSMS. Le proprietà in modalità MALDI-MS dei peptidi dansilati sono state già studiate in un precedente lavoro (16). E' stato dimostrato che l'introduzione di un gruppo

dimetilammino-naftalenico, che ha un massimo di assorbimento alla lunghezza d'onda del laser utilizzato nelle comuni sorgenti MALDI, permette di migliorare il rapporto segnale rumore dei peptidi modificati in modalità MS. Inoltre è stato osservato che la marcatura degli idrolizzati triptici cambia la tipica "impronta digitale" di una proteina ottenuta mediante analisi MALDI-MS. Quest'ultimo effetto è dovuto alla natura della modifica introdotta, che cambia la gerarchia dei profili di ionizzazione, permettendo l'identificazione di peptidi non rivelati mediante un approccio classico, tuttavia a discapito di altri normalmente osservati. Gli autori hanno dunque proposto una strategia che prevede l'idrolisi delle proteine in esame, la marcatura con DNS-Cl di un'aliquota delle risultanti miscele peptidiche ed infine l'analisi in parallelo delle due miscele ottenute mediante *Peptide Mass Fingerprint* (16). La complementarietà dei risultati generati dall'analisi delle miscele marcate e non marcate, permette di ottenere considerevoli miglioramenti nell'attendibilità dei dati statistici e nella copertura di sequenza. In questo lavoro di tesi sono state migliorate le condizioni di reazione avvantaggiandosi dell'utilizzo delle micro-onde. Inoltre i dati sopra citati sono stati confermati mediante l'utilizzo di uno spettrometro di massa d'ultima generazione MALDI-TOFTOF. È stato realizzato uno studio più approfondito rivolto a comprendere l'effetto di variazione dei profili di ionizzazione dopo la marcatura, mediante l'utilizzo di un numero elevato di peptidi e di dati ottenuti da esperimenti MSMS. Da questo studio risulta che la modifica dell'ammina N-Terminale con un gruppo che assorbe la radiazione UV, aumenta il trasferimento di energia dalla sorgente laser al sistema matrice/campione, favorendo il desorbimento e la ionizzazione soprattutto dei peptidi dotati di  $m/z$  più bassi. Tuttavia la sulfonazione dei gruppi amminici causa una netta diminuzione del  $pK_a$  di questi residui, comportando nei peptidi una minore tendenza a formare addotti  $MH^+$ . Mentre questo effetto è irrilevante per la conversione dell'ammina N-terminale ( $pK_a \approx 8,0$ ), è stato osservato che il 91% dei peptidi non identificati in seguito alla marcatura conteneva un residuo di lisina ( $pK_a \approx 12,0$ ), in posizione C-Terminale. I dati ottenuti spiegano la complementarietà osservata a seguito della marcatura con DNS-Cl, che ha permesso di identificare per la BSA 18 peptidi normalmente non osservati. In questo studio sono anche state valutate le caratteristiche di frammentazione dei peptidi dansilati in modalità *Post Source Decay* mediante uno spettrometro di massa MALDI-TOFTOF. Risulta che la presenza del residuo di dansile in posizione N-terminale permette di ottenere una migliore copertura della sequenza aminoacidica ricavata dall'interpretazione degli spettri MSMS. Infatti in fase di ionizzazione, il gruppo dimetilammino-naftalenico assorbe discrete quantità di energia che è ridistribuita nei vari sottolivelli vibro-rotazionali dei legami chimici lungo la catena peptidica. Questo comporta un aumento della probabilità di frammentazione del legame peptidico in prossimità del sito di dansilazione, infatti lo spettro MSMS risulta essere caratterizzato da una maggiore presenza di segnali relativi alla regione N-Terminale. In definitiva l'analisi complementare mediante la dansilazione dei peptidi triptici è vantaggiosa per aumentare la copertura di sequenza e l'attendibilità dei dati statistici anche per l'analisi LC-MALDI/MSMS. Ciò è stato verificato su scala proteomica dall'analisi di miscele complesse di estratti proteici di *E.coli*. L'ultimo oggetto di studio affrontato in questo progetto di tesi è rivolto allo sviluppo di una procedura in grado di permettere l'analisi dei differenti stati di ossidazione dei residui tiolici *in vivo*. Tale problematica è attualmente di grande interesse in quanto la transduzione di importanti segnali biologici è regolata dalla modifica ossidativa reversibile dei residui di cisteina (17). Inoltre è stato osservato che diversi fenomeni patologici sembrano relazionati a una incorretta ossidazione di tali amminoacidi a

seguito di eventi di stress ossidativo (18). I metodi dell'analisi Proteomica classica non sono sempre efficaci per la definizione dello stato di ossidazione delle cisteine. Questo perché la più parte delle modifiche è reversibile e quindi fortemente suscettibile ai tamponi normalmente impiegati per l'estrazione delle proteine e il frazionamento elettroforetico. Per questi motivi sono stati studiati approcci alternativi che consistono nell'alchilazione differenziale dei tioli, in tamponi riducenti a selettività decrescente (19). La pleora dei reagenti alchilanti impiegati permette oggi di valutare le variazioni dello stato ossidativo dei tioli mediante le classiche tecniche di Proteomica. Tuttavia i reagenti utilizzati non sempre favoriscono tutti i passaggi analitici che caratterizzano l'approccio proteomico. In questo progetto di tesi sono stati effettuati studi preliminari per valutare l'applicabilità dei derivati del dansil nella caratterizzazione delle modifiche post-traduzionali connesse allo stato d'ossidazione dei tioli. Infatti, oltre alle eccezionali caratteristiche di spettrometria di massa mostrate nei precedenti studi di questo progetto di tesi, i dansil derivati possono essere impiegati per la rivelazione di fluorescenza di proteine frazionate per elettroforesi (20). Inoltre in bibliografia sono presenti diverse metodologie che prevedono l'utilizzo dei dansil-derivati nelle tecniche di istochimica (21) e citometria a flusso (22). Dunque sembrerebbe possibile sviluppare per la prima volta una metodologia che prevede l'utilizzo di un unico reagente per la determinazione dello stato ossidativo dei tioli nei tessuti e cellule compatibile con il frazionamento elettroforetico e l'analisi di spettrometria di massa. La strategia prevede la marcatura dei tioli con il reagente dansil-aziridina (DAZ) e successiva alchilazione con iodoacetammide in un tampone riducente. Per raggiungere questo scopo sono state ottimizzate le condizioni di reazione ed è stata verificata la selettività del reagente utilizzando come proteina standard la BSA, caratterizzata da 34 cisteine ossidate in 17 ponti disolfuri e una in forma ridotta. Verificata l'efficienza della reazione, la BSA modificata con DAZ è stata frazionata mediante SDS-PAGE per valutare la sensibilità della rivelazione di fluorescenza che è stata stimata compresa tra 1 e 10ng di proteina marcata. È stata inoltre valutata la possibilità di apprezzare ossidazioni delle cisteine mediante variazione dell'intensità di fluorescenza in proteine frazionate mediante elettroforesi. Questo è stato realizzato facendo reagire la BSA con una soluzione 1 mM di H<sub>2</sub>O<sub>2</sub> e successivamente applicando il protocollo di marcatura ottimizzato. È stato osservato che la banda corrispondente alla BSA ossidata presentava un'evidente diminuzione della fluorescenza dovuta alla minore disponibilità di tioli liberi dopo la reazione di ossidazione. Questo tipo di analisi è stata anche estesa ad un estratto proteico di *E.coli* permettendo di confermare la specificità e l'applicabilità del metodo su scala proteomica. In questo progetto di tesi sono state anche ottimizzate le condizioni di reazione per realizzare la marcatura dei tioli intra-cellulari. Questo è stato possibile perché i dansil derivati sono permeabili alla membrana cellulare. È stato verificato che la quantità di reagente utilizzato non fosse stata nociva per le cellule batteriche ed umane mediante test del blu tripano, microscopia in fluorescenza e citometria a flusso. Dunque, cellule batteriche e umane sono state sottoposte a stress ossidativo indotto da H<sub>2</sub>O<sub>2</sub> ed inseguito trattate con dansil-aziridina. Mediante citometria a flusso è stato possibile discriminare la popolazione di cellule sottoposte a stress in quanto presentava una minore emissione fluorescenza rispetto al controllo. Inoltre dall'analisi dell'immagine dei gel 2DE degli estratti cellulari relativi ai campioni sopra citati è stato possibile identificare le proteine coinvolte nei processi ossidativi. Allo stato attuale la strategia presentata deve ancora essere ottimizzata in alcuni punti. Infatti, devono essere valutate eventuali differenze tra la marcatura *in vitro* ed *in vivo*, dovute alla differente

accessibilità dei residui di cisteina da parte del reagente. In caso affermativo si potrebbe considerare la possibilità di estendere la procedura anche a studi conformazionali e di interattomica. Inoltre allo stato attuale la strategia, come tutte le altre metodologie presenti in letteratura, anche se permette di identificare la proteina coinvolta nel processo di ossidazione non consente sempre in maniera univoca la determinazione del sito di modifica. Questo scopo sarà raggiunto, nel prosieguo di questo progetto, quando saranno sintetizzati analoghi del dansile arricchiti della loro componente isotopica.

## Bibliografia

1. Radi R., *Proc. Natl. Acad. Sci. U S A* **2004**, 101(12):4003-4008.
2. Ohshima H., Friesen M., Brouet I., Bartsch H., *Food Chem. Toxicol.* **1990** 28(9): 647-52
3. Sacksteder C.A., Qian W.J., Knyushko T.V., Wang H., Chin M.H., Lacan G., Melega W.P., Camp D.G., Smith R.D., Smith D.J., Squier T.C., Bigelow D.J., *Biochemistry* **2006**, 45(26):8009-22
4. Kanski J., Behring A., Pelling J., Schöneich C., *Am. J. Physiol. Heart Circ. Physiol.* **2005**, 288: H371–H381;.
5. Sarver, A., Scheffler N.K., Shetlar M.D.; Gibson B.W., *J. Am. Soc. Mass Spectrom.* **2001**, 12:439–448.
6. Thomson L., Christie J., Vadseth C., Lanken P.N., Fu X., Hazen S.L., Ischiropoulos H., *Am J Respir Cell Mol Biol.* **2007**, 6(2):152-7
7. Nikov G., Bhat V., Wishnok J.S. and Tannenbaum S.R., *Anal. Biochem.* **2003**, 320, 214-222.
8. Amoresano A., Monti G., Cirulli C., Marino G., *Rapid Commun. Mass Spectrom.* **2006**, 20:1400-1404.
9. Amoresano A., Chiappetta G., Pucci P., D'Ischia M., Marino G., *Anal. Chem.* **2007**, 79(5):2109-17
10. Zheng, L., Nukuna, B., Brennan, M. L., Sun, M., Goormastic, M., Settle, M., Schmitt D., Fu X., Thomson L, Fox P. L., Ischiropoulos H., Smith J. D., Kinter M., and Hazen S. L., *Clin. Invest.* **2004**, 114: 529–541
11. Leeuwenburgh C., Hardy M.M., Hazen S. L., Wagner P., Oh-ishi S., Steinbrecher U. P., *J. Biol. Chem.* **1997**. 272: 1433–1436.
12. Ross P.L., Huang Y.N., Marchese J.N., Williamson B., Parker K., Hattan S., Khainovski N., Pillai S., Dey S., Daniels S., Purkayastha S., Juhasz P., Martin S., Bartlet-Jones M., He F., Jacobson A., Pappin D.J., *Mol. Cell. Proteomics.* **2004**, 3(12):1154-69.
13. Chiappetta G., Corbo C., Palmese A., Marino G., Amoresano A, *Proteomics* **2008** in press
14. Pashkova A., Chen H.S., Rejtar T., Zang X., Giese R., Andreev V., Moskovets E., Karger B.L., *Anal. Chem.* **2005**, 77(7): 2085-2096
15. Wysocki V.H., Tsaprailis G., Smith L.L., Brezi L.A., *J. Mass Spectrom.* **2000**, 35: 1399–1406
16. Park S.J.. Song J.S.. Kim HJ.. *Rapid Commun. Mass Spectrom.* **2005**. 19(21):3089-96
17. Biswas S., Chida A.S., Rahman I., *Biochem. Pharmacol.* **2006**, 71:551-564
18. Dafre A.S., Artenib N.S., Siqueirab I.R. and Netto C.A., *Neuroscience Letters* **2003**, 345 (1): 65-68
19. Leichert L.I., Jakob U., *PLoS Biol.* **2004**, 2: e333,

20. Hsi K.L, O'Neill S.A., Dupont D.R., and Yuan P.M., *Anal. Biochem.* **1998**, 258: 38-47
21. Braga-Vilela A.S., de Campos Vidal B., *Acta Histochem.* **2006**, 108(2):125-32.
22. Jones R.J., Barber J.P., Vala M.S., Collector M.I., Kaufmann S.H., Ludeman S.M., Colvin O.M., Hilton J., *Blood.* **1995**, 85(10):2742-6

## Résumé

Le travail de thèse présenté dans ce mémoire consiste en la mise au point de nouvelles méthodologies d'analyse pour les études protéomiques. Le sujet principal de ce travail de thèse a été l'optimisation de procédures innovantes qui se basent sur la manipulation chimique de mélanges peptidiques et sur l'analyse avancée par spectrométrie de masse MS3, et qui ont pour objectif d'améliorer les capacités d'identification et quantification des modifications post-traductionnelles par une approche protéomique.

Une nouvelle procédure d'identification des sites de nitration des protéines a été mise au point, par le moyen d'une modification sélective des peptides nitrés après dansylation et par l'analyse par spectrométrie de masse en modalité Precursor Ion Scan/MS3. Une telle stratégie permet de surmonter quelques unes des limites classiques de l'analyse des sites de nitration des protéines, comme la nécessité d'utiliser des techniques d'enrichissement chromatographique mais permet aussi de surmonter les difficultés d'identification des peptides nitrés par spectrométrie de masse. Il a également été optimisé une procédure pour l'identification et la quantification des sites de nitration des protéines par le biais d'une modification sélective des peptides nitrés avec le réactif iTRAQ et par une analyse successive par spectrométrie de masse en modalité Precursor Ion Scan. Cette technique peut être considérée comme étant la première stratégie capable simultanément d'identifier et de quantifier les sites de nitration des protéines par spectrométrie de masse. En outre, différentes conditions d'analyses pour l'identification des phosphopeptides dans des mélanges biologiques ont été évaluées par analyse LC-MSMS en modalité neutral loss et precursor ion scan. De plus, une nouvelle procédure qui utilise la chimie des micro-ondes afin d'améliorer les analyses LC-MALDI-MSMS a également été optimisée, par un marquage extensif des mélanges peptidiques analysés avec du chlorure de dansyle. Cette étude a également permis de comprendre les caractéristiques de la fragmentation des peptides dansylés dans des expériences de post source decay. Enfin, des expériences préliminaires ont été réalisées afin de vérifier la possibilité d'utiliser les dérivés de la dansylation pour développer une nouvelle procédure finalisée à l'identification des états d'oxydation des résidus de cystéine des protéines séparées par une électrophorèse bi-dimensionnelle. Les résultats obtenus indiquent que les dérivés du dansyle permettent de déterminer les variations des états d'oxydation des cystéines par des techniques de cytométrie en flux, électrophorèse bidimensionnelle et spectrométrie de masse.

## **1. INTRODUCTION**

### **1.1 Proteomics impact on modern Biotechnologies**

In modern terms, Molecular Biotechnology has come to mean the use of cells and tissue cultures, molecular biology, and in particular recombinant DNA technology, to generate unique organisms with new features leading to produce specific products, that many times are proteins. On this basis, the fields of the Industrial (white) Biotechnology, Medical (red) Biotechnology, Vegetal (green) Biotechnology, can be distinguished if these tools are applied to the development of industrial processes, molecular studies of the diseases and drug discovery, agricultural and food production improvement respectively. Most of the biotechnological products result from the use of recombinant DNA technology, where a recombinant production system is set up, based on a genetically modified host cell, using either microbial fermentation or mammalian cell cultures. In addition to fermentation, the extraction and subsequent purification of the desired bio-product from the fermentation broth is an important part of the overall production process. These downstream procedures form a major part of the overall process development and are important in the determination of the final productivity and characteristics of the product. Traditionally, process development involves designing and optimizing upstream and downstream processes based on empirical data, with only incomplete or limited understanding at the cellular level. The advent of Genomic and Proteomic technologies, which can provide details at the molecular level, has generated interest in the application of these tools for the development of biotechnological processes.

Genomics is the comprehensive analysis of the genetic content of an organism. It also often refers to genome wide studies of mRNA expression (1). Already during the “genomic era” that ended with the sequencing of Human Genome in the year 2003, the scientific community realized that the identification of coding sequences is insufficient to understand the molecular mechanisms of cell activity. Therefore, the attention increasingly focused on the products of the genome: the proteins and enzymes that determine cellular architecture and function. According to the current annotation, the human genome consists of about 25000 genes, scattered among 3 billions nucleotides of chromosome-based DNA code (2). This represents a huge amount of static information, which needs to be correlated with dynamic information coming from gene products and their interactions. In contrast to the genome, the proteome is dynamic and is in constantly modulated because of a combination of factors, which include mRNAs differential splicing, post translational modifications (PTMs), as well as temporal and functional regulation of gene expression as well as the formation of multi-protein complexes.

Proteomics provides methods for correlating the vast amount of genomics information that is becoming available with the equally vast protein information that is being produced through analysis of cells under normal versus altered states (3). In the last few years Proteomics has become a powerful tool for the investigation of complex biochemical processes and protein-protein interactions (4-5). In medical sciences, the discovery and the use of disease biomarkers, especially in cancer and neurodegenerative diseases, has become a routine analysis for a better and more targeted medical treatment (5–8). Currently, Proteomic methods are widely used in food biotechnology as quality control so the terms “industrial process proteomics” (9) and “industrial proteomics” (10) are currently used. It has also been shown that proteomic technology can be very useful in the development of production processes

for therapeutic proteins by using genetically engineered animal cells (11-12) or human stem cells (13). In “classical” fermentation industry, Proteomic methods can also be used for the identification of targets for bioprocess improvement (14). Unlike mammalian cells that are used almost exclusively for production of protein-based therapeutics (15), microbial cells are also widely used for production of small molecules (14). Microbial fermentation in food processing has been a tradition for thousands of years (16). Besides optimization of the fermentation process, purification, optimization of yield and purity, the characterization of the final process are crucial steps in integral process development.

In the near future, in parallel with genomics and metabolomics, proteomics will play an important role in process development. These technologies will be used to enhance productivity of microbial cells or to influence targeted properties of the final product. Knowledge of the cell proteomics will be helpful to predict the cellular response to environmental change and its adaptation to different substrates. Finally, proteomics are important for optimization of downstream processing and for thorough analytical investigation of the final products.

## **1.2 Proteomics analysis**

The terms Proteomics is associated to the set of analytical tools used to depict the protein compartment of a cell. This innovative “biotechnology” is the natural continuation of Genomics approach. It moves away from classical Protein Chemistry, also if from the latter, taking advantages of all the heritage of knowledge and methods developed from the latter. In fact, the great innovation of the Proteomics analysis is the idea that to study the cellular molecular mechanisms, in which proteins play a key role, it is necessary to study the entire proteome as a “single analyte”. Meaning that, the proteins target of the analysis are no more purified and isolated from their highly complexity context found in living systems. Indeed, they are analyzed all together in order to obtain a real snapshot of the proteome, related to a particular cell state. From this general definition it may distinguish two main area of interest: *i)* “expression proteomics” that is focused to the characterization of the change in protein expression levels and definition of PTMs (17), *ii)* “functional proteomics” aimed to understand protein-protein interactions (18), signal pathways (19) and structure function relations.

However, the proteome analysis is hindered by several analytical problems. First of all is the large range of protein concentration present in the samples. For example, in the human serum the 50 most abundant proteins represent about 99% of the total amount of protein mass but only less than 0.1% in number (20). Another important challenge is surely the detection of PTMs. In fact only a minor part of the proteins of interest are post translationally modified, for instance just 1 in  $10^6$  tyrosines are nitrated (21). The high sample complexity, in terms of number of analytes, is also a feature that has to be taken in account, in fact for about 21000 human protein-encoding genes are estimated around  $10^6$  human proteins (22). For these reasons the Proteomics analysis needs a pool of methodologies and technologies that are high throughput, sensitive, selective toward the proteins target of the analysis and with large dynamic range effectiveness.

Currently, Proteomics may rely on many chromatographic and electrophoresis tools to fractionate the analytes. However, if different approaches are in relation to these techniques of separation, all the strategies have a common essential final step: the mass spectrometry (MS) analysis of peptides or proteins.

### **-1.2.1 Mass spectrometry tools for Proteomics analysis**

#### **a) Principles and instrumentation**

Mass spectrometers consist of three basic components: an ion source, a mass analyser, and an ion detector. Molecular mass measurements are carried out indirectly, calculating the mass charge ratio ( $m/z$ ), by the analysis of kinetics behaviour of the ionized analytes in the gas phase and in electromagnetic fields. The need of a method that transfers efficiently intact molecules from solution or solid phase into the gas phase, was the limit that for many years excluded proteins and peptides from this powerful technique. With the development and the commercialization of mass spectrometers based on the ion source technologies of “*Matrix-Assisted Laser Desorption/Ionisation*” (MALDI) (23) and “*Electrospray Ionisation*” (ESI) (24) the gas phase ionization of polar analytes has also become possible. Both MALDI and ESI are considered as soft ionisation techniques with which the generated ions undergo minor fragmentation.

In MALDI technique, samples are co-crystallised with a weak aromatic acid matrix on a metal target. A pulsed laser is used to excite the matrix, which causes rapid thermal heating of the molecules and desorption of ions into the gas phase in a *pulsed beam* fashion. After the laser activation, the weak acid nature of the matrix drives to generate single-charged ions in the form of  $MH^+$  adduct. The one-one analyte-MS signal relation in MALDI-MS makes possible to analyze also multi-component mixtures without any interpretation difficulties caused by the peaks overlapping.

ESI creates ions by spraying an electrically generated fine mist of ions into the inlet of a mass spectrometer at atmospheric pressure. By creating a potential difference between the capillary, through which the liquid flows, and the inlet of the mass spectrometer, small droplets of liquid are formed. These are transferred into a heated device to induce efficient evaporation of solvent. Once the droplets have reached the Rayleigh limit, ions are desorbed from the droplet generating gas-phase ions in a *continuous beam* fashion. The ions produced by ESI sources are multiply charged adducts  $MH_n^{n+}$ , where the number of protons incorporated depends on the statistical acid/basic equilibrium of the analytes. This situation complicates the spectra interpretation because each analyte may give rise to many signals in the spectrum. For this reason it is not possible to analyze complex mixture without a previous fractionation. However, because the ionization is carried on a liquid flow, ESI source may be simply coupled to liquid chromatography systems. The most notable improvement of ESI technique has come from the reduction of the liquid flow rate used to create the electrospray to *nano-scale* level. This device leads to create ions more efficiently (25) because the charge density at the Rayleigh limit increases significantly with decreasing droplet size ( $z_R \propto 8R^{3/2}$  where  $R$  is the droplet radius). Another advantage using separation techniques with low flow rate ESI is the increase in the concentration of the analyte as it elutes off the column.

After ionisation, the analytes reach the mass analyzer, which separates ions by their mass-to-charge ( $m/z$ ) ratios. Ion motion in the mass analyser can be manipulated by electric or magnetic fields to direct ions to a detector, usually an electro-multiplier, which records the numbers of ions at each individual  $m/z$  value converting the signals

in current. In Proteomic research, four basic kinds of mass analysers are currently

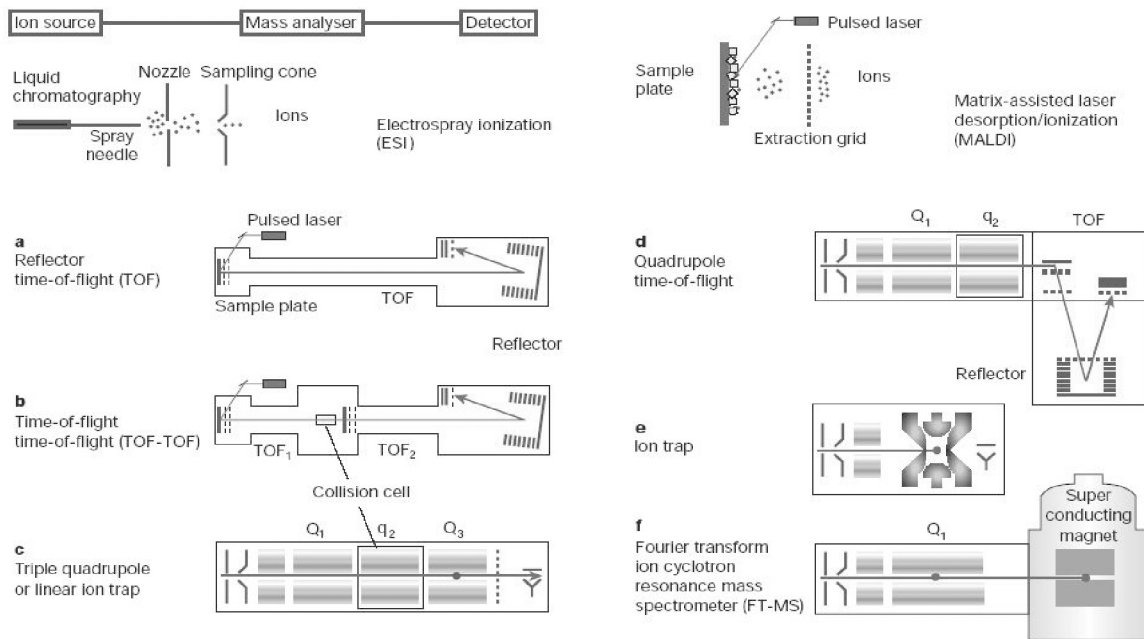


**Fig.1.1** Main components of Proteomics commonly used mass spectrometers

used: *time-of-flight (TOF)*, *ion trap (IT)*, *quadrupole (Q)*, and *Fourier transform ion cyclotron resonance (FTICR)* analysers (Fig.1.1). All four differ considerably in sensitivity, resolution, mass accuracy and the possibility to fragment peptide ions. By using a *TOF* analyzer the mass spectrum is measured by determining the flight time of ions after the extraction and the acceleration from the source by an electric potential. The ions are separated in a field-free flight tube. The ions time-of-flight is related to their  $m/z$  values:

$$m/z = 2Et^2/d^2, \quad E = \text{potential of extraction, } t = \text{time of flight, } d = \text{length of the tube}$$

The experimental arrival times of each ion to the end of the flight tube can be a mass spectrum can be acquired. The two main improvements to enhance the resolution of this technique were the “delayed extraction” that corrects the initial velocity vectors and the “reflectron” (26) that increases the ions path, curving their trajectories. TOF based instruments have high resolution and accuracy characteristics and they are usually coupled to pulsed beam type sources.

The simpler mass analyzer is the *quadrupole* that consists of four precisely straight and parallel rods that are aligned in the axial direction of ion beam. A voltage combining a DC component and a radio frequency (RF) component is applied between adjacent rods but with inverse polarity, opposite rods are electrically connected. Once inside the quadrupole the ions will oscillate in the (x) (y) direction as a result of the electric field. The differential equation which describes the motion of the charged particle along the x or the y-axis is:

$$d^2f/d\tau^2 = -[a - 2q\cos(2\tau)]f \quad \text{with} \quad a = -4/\omega^2 r_o^2 (e/m)U, \quad q = -2/\omega^2 r_o^2 (e/m)V, \quad \tau = \omega t/2$$

(with  $\omega$  the frequency of RF,  $r_0$  the radius between the electrodes,  $U$  is the constant DC voltage,  $V$  the maximum RF voltage,  $m$  the ion mass and  $e$  its charge). The general solution of this differential equation was found by Mathieu and has the form:

$$f = Ae^{\mu\tau}F(\tau) + B^{-\mu\tau}(-\tau), \text{ with } \mu(a, q) = \alpha + i\beta$$

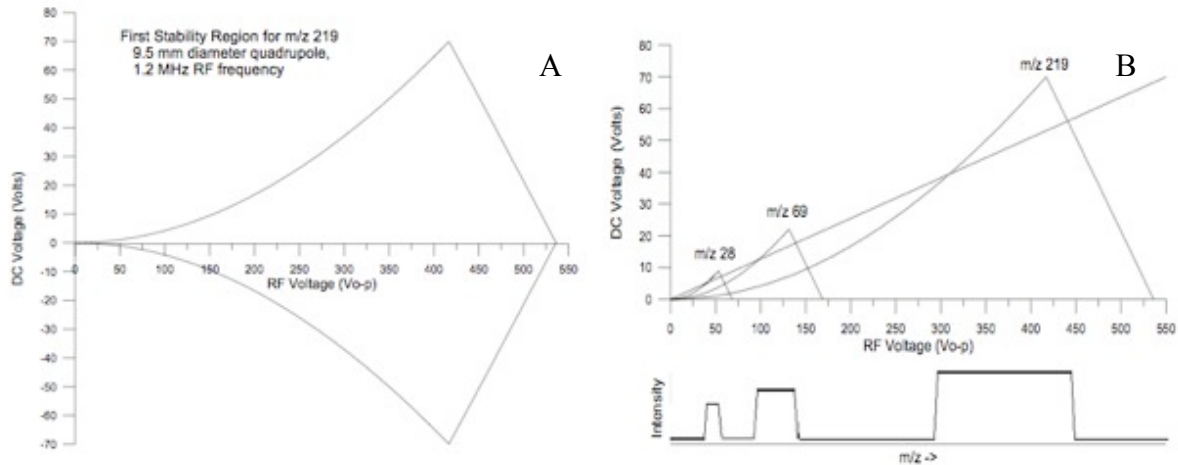


**Fig. 1.2 Panel A** shows a RF voltage vs DC voltage diagram of Mathieu stable solution for the ion 219 m/z in a 9.5 mm diameter quadrupole. All the RF-DC couples of voltage values inside the curve give to the ion stable trajectories and may be detected. **Panel B** shows the effect of the quadrupole scanning. In the RF voltage VS DC voltage diagram are represented three stability curves for the ions 28 m/z, 69 m/z and 219 m/z. The "operative line" starting from the origin represents the RF and DC ratio used during the scan in function of the time. When the line crosses the stability region of an ion it means that it is actually scanned. By this representation it is showed that with a linear scan line through the origin, the peak width increase geometrically with increasing mass. By using higher DC/RF ratio the operative line increase its slope and it passes through less stability regions resulting in higher resolution scan.

**A** and **B** are the constant of integration while  $\alpha$  and  $\beta$  are real function of  $a$  and  $q$  (27). It is possible to demonstrate that for a given m/z value ion oscillations are stable only for a restricted couple of  $a$  and  $q$  values that are operative depending respectively by the DC and RF voltage. Otherwise the ions have very large x,y coordinates and strike the rods and dissipate. The family of Mathieu stable solutions may be graphically represented in function of RF and DC. The resulting diagram helps to understand for a given m/z for what couple of RF and DC values it would have stable trajectories (Fig.1.2A). The symmetry around the DC voltage =0 means that in only RF mode the quadrupole lets pass all the ions. The mass filtering is realized by changing in time the DC voltage and the RF frequency, keeping constant their ratio (Fig.1.2B), therefore instantly varying the ions that are in their boundary stability condition.

The three-dimensional *ion traps* (IT) are composed of three hyperbolic electrodes: two end-caps and one ring. The ring electrode defines the radial direction and the end-cap electrodes define the axial direction. One end-cap electrode will usually have a hole in it to allow ions to enter the trapping volume. The ions are injected axially with kinetic energies that lead to pass the fringing field barrier near the end-cap hole. However, to overcome the exit of the ions, their high kinetic energy is dissipated by cooling them by collision with neutral gas by filling the trap with helium (28). In the IT ion trajectories undergo the same quadrupole rules and motion

equations showed before. However, the geometry of the electric field used gives to the ions an elliptical trajectory in the radial plane so they are confined inside the volume of the electrodes, and maintains a stable periodic motion in the axial direction with a peculiar secular frequency  $\omega_z$  for each  $m/z$  (29). By applying a supplementary voltage at the frequency  $\omega_z$ , the axial oscillation is increased causing the ions ejection from the trap. By timely changing the frequency it is possible to scan the mass range. Mass spectrometer equipped with IT technology has good sensitivity but low resolution and mass accuracy.

The most common *FTICR* analyzer consists of a cell composed of six plates arranged in the shape of a cube (30). This cell is oriented in a magnetic field (4,7-13 Tesla) so that one opposing pair of plates is orthogonal to the direction of the magnetic field lines. It is common for trapping electrodes of cubic cells to have openings that permit electrons or ions to enter the cell along the magnetic field lines. The four remaining plates are used for ion excitation and ion detection. When the ions pass into the magnetic field they are bent into a circular motion in a plane perpendicular to the field by the Lorentz Force. The cyclotron frequency of the ions rotation is dependent on their  $m/z$  ratio

$$\omega_c = eB/2\pi m, \quad \omega_c, \text{ secular frequency, } B = \text{magnetic field}$$

At this stage, no signal is observed because the radius of the motion is very small. The excitation of each individual  $m/z$  is achieved by a RF pulse across the plates of the cell. Each individual excitation frequency, corresponding to the peculiar  $\omega_c$  value, will excite the ions natural motion to a higher orbit inducing an alternating current between the cell plates. When the RF goes off resonance for that particular  $m/z$  value, the ions relax to their natural orbit and the next  $m/z$  packet is excited. Although the RF sweep is made up of a series of stepped frequencies, it can be considered as all frequencies simultaneously. This results in the measurement of all the ions together producing a complex frequency vs. time spectrum containing all the signals. The deconvolution of this signal by Fourier transform methods results in a frequency vs intensity spectrum, which is finally converted to the mass vs. intensity spectrum. FTICR mass spectrometers are the most accurate and the highest resolving power instruments currently available. (31)

### **b) Tandem Mass Spectrometry**

Conventional MS produces ions that are separated by  $m/z$  and analyzed directly. If a soft ionization method is used, the mass spectrum will lead to calculate the molecular weight values of compounds present in the analyte but with little or no structural information. In a tandem mass spectrometer, ions of a particular mass (parent or precursor ion) are selected by the first mass analyzer (MS1) can be subjected to collisions with neutral gas atoms or molecules. This process is known as *Collision Induced Dissociation* (CID). The ionic fragments (daughter ions) are then separated in a second analyzer (MS2), giving structural information such as the amino acid sequence of a peptide. Therefore, to realize the multi-stage MS analysis many mass spectrometers equipped with hybrid combinations of analyzer were commercialized. Triple quadrupole (QqQ) (32), quadrupole/ time of flight (QqTOF) (33) and time of flight/ time of flight (TOFTOF) (34) may perform “*space separated*” tandem MS. Ion trap analyzer by itself may realize tandem MS experiments. This is accomplished by the expulsion of the ions trapped in MS mode, isolating the parent ion. This one is further fragmented by collision and the produced ions are first accumulated, then

scanned and detected. This “time separated” operative mode allows to realize very sensitive MS<sup>n</sup> experiments with simple equipments. However, the usage of a unique quadrupole trap analyzer leads to record MS<sup>n</sup> spectra with low mass range cut-off. In fact, during their generation the daughter ions have experience of the RF and DC values used to trap the precursor ion.

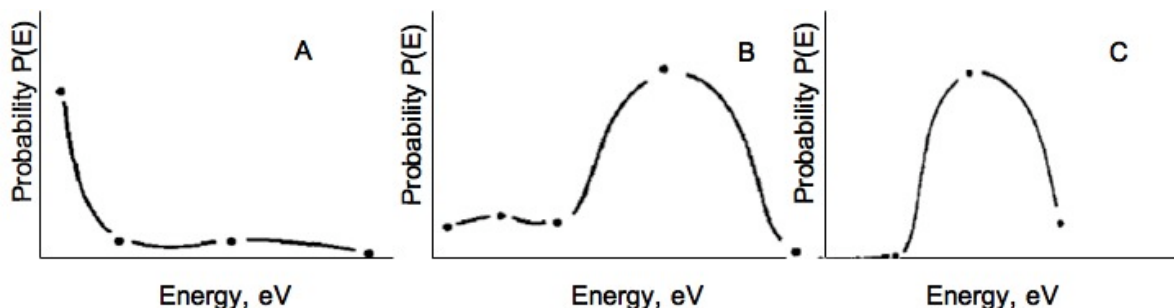


**Fig.1.3** Panel A shows the internal energy distribution for an ion population after a rapid activation High Energy CID (7keV). In these condition the collision are rare and high energetic. Thus, it appears that only a restricted number of ions increases their internal energy with high increment resulting in poor sample utilization and drastic fragmentation. Panel B shows the ions internal energy distribution after a slow activation Low Energy CID (28 eV). In these conditions the collisions are more probable and the ions are cooled by the higher operative pressure (0,5 mtorr). Thus, it results that a large number of ions increases their internal energy favoring peptide  $b_n$ ,  $y_n$  and immonium ions generation. Panel C shows the ions internal energy distribution after a slow activation Very Low Energy CID (26 eV). The higher operative pressure (2 mtorr) and the lower ions kinetic energies lead to a very slow activation compatible with the formation of a reaction intermediate. It results in a Gaussian curve without high energy tail. Thus, the fragmentations follow the Arrhenius theory producing mainly  $b_n$ ,  $y_n$  ions

These couple of potential values are in the stable region of Mathieu graphic for ions with  $m/z$  within 60% of the parent ion  $m/z$ , thus resulting in the complete loss of the smaller fragments (28). The chemistry of the fragmentation depends on many factors as the energy transferred to the ions, the time elapsing between the activation and the dissociation, the distribution of the internal energy (35). The amount of energy that can be deposited in an ion depends on the relative collision energy of the colliding ion/neutral pair under the classical impact rules. Considering that the neutral gas molecules have no velocity component the maximum centre-of-mass energy is:

$$E_{com} = \left( \frac{N}{N+m} \right) E_{kin}$$

with  $N$  the neutral gas the mass,  $m$  the ion mass,  $E_{kin}$  the parent ion kinetic energy (36-37). It results that heavier ions are more difficult to fragment and, by using heavier neutral gas, higher amount of energy are transferred to the parent ion. The  $E_{kin}$  value depends on the mass spectrometer optics and the operative mode. It is also related to the energy transfer kinetics and to the distribution in internal degrees of freedom. CID experiments of peptides and proteins are realized in three different modes: “High Energy”, “Low Energy” and “Very Low Energy”. High Energy CID processes involve keV kinetic energy of the parent ion and they are carried out by sector-based instruments (38). The gas pressure inside the spectrometer is kept low, thus 1-5 collisions take place between the fragmentation events. Consequently a large part of ion population increments the internal energy of few eV while the remaining has high energy favouring only a restrict number of critical sequential dissociation (Fig.1.3A). Therefore the efficiency of the process is low (10%) and the spectra consist principally of  $d$  and  $w$  ions characterized by side chain fragmentations

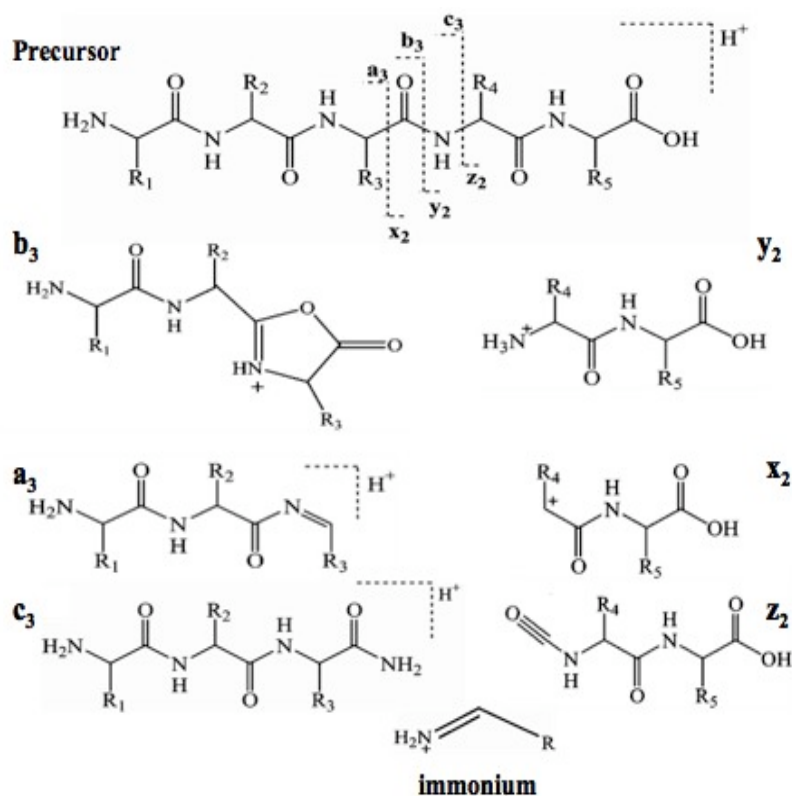


**Fig.1.4** Principal fragmentations of Low and Very Low Energy CID

Low Energy and Very Low Energy CID is essentially due to the “beam type” and “no beam type” features of the spectrometers. In fact the ions in QqQ and QTOF instruments have higher kinetic energy that may cause with the classical *b* and *y* ions also internal fragments as immonium ions (Fig.1.4) or *a* and *x* ions generated by the cleavage of  $\alpha$ -C and carbonyl-C. On the contrary in the Ion Trap the ions are “cooled” resulting in lower energy fragmentations with enhanced efficiency (50-100%)(39). The peptide bond cleavage is the principal event using Low and Very Low Energy CID, giving rise to *b* and *y* ions if the charge is retained on the N-Terminal or C-Terminal containing moiety respectively (Fig.1.4). It is commonly accepted that the cleavage occurs predominantly through charge-directed pathways. In practice the fragmentation is initiated by a charge that is transferred to the vicinity of the cleavage site after the hydrogen rearrangement as described by the mobile proton model (40). This interaction of the charge and the heteroatoms is more important in the gas phase because the solvent molecules that typically stabilize the molecules in the solution phase are not present in the gas. However, a charge-remote component is also observed in peptides CID fragmentation by which the acquired proton is localized on the more basic sites and takes no part to the fragmentation mechanism. In this pathway the peptide bond cleavage takes place by internal proton rearrangements, with charge retention on the initial protonated moiety. During this hybrid fragmentation pathway, singly-charged tryptic peptides give rise predominantly to *y* ions, by the presence of a strong basic lysine or arginine in C-Terminal position. The ions of *b* series are better visualized in multiply-charged peptides where the probability to have a N-Terminal charge retention is higher. The resulting Low Energy CID fragmentation spectra recorded with the common mass

only useful to discriminate isobaric amino acids (38). Low Energy and Very Low Energy CID processes involve 1-100 eV kinetic energy realized by using QqQ and QTOF and Ion Trap instruments respectively. Higher gas pressures are applied leading to 10-100 collisions between dissociations events. Under multiple collision conditions, energy is deposited in small increments, thus such activation effectively gives rise to a statistical internal energy distribution without higher component (Fig.1.3B and C). Consequently, no *d* or *w* ions or sequential dissociation is observed. The difference between

spectrometer consist of a large number of peaks related mainly to the *b* and *y* series ions and also to eventual neutral loss of NH<sub>3</sub>, CO and H<sub>2</sub>O. By the interpretation of these spectra it is very simple to reconstruct the peptide sequences calculating the difference between the mass values relative to the ions belonging at the same series. This procedure may be also automated by using special algorithms (41-42) leading to the *de novo* sequencing or the protein database searching (43-44).

### **-1.2.2 The first generation of the Proteomic analysis**

Proteomic analysis is aimed to analyze the whole proteome as a single analyte. However, the high complexity of the mixture examined imposes to use fractionation procedures in order to simplify the analysis without losing a global view of all the protein component of the samples. Bidimensional electrophoresis was the first technique leading to study the proteins on Proteomic scale and it is currently the leader technique in this field. Although 2DE development was realized many years before the *post-genomic era* (O'farrel et al. 1975) (45) the usage of this technique is still of high value because it allows to separate protein with high resolution (up to 10000) (46) giving rise at the same time to protein maps of the biological matrix examined. 2DE consists of a first fractionation step by Iso-Electric Focusing (IEF) leading to separate proteins by their typical iso-electric point. In the second step, co-focalized proteins are orthogonally separated by their hydrodynamic volume by SDS-PAGE. 2DE conversion from only-imaging technique to Proteomic leader technique was favoured both by the commercialization of the first MALDI-MS instruments and by the enrichment of sequence database using genomic data. Thus, the synergy between 2DE separation features, MALDI-TOF accurate and sensitive mass measurement, the sequencing database software versatility, lead to develop in 1993 the *Peptide Mass Fingerprinting* (PMF) (47-49) strategy that may be considered the first Proteomic high throughput methodology. PMF is based on the idea that a protein digested by an enzyme with known specificity produces a peptides pool that may be used as discriminatory for its identification. MALDI-TOF analysis produces a unique spectrum giving the accurate monoisotopic mass of all the peptides produced by the protein digestion, producing peculiar molecular masses map for each protein. This map is then compared to the ones generated *in silico* by the virtual digestion of all the protein sequences present in the genomic database. The results are statistically analyzed to find the best match. Therefore, such gel based strategy consists of six analytical steps: I) protein recovery from biological matrix II) 2DE fractionation III) Image analysis IV) in gel protein digestion V) MS analysis VI) Data base searching. The statistic nature of the protein identification, without any information about the amino acid sequence, implies a high hydrolysis yielding optimize the sequence coverage. In addition, in order to avoid misunderstanding results high protein purification and high mass accuracy of the mass measurements is also important. While the last two features are achieved by coupling 2DE and MALDI-TOF, it must be considered that the *in gel* hydrolysis leads to poor sequence recovery. This characteristic was the most important limitation of the first generation Proteomic analysis. The introduction of MS<sup>2</sup> This problem was in part overcome with the introduction of nanoLC-MS<sup>2</sup> technique in 1996, leading to determinate peptide amino acid sequence (50-51). So, the association of molecular weight and amino acid sequence for each given peptide is a milestone of Proteomic evolution. The statistic relevance of the sequence data coupled to the mass measurement allows to the unambiguous protein identification, even if a reduced number of peptides is detected. In

the last 10 years many technological progresses have changed the materials and methods of the gel-based Proteomics. New gel dyes were introduced in order to enhance the 2DE sensitivity (Brilliant Blue Coomassie, Sypro, DIGE) (52-53) and the selectivity toward the post-translational modifications (Pro Q diamond, Pro Q emerald) (54-55). Mass spectrometry analysis has been improved by using new instruments with higher resolution power and faster scan rates. The electrophoresis techniques are radically changed with the introduction of the first dimension gel strip with pre-formed gradient. Also research algorithms were powered and protein database were enriched, in particular considering the complete human genome sequencing in 2003. This overall evolution of modern Proteomic is driven by the methodological revolutions in the protein analysis over the years 1993-1995. This is particularly true if we consider that the six steps procedure is still currently un-varied in many Proteomic applications of the more recent research lines (56-57).

### **-1.2.3 The second generation of the Proteomic analysis**

The great results reached by the coupling of the 2DE high resolution power and MS flexibility were the driving force for the development of modern technologies and high throughput strategies. In fact, the analysis carried out by 2DE-MS presents many constitutive limitations for the study of some kinds of Biological aspects. For example, the analysis of membrane proteins is still a challenge, because of the poor solubility of the sample and the low recovery after the extraction procedures. To avoid 2DE high conductivity, that may induce the gel over-warming, low quantity of sample must be analyzed. Under this condition a high percentage of less abundant proteins never reaches the detection limits and remains un-analyzed. For the same reason the PTMs identification is a challenge because of the sub-stoichiometric characteristics of the biological modifications. In addition the 2DE-MS strategy is not a high throughput approach. To identify the detected proteins a large number of spots have to be processed, however the method is time consuming and it requires an intensive work of skilled operators. This is very limiting because the modern Proteomic studies relies on reproducible analysis of large numbers of proteins and samples that is realizable only with a high automation of the procedures. Moreover, the 2DE has also low reproducibility and triplicates of the analysis are required. In order to overcome this problem and make accessible all the fields of analysis, a new generation of Proteomic strategies was implemented. It consists in the extensive hydrolysis of protein extracts without gel-based separation. By this “shotgun” method, theoretically all the proteins present in the sample may be identified, also the ones with low solubility, if enzymes capable to achieve heterogeneous phase digestion as trypsin are used. However, the resulting peptide mixtures are too complex to be directly analyzed by RP/LC-MS<sup>2</sup> (58). The optimization of the multidimensional chromatography techniques followed by improved MS methods makes possible to realize this approach. The most common one employs  $\mu$ LC column packed with strong cationic exchange (SCX) and RP materials. Peptides are separated first by their electrostatic charge features then by their hydrophobicity followed by online MS<sup>2</sup> analysis. In parallel the evolution of the MS technique played a key role in the achievement of the gel free approach. In fact the introduction of high scan rate mass spectrometers, the realization of routinely data dependent methods to survey the LC separations make possible to manage a large number of samples and to analyze large amount of peptides in a full automated mode, resulting in a definitive high throughput strategy. However the large dynamic range of protein concentration in

biological samples is a major concern in gel free approach. The routine strategy combines a succession of one survey MS scan, the selection of the most intense precursors and the MS<sup>2</sup> fragmentation of the selected ions. When applied to complex peptide mixtures the shotgun approach is limited by the LC co-elution effects. A large number of redundant peptides can be repetitively fragmented leading to the identification of the more abundant proteins. To overcome this problem Aebersold's group introduced an innovative strategy called ICAT (Isotope Coded Affinity Tag) (59). It is based on the consideration that the modern database software leads to unambiguous protein identifications by using accurate peptide mass measure and just short primary sequence passage. Thus to lower the complexity of the peptide mixtures they based the analysis on a reduced number of peptides *per* protein containing cysteine residue. This amino acid was chosen by the evidence that it is present in 92% of *Saccharomyces cerevisiae* proteins and by their hydrolysis with trypsin only 10% of the resulting peptides contain a cysteine residue (60). The global strategy consists in a three dimensional chromatography. To enrich the mixture with cysteine containing peptides, they are labelled with a thiol reactive biotin and purified by streptavidin affinity chromatography before the bidimensional LC-MSMS. On this basis many other labelling strategies are available aimed to enhance both the global protein identification and more specific PTMs. Despite 2DE is still a standard proteomic tool, the shotgun approach is the higher throughput approach for the extensive Proteomic analysis.

#### **-1.2.4 Quantitative Proteomics**

The estimation of protein expression changes is one of the main aims of Proteomics analysis. Therefore, more than an absolute quantification of peptides and proteins it is interesting to evaluate the relative variation of concentration.

The different techniques introduced in the last years follow the parallel development of the analytical tools cited above. Gel-based strategy allows to obtain quantitative data because stained 2DE spot intensity can be directly related to the protein amount. Coomassie or silver stained gel images of different samples are digitized and aligned to be further compared spot by spot. There are many software consenting to carry out the spot alignments and the quantification. With the dual channel visualization (61) two gel images are discharged of their colours leaving respectively only the red and the green channel. By superposing the images the common spots appear orange, which tonality leads to calculate the relative contribution of the original base colour and so to obtain the relative quantitative estimations. However, Coomassie and silver stained spots have short range of chromatic linear variation in function of the concentration. In addition the low reproducibility of the 2DE technique makes it problematic to compare different gels. A solution to this problem was proposed by the Differential Gel Electrophoresis (DIGE) (53). It consists in the differential labelling of up to three protein extracts with MS compatible chromophore molecules. Then the extracts are pooled and analyzed by a unique 2DE gel. In this way the problems related to the migration reproducibility are overcome and the differential visualization of the samples is realized by using a scanner that acquires images at different wavelength. From the resulting three component colours it is possible to obtain quantitative information as discussed above. Also in this case the 2DE resolution limits affect the analysis: in particular the presence of overlapping protein species in the gel spots may invalidate the correct quantitative measure.

The shotgun approach allows the quantitative analysis by using MS. The signal intensity recorded by a mass spectrometer is directly related to the amount of ion species analyzed. However, the amount of ionized analytes detected depends on the ionization efficiency that is specific to each chemical species and that is also related to the instantaneous conditions of the source and the buffers. For these reasons it is possible to compare the MS signal intensity just

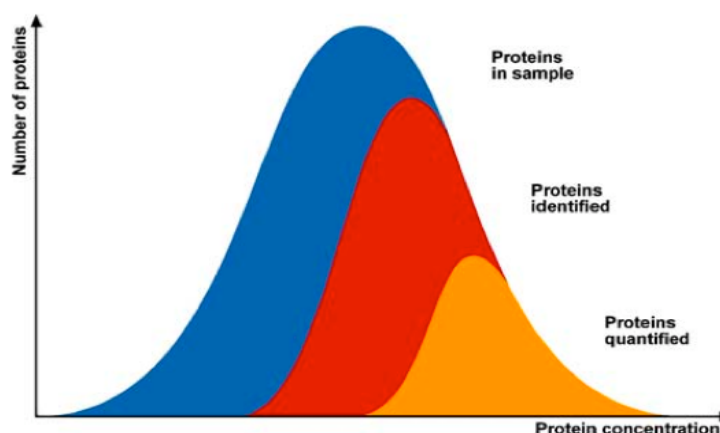


**Fig. 1.5** Estimated Serum Proteomics capacity. More than 50% of the less abundant proteins rests not identified and the quantification is realizable just on a restrict number of more concentrated proteins

between isotope molecules in the same mass spectra. This is realized in different proteomic approaches by labelling the protein or the peptide of different samples with isotope enriched tags. In fact by this modification the differentially labelled species have an identical chemical and chromatographic behaviour but are distinguishable by MS analysis using their isotopic composition. ICAT reagent for example is commercialized in two different isotopic forms with a different distribution of  $^{12}\text{C}/^{13}\text{C}$  atoms that consents the relative quantitative estimation between two samples in MS mode (62). Major impact has had the iTRAQ strategy (63) that by a combination of C, N, and O isotope makes possible a peptide isobaric labelling consenting the MS<sup>2</sup> quantification without any complication of MS spectra. Isotope dilution may be also achieved by enzymatic reaction, *in vitro* introducing two  $^{18}\text{O}$  atoms in the peptide C-Terminus by trypsin hydrolysis in  $\text{H}_2^{18}\text{O}$  (64) or *in vivo* by SILAC (Stable Isotope Labelling with Amino acids in Cell cultures) (65) strategy based on the cell growth in isotope enriched amino acid medium. Although, each method has its strong and weak points in terms of flexibility, efficiency of the labelling, mass difference introduced, SILAC is considered the most powerful strategy. Because the reactions are quantitative and driven into the cell, the samples are pooled by the protein extraction minimizing systematic errors, the  $\Delta M$  are high (9 Da) and no tag is linked to proteins or peptides. The wide application of this strategy is just limited by the relevant cost of the kit. Some alternative methods have been recently proposed to avoid the expensive costs of isotopic enriched reagent. The use of Rare Earth Elements (REE) was demonstrated (66) a valid alternative. In fact the peptides coordinating different REE have identical LC retention times. In addition the metallic centre allows to perform the analysis by Inductively Coupled Plasma (ICP) MS, which sensitivity and signal independence by the chemical structure make it the best tool for the quantitative analysis. Despite the important advances in the chromatographic and MS techniques, the “quantitative identification” of all the proteins in a biological system remains still a challenge, in particular for the bad data quality relative to the less abundant species (Fig.1.5).

### 1.3 Oxidative stress

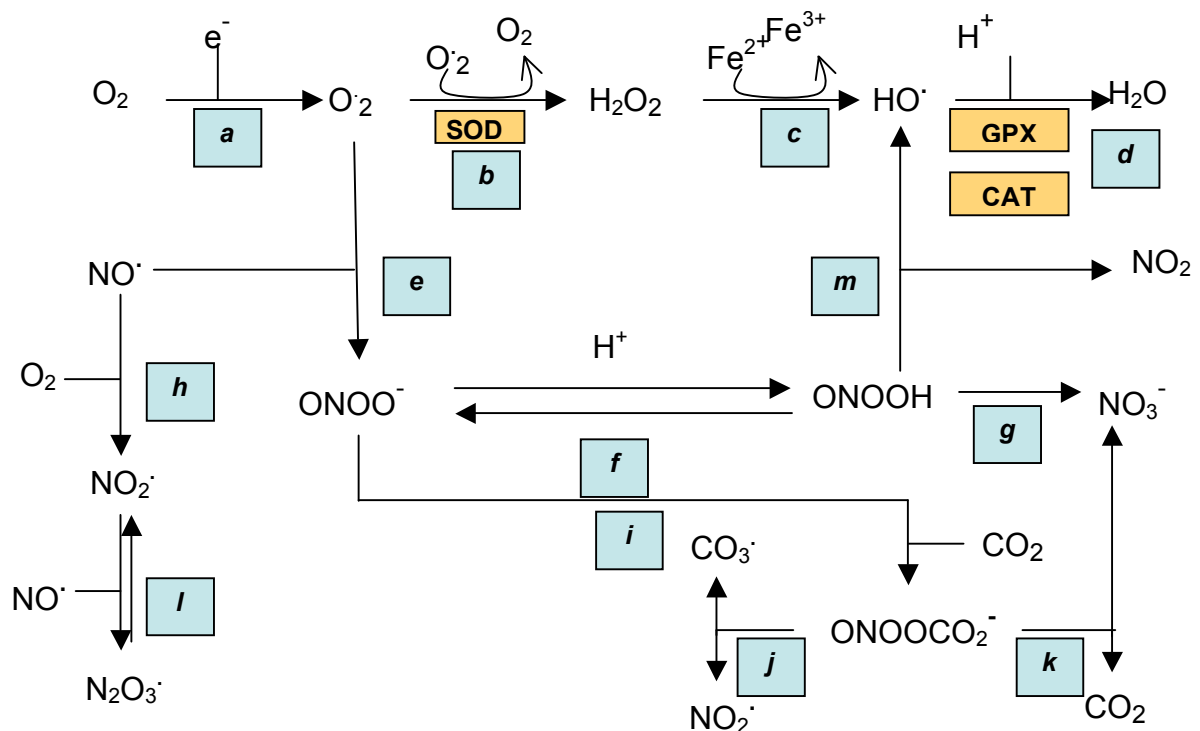
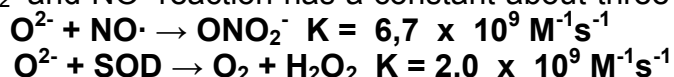


**Fig.1.6** Main *in vivo* ROS/RNS pathway

Disturbances in the intracellular redox equilibrium are often associated with disease (67). Oxidative stress, for instance, is an imbalance of the intracellular redox status that is found in many human diseases, such as rheumatoid arthritis, autoinflammatory and neurodegenerative diseases, and cancer (68-70). However, in most disorders, oxidative/nitrosative stress is a consequence and not a cause of the primary disease process. Oxidative stress is associated with a significant increase in the level of intracellular oxidising species, such as hydrogen peroxide, lipid peroxides, superoxide, peroxy radicals (reactive oxygen species, ROS) (71). Mitochondria are the main cellular producers of ROS (72). Low concentrations of these metabolites *in vivo* have a key role in many physiologic functions as signal transduction, regulation of genetic expression and defence action against pathogen agents (73-75). It was estimated that in normal conditions 1% of the mitochondrial electron flow leads to the formation of the superoxide anion ( $O_2^{\cdot-}$ ) (Fig.1.6, reaction a). Interfering with this mechanism may influence the production of  $O_2^{\cdot-}$  and increase its cellular concentration (76). In these cases  $O_2^{\cdot-}$  is rapidly converted in hydrogen peroxide  $H_2O_2$  and oxygen  $O_2$  by the action of Superoxide Dismutase (SOD) action (Fig.1.6, reaction b), that is the main cellular  $O_2^{\cdot-}$  concentration regulator (77). However,  $H_2O_2$  by reaction with transition metals may give rise to the hydroxyl radical ( $\cdot OH$ ) (Fig.1.6, reaction c) that is a very reactive and toxic species (78). The main  $H_2O_2$  removal mechanism consists in the conversion in water by Catalase and Peroxidase activity (Fig.1.6. reaction d) (76). Reactive nitrogen species (RNS) as the nitric oxide ( $NO\cdot$ ) and the nitrite ( $NO_2\cdot$ ), have many physiological roles (79). However, it must be considered that these species can induce strong modifications in many biological macro-molecules (80). Nitric oxide is an ubiquitous inter-cellular messenger

deputed to the blood flux regulation, of the neural activity and it also has an important role in the un-specific immune defence against the tumours. Nitric oxide is synthesized *in vivo* by the oxidation NADPH-dependent of the L-arginine catalyzed by the Nitric Oxide Synthetase (81). A large part of NO-signaling functions are accomplished by its reaction with Heme prosthetic group or by cysteine S-nitrosilation. However, in contrast with these important functions the NO cytopathic nature is increased when this molecule reacts with ROS producing a class of derivatives that are very reactive toward proteins, lipids, and DNA (82). For instance, when NO· concentration in the tissues makes comparable the rate of the reactions with O<sub>2</sub><sup>-</sup> and SOD, it is produced a relevant amount of peroxynitrite (ONO<sub>2</sub><sup>-</sup>) (Fig1.6, reaction e). In fact, O<sub>2</sub><sup>-</sup> and NO· reaction has a constant about three folds higher the one with SOD (76):



The ONO<sub>2</sub><sup>-</sup> pK<sub>a</sub> is 6.8, so at physiological pH only the 20 % is protonated and converted to peroxynitrous acid (ONO<sub>2</sub>H) (Fig. 1.6, reaction f) (83). The last one is a high oxidative species that rapidly undergoes to homolytic rupture of N-O bond yielding to the nitrogen dioxide (·NO<sub>2</sub>) and the oxyhydril radical (·OH), two species directly involved in the *in vivo* protein nitration (83). The ONO<sub>2</sub><sup>-</sup> toxicity is mainly due to its physiologic stability in the *cis* form (Fig.1.7) that may not isomerize to less reactive species as the nitrate (NO<sub>3</sub><sup>-</sup>) (84) (Fig.1.6, reaction g). High quantity of ·NO<sub>2</sub> may also be generated by the reaction of the H<sub>2</sub>O<sub>2</sub>-dependent Myeloperoxidase in presence of low concentration of nitrite (NO<sub>2</sub><sup>-</sup>) (85) or also by the reaction between NO· e O<sub>2</sub> (Fig.1.6, reaction h). Peroxynitrite reactivity may be increased in presence of carbonic anhydride (CO<sub>2</sub>) (Fig.1.6, reaction i) rapidly producing peroxycarbonate

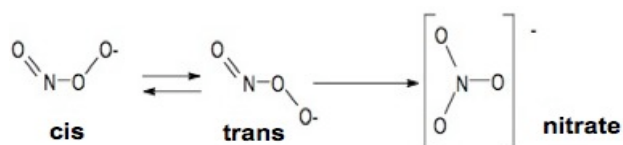


**Fig.1.7** *Cis-Trans peroxynitrite conformation*

(ONO<sub>2</sub>CO<sub>2</sub><sup>-</sup>) that is considered the main cellular nitrating agent (83). However, ONO<sub>2</sub>CO<sub>2</sub><sup>-</sup> has a short life-time (3 ms) and it is rapidly converted (Fig.1.6, reactions j and k). Obviously both the enzymatic and un-enzymatic systems protect the cells and the tissues by the toxic effects of ROS/RNS produced by the metabolism. However, in inflammatory pathologic states the concentration of such species may exceed the cell antioxidant faculties making relevant the effects showed above.

#### **1.4 Oxidative stress related PTMs**

The posttranslational modification of proteins by reactive oxygen and nitrogen species is associated with a large number of pathologies and also with biological aging (68-70). There is no question that some of these PTMs affect the structural and functional integrity of specific proteins. Most of such oxidants will react with several amino acids yielding to multiple products. However, only a few of these reactions will lead to stable and specific products, characteristic for a selected oxidant, which can then be used as a signature for the reaction of one specific individual reactive species with a protein *in vivo*.

### -1.4.1 Protein nitration

Protein nitration consists in the addition of a nitro group ( $\text{NO}_2$ ) moiety to the side chain of the amino acids. The more susceptible substrate is the aromatic amino acids and most of all the tyrosine whose phenolic ring is activated toward such type of aromatic substitution. There are two more probable *in vivo* mechanisms (Fig.1.11) both involving the formation of a tyrosyl radical ( $\cdot\text{Tyr}$ ) (86). The generation of this specie seems to be the steady state of the reaction yielding 3-nitrotyrosine ( $\text{NO}_2\text{Tyr}$ ) and it is mediated by the presence of some ROS ( $\text{CO}_3^{\cdot-}$ ,  $\text{OH}\cdot$ ) mainly formed by  $\text{ONO}_2^-$  reactions (cfr.par.1.3)(86). The tyrosyl radical reacts with  $\text{NO}_2\cdot$  with the reaction rate controlled just by the diffusion of the two reagents ( $K = 3 \times 10^9 \text{ M}^{-1}\text{s}^{-1}$ ) finally generating  $\text{NO}_2\text{Tyr}$ . The dimerization of two  $\cdot\text{Tyr}$  equivalents producing the 3,3'-diytrosine is a competent process. However, this kind of inter-molecular stabilization is limited by diffusional and steric effects, leaving the tyrosine nitration the main process (Fig.1.8). An alternative, less probable, way to  $\text{NO}_2\text{Tyr}$  formation is the reaction between  $\cdot\text{Tyr}$  and  $\text{NO}\cdot$  generating the intermediate 3-nitrosotyrosine ( $\text{NOTyr}$ ) that it is further oxidized to  $\text{NO}_2\text{Tyr}$  by transferring two electron with the formation of the iminoxyl radical (Fig.1.8)(87).

The  $\text{NO}_2$  tyrosine ortho-substitution implies the oxydryl  $\text{pK}_a$  decreasing from 10.1 to 7.2 (88). Therefore, at physiological pH about 50% of  $\text{NO}_2\text{Tyr}$  groups are deprotonated so a negative charge is introduced also in hydrophobic regions inducing protein conformation modification and altering its biological activity. Protein tyrosine nitration exhibits a certain degree of selectivity, and not all tyrosine residues are nitrated. Tyrosine nitration sites are localized within specific functional domains of

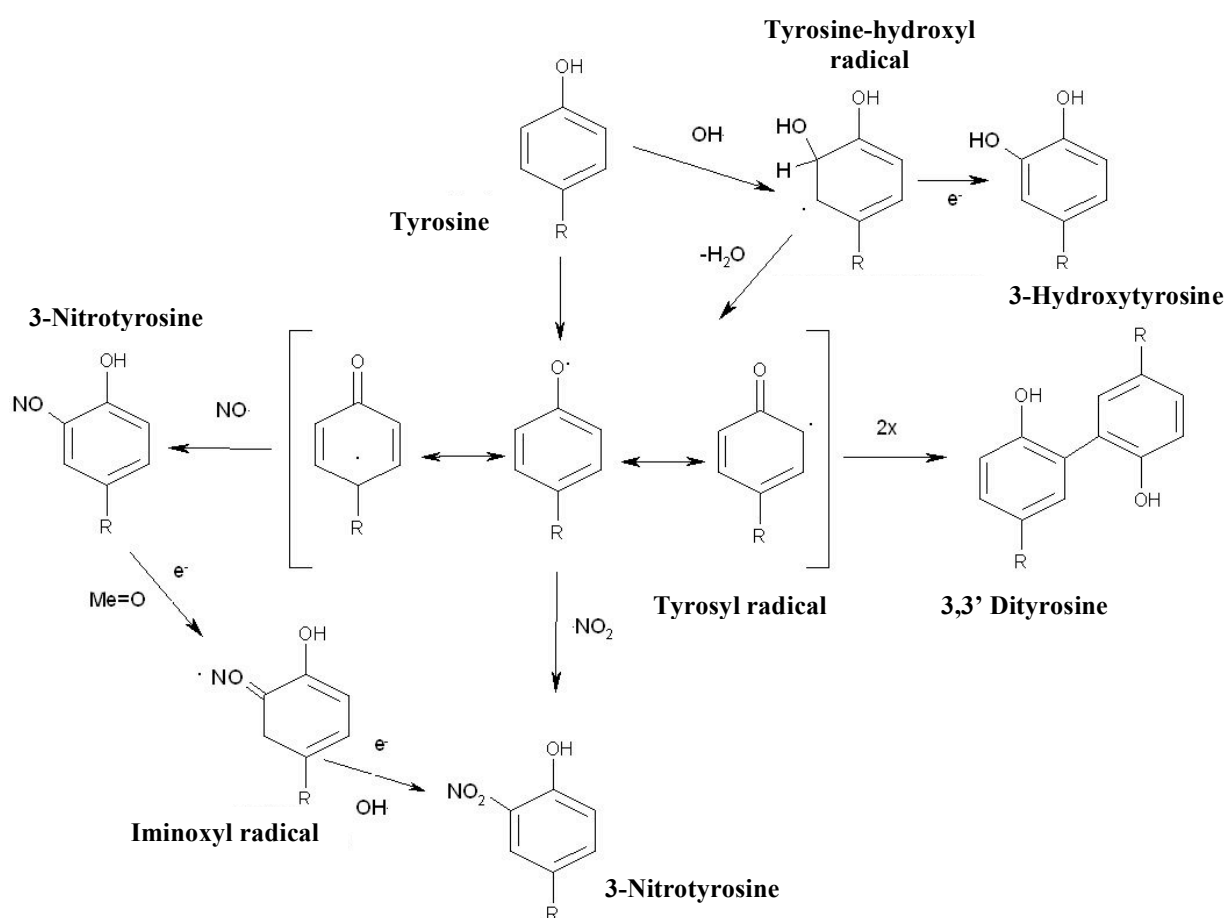


Fig. 1.8 *In vivo* 3-Nitrotyrosine generation main pathway

nitrated proteins (89). The factors that control site- and protein-specificity in tyrosine nitration are the proximity to the site of nitrating agent, the abundance of the protein and the number of tyrosine residues within a single protein (90), finally it may be the amino acid sequence or a specific nitrating environment (91). Tyrosine nitration occurs at inflammatory sites within specific cell types (92), suggesting that the proximity to the sites of nitrating agent formation is critical in inducing site- and protein-specific tyrosine nitration. Protein tyrosine nitration usually occurs near acidic residues in loop regions (89, 90) in areas free of steric hindrances. The location of tyrosine residues in favourable environments for nitration within the secondary and tertiary protein structure may also influence site-specific nitration. Tyrosine nitration is one of the not-abundant PTMs related to ROS/RNS that is stable *in vivo* and its generation it is increased directly with the incurring of inflammatory events associated to the iper-production of nitric oxide (92). For these reasons NO<sub>2</sub>Tyr is currently considered the best biomarker for the identification and quantification of stress oxidative event related to the RNS (93).

### -1.4.2 Thiol oxydation

The redox chemistry of thiol in cysteine involved typically its anionic state (94). The features of the protein microenvironment controls thiol reactivity and the stability of the resulting modifications (95). For many proteins the first product of cysteine oxidation by ROS is the cysteine sulfenic acid (R-SOH) (Fig. 1.9). It undergoes a rapid condensation either with another protein thiol by an intramolecular or intermolecular interaction or with a small molecule thiol-like as glutathione or cysteine

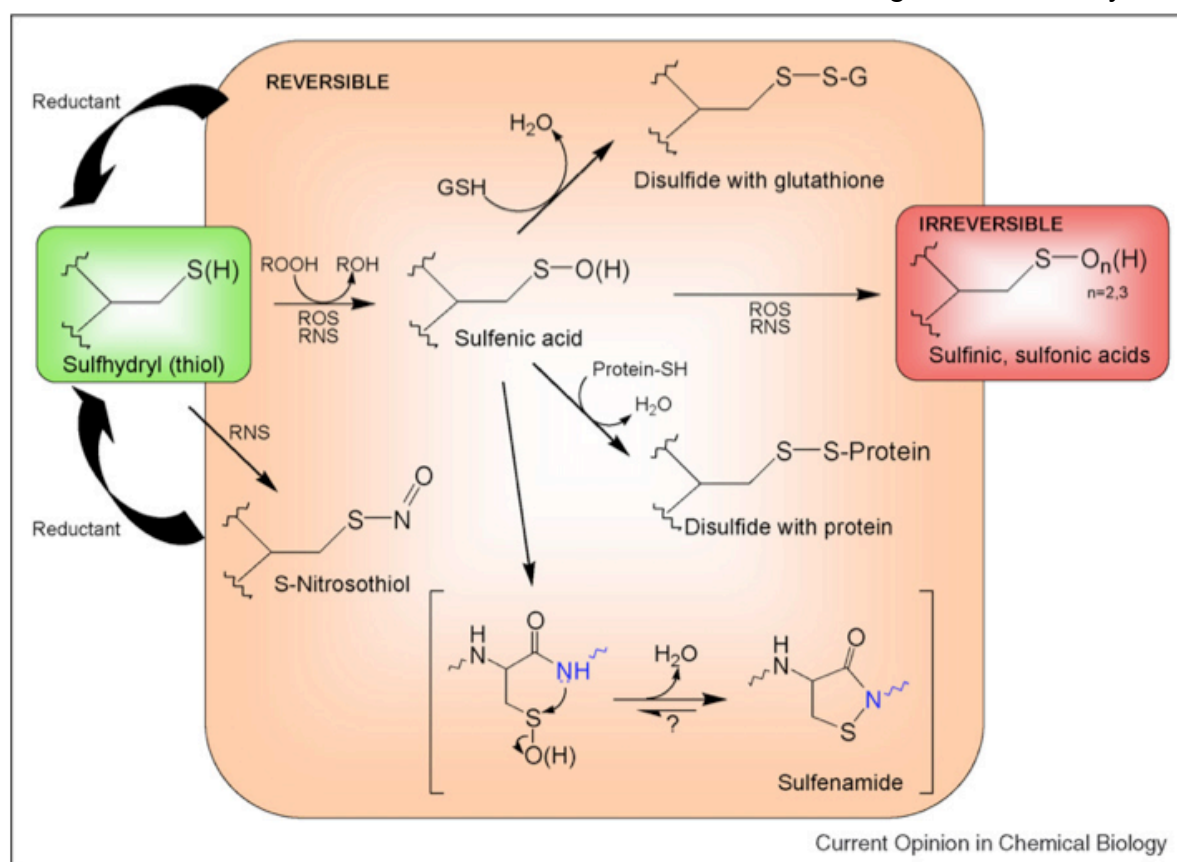


Fig.1.9 Stress oxidative related thiol PTMs

to form a disulfide bond. Then, thiol-based reductants may also return these species to the fully reduced thiol state (Fig. 1.9). Disulfide bonds can stabilize extracellular proteins, protect against irreversible inactivation, stabilize associations within protein complexes, modify structures to create, destroy or modulate functional sites, and also regulate enzymatic or transcriptional activity of proteins. Under conditions where ROS/RNS are generated, in addition to the typical ROS-generated products, reversible S-nitrosation may also play an important signaling role (96). In certain cases, the initial sulfenic acid may be stabilized by the protein microenvironment. However, in this case the protein sulfenic acid is vulnerable to the hyper-oxidation to the irreversible sulfinic or sulfonic acids (Fig. 1.9). These further modifications could, in spite of their typically irreversible status, also provide a signaling role analogous to a 'fire alarm' regarding cellular redox status (97). Sulfenamide (sulfenyl-amide) has recently been recognized as another stabilized oxidation product generated by the condensation of the sulfenic acid with a neighbouring backbone amide nitrogen (Fig. 1.9). The resulting 5-membered ring structure appears to represent a form of oxidized cysteine resistant to the hyper-oxidation (98). A functional role for the generation of the sulfenamide was related to the changes in structure imparted to the tyrosine phosphatases active site, changes that may enhance the access by reductants and/or modulate interactions with other domains (99-100). Several studies have shown that cysteine oxidation is involved in several neurodegenerative diseases. Changes in the thiol/disulphide status were evaluated in ischemia events (101). Parkinson's disease protective properties of protein DJ-1 were demonstrated to be carried out by the correct oxidation of cysteine 106 to sulfinic acid (102). Recently, S-glutathionated proteins were found related to Alzheimer's disease (103) and the thiol-protease oxidation was implicated in Alzheimer's disease of the hippocampus and cerebellum (104). As far as the first aspect is concerned, oxidation of cysteine within proteins may result in various changes of the protein's structure and function, not all of which are detrimental. There are many examples of oxidative activation as well as inactivation, some of which are based on modifications to active-site residues, while others are the result of conformational changes. For instance, activation of a protein may be the result of the oxidative removal of an undesired thiolate ligand, as observed for matrix metallo-proteinases (105-106). From a structural point of view, thiol oxidation may lead to covalent disulfide bridges between cysteine residues or more highly oxidised sulfur species with distinct negative charges and steric requirements. These changes may be introduced by 'random' thiol oxidation during oxidative stress, or as part of a controlled enzymatic process involving thiol oxidases or thiol/disulfide oxido-reductases, (107). Such structural changes induced by oxidation are particularly beneficial in the context of the folding, oligomerisation and associated redox activation of proteins able to counteract oxidative stress.

It is increasingly clear that a major component of the ROS-linked modulation of cell signaling pathways is the dynamic regulation of protein function by thiol modification. Redox signaling is known to affect gene transcription, at least four well-known transcription factors are known to be modulated by NO through S-nitrosylation (108-109). For example, irreversible oxidation of certain cysteine residues to sulfinic or sulfonic acid might inhibit enzyme activity or serve as a signal for protein degradation. According to the 'N-end rule' pathway for protein degradation in mammalian cells, oxidation of N-terminal cysteine residues in certain proteins to a sulfinic or sulfonic acid is required for arginylation and subsequent degradation (110).

## **1.6 References**

1. EPA Interim Genomics Policy
2. International Human Genome Sequencing Consortium, *Nature* **2004**, 431 (7011): 931-945.
3. Anderson N.L., Anderson N.G., *Electrophoresis*. **1998**, 19(11): 1853-1861
4. Zhou M., Veenstra T.D., *Proteomics* **2007**, 7: 2688–2697.
5. Josic D., Clifton J. G., *Proteomics* **2007**, 7: 3010–3029
6. Le Naour F., André M., Greco C., Billard M., Sordat B., Emile J.F., Lanza F., Boucheix C., Rubinstein E., *Mol Cell Proteomics*. **2006**, 5(5): 845-57
7. Mei J., Kolbin D., Kao H.T., Porton B., *Schizophrenia Res.* **2006**, 84 204–213.
8. Cox J., Mann M., *Cell* **2007**, 130: 395–398.
9. Incamps A., Hély-Joly F., Chagvardieff P., Rambourg J.C., Dedieu A., Linares E., Quéméneur E., *Biotechnol Bioeng.* **2005**, 91(4): 447-459
10. Josic D., Brown M.K., Huang F., Lim Y.P., Rucevic M., Clifton J.G., Hixson D.C., *Proteomics* **2006**, 6(9): 2874-85
11. Gupta P., Lee K. H., *Trends Biotechnol.* **2007**, 25: 324–330.
12. AlFageeh M.B., Marchant R.J., Carden M.J., Smales C.M., *Biotech. Bioeng.* **2005**, 93: 829–835.
13. Li Y., Powell S., Brunette E., Lebkowski J., Mandalam R., *Biotechnol. Bioeng.* **2005**, 91: 688–698.
14. Wang W., Sun J., Hartlep M., Deckwer W.D., Zeng A.P., *Biotechnol. Bioeng.* **2003**, 8: 525–536.
15. Pieiro C., Barros-Velázquez J., Velázquez J., Figueras A., Gallardo J.M., *J. Proteome Res.* **2003**, 2: 127–135
16. Kern A., Tilley E., Hunter I.S., Legisa M., Glieder A., *J. Biotechnol.* **2007**, 129: 6–29.
17. Mirza S.P., Olivier M., *Physiol Genomics*. **2008**, 33(1):3-11
18. Köcher T., Superti-Furga G., *Nat. Methods*. **2007**, 4(10):807-815.
19. Ratushny V., Golemis E., *Biotechniques* **2008**, 44(5): 655-662
20. Issaq H.J., Conrads T.P., Janini G.M. and Veenstra T.D., *Electrophoresis* **2002**, 30(4844(5):655-662
21. Shigenaga M.K., Lee H.H., Blount B.C., Christen S., Shigeno E.T., Yip H., Ames B.N., *Proc. Natl. Acad. Sci. U S A* **1997**, 94(7):3211-6
22. Jensen O.N., *Curr. Opin. Chem. Biol.* **2004**, 8: 33-41
23. Fenn J. B., Mann M., Meng C. K., Wong S. F., and Whitehouse C. M., *Science* **1989**, 246: 64–71.
24. Karas M. and Hillenkamp F., *Anal. Chem.* **1988**, 60: 2299–2301.
25. Emmett M.R., Caprioli R.M., *J. Am. Soc. Mass Spectrom* **1994**, 5: 605–613
26. Cornish T.J., Cotter R.J., *Rapid Commun. Mass Spectrom.* **1993**, 7(11):1037-40
27. Pedder R.E., *49<sup>th</sup> ASMS Conference on Mass Spectrometry and Allied Topics*, May 28 - June 1, **2001**.
28. Payne A.H., Glish G.L., *Methods Enzymol.* **2005**, 402:109-48
29. Nappia M., Weila C., Clevener C. D., Horna L. A., Wollnikb H. and Cooksa R. G. *Int J Mass Spectrom Ion Process.* **1997**, 161: 77-85
30. Marshall A.G., Hendrickson C.L., Jackson G.S., *Mass Spectrom Rev.* **1998** 17(1):1-35
31. Domon B., Aebersold R., *Science* **2006**, 312: 212
32. Yost R. A. and Boyd R. K., *Methods Enzymol.* **1990**, 193: 154–200.

33. Morris H. R., Paxton T., Dell A., Langhorne J., Berg M., Bordoli R. S., Hoyes J. and Bateman R. H., *Rapid Commun. Mass Spectrom.* **1996**, 10: 889–896.
34. Medzihradzky K.F., Campbell J.M., Baldwin M.A., Falick A.M., Juhasz P., Vestal M.L., Burlingame A.L., *Anal Chem.* **2000**, 72(3): 552-558
35. Vachet R. W., Winders A. D. and Glish G. L., *Anal. Chem.* **1996**, 68: 522–526
36. McLuckey S. A., Goeringer D. E. and Glish, G. L., *Anal. Chem.* **1992**, 64: 1455–1460
37. Shukla A. K. and Futrell J. H., *J. Mass Spectrom.* **2000**, 35: 1069–1090
38. Biemann K. and Papayannopoulos I. A., *Acc. Chem. Res.* **1994**, 27: 370–378
39. Wells J.M., McLuckey S.A., *Methods Enzymol.* **2005**, 402: 148-185
40. Wysocki V.H., Tsaprailis G., Smith L.L., Breci L.A., *J. Mass Spectrom.* **2000**, 35: 1399–1406
41. Ferro M., Tardif M., Reguer E., Cahuzac R., Bruley C., Verinat T., Nugues E., Vigouroux M., Vandembrouck Y., Garin J., Viari A., *J. Proteome Res.* **2008**, 7(5):1873-83.
42. Waridel P., Frank A., Thomas H., Surendranath V., Sunyaev S., Pevzner P., Shevchenko A., *Proteomics* **2007**, 7(14):2318-23 Hirose M, Hoshida M,
43. Ishikawa M., Toya T., *Comput Appl Biosci.* **1993**, 9(2):161-167
44. Xu H., Yang L., Freitas M.A. *BMC Bioinformatics* **2008**, 9 (1):347
45. O'Farrell P.H., *J. Biol. Chem.* **1975**, 250:4007–4021
46. Klose J., Kobalz U., *Electrophoresis* **1995**, 16:1034–1059
47. Pappin D.J., Hojrup P., Bleasby A.J., *Curr. Biol.* **1993**, 3(6): 327–332.
48. Henzel W.J., Billeci T.M., Stults J.T. Wong S.C., Grimley C., Watanabe C., *Proc. Natl. Acad. Sci. U.S.A* **1993**, 90(11): 5011–5015.
49. Mann M., Hojrup P., Roepstorff P., *Biol. Mass Spectrom.* **1993**, 22(6): 338–45.
50. Wilm M., Shevchenko A., Houthaeve T. Breit S., Schweigerer L., Fotsis T. and Mann M., *Nature* **1996**, 379: 466 – 469
51. Wilm M. and Mann M., *Anal. Chem.* **1996**, 68: 1– 8
52. Valdes I., Pitarch A., Gil C., Bermúdez A., Llorente M., Nombela C., Méndez E., *J.Mass Spectrom.* **2000**, 35(6):672-82
53. Tonge R., Shaw J., Middleton B., Rowlinson R., Rayner S., Young J., Pognan F., Hawkins E., Currie I., Davison M. *Proteomics*, **2001**, 1(3):377-96
54. Martin K., Steinberg T.H., Goodman T., Schulenberg B., Kilgore J.A., Gee K.R., Beechem J.M., Patton W.F., *Comb. Chem. High Throughput Screen.* **2003**, 6(4):331-9
55. Steinberg T.H., Pretty On Top K., Berggren K.N., Kemper C., Jones L., Diwu Z, Haugland R.P., Patton W.F., *Proteomics* **2001**, 1(7):841-55
56. Ravalason H., Jan G., Mollé D., Pasco M., Coutinho P.M., Lapierre C., Pollet B., Bertaud F., Petit-Conil M., Grisel S., Sigoillot J.C., Asther M., Herpoël-Gimbert I., *Appl Microbiol Biotechnol.* **2008**, 80(4): 719-33.
57. Pocaly M., Lagarde V., Etienne G., Dupouy M., Lapailierie D., Claverol S., Vilain S., Bonneu M., Turcq B., Mahon F.X., Pasquet J.M., *Proteomics* **2008**, 8(12):2394-406
58. Wolters D.A., Washburn M.P., Yates J.R., *Anal Chem.* **2001**, 73(23):5683-90
59. Gygi S. P., Rist B., Gerber S. A., Turecek F., Gelb M. H. and Aebersold, R. *Nat. Biotechnol.* **1999**, 17: 994–999
60. Fenyo D., Qin J. and Chait B. T., *Electrophoresis* **1998**, 19: 998–1005
61. Bernhardt J., Büttner K., Scharf C., Hecker M., *Electrophoresis* **1999**, 20(11): 2225-2240

62. Yi E.C., Li X.J., Cooke K., Lee H., Raught B., Page A., Aneliunas V., Hieter P., Goodlett D.R., Aebersold R., *Proteomics* **2005**, 5(2):380-387
63. Ross P.L., Huang Y.N., Marchese J.N., Williamson B., Parker K., Hattan S., Khainovski N., Pillai S., Dey S., Daniels S., Purkayastha S., Juhasz P., Martin S., Bartlett-Jones M., He F., Jacobson A., Pappin D.J., *Mol. Cell. Proteomics* **2004**, 3(12):1154-1169
64. Stewart I.I., Thomson T., Figeys D., *Rapid Commun. Mass Spectrom.* **2001**;15(24):2456-2465
65. Ong S.E., Blagoev B., Kratchmarova I., Kristensen D.B., Steen H., Pandey A. and Mann M., *Mol. Cell. Proteomics* **2002** 1, 376-386.
66. Ahrends R., Pieper S., Kühn A., Weisshoff H., Hamester M., Lindemann T., Scheler C., Lehmann K., Taubner K., Linscheid M.W., *Mol. Cell. Proteomics* **2007**, 6(11):1907-1916
67. Sies H., *Exp. Physiol.* **1997**, 82(2):291-5.
68. McMahon M., Grossman J., FitzGerald J., Dahlin-Lee E., Wallace D.J., Thong B.Y., Badsha H., Kalunian K., Charles C., Navab M., Fogelman A.M., Hahn B.H., *Arthritis Rheum.* **2006**, 54(8):2541-9
69. Emerit J., Edeas M., Bricaire F., *Biomed. Pharmacother.* **2004**, 58(1):39-46
70. Matés J.M., Segura J.A., Alonso F.J., Márquez J., *Arch Toxicol.* **2008**, 82(5): 273-299.
71. Bergamini C.M., Gambetti S., Dondi A., Cervellati C., *Curr. Pharm. Des.* **2004**, 10(14):1611-26
72. Ishii N., *Cornea* **2007**, 26(9 Suppl 1):S3-9
73. Lee M.Y., Griendling K.K., *Antioxid. Redox Signal.* **2008**, 10(6):1045-59
74. Calabrese V., Guagliano E., Sapienza M., Mancuso C., Butterfield D.A., Stella A.M., *Ital. J. Biochem.* **2006** 55(3-4):263-282
75. Fialkow L., Wang Y., Downey G.P., *Free Radic Biol. Med.* **2007**, 42(2):153-64.
76. Dalle Donne I., Scaloni A., Giustarini D., Cavarra E., Tell G., Lungarella G., Colombo R., Rossi R., Milzani A., *Mass Spectrom. Rev.* **2005**, 24(1):55-99
77. Bannister J.V., Bannister W.H., Rotilio G., *CRC Crit. Rev. Biochem.* **1987**, 22(2):111-80
78. Afanas'ev I.B., *Mol. Biotechnol.* **2007**, 37(1): 2-4
79. Lundberg J.O., Weitzberg E., Gladwin M.T., *Nat. Rev. Drug Discov.* **2008** 7(2):156-67
80. Murad F., *Biosci. Rep.* **2004**, 24(4-5):452-74
81. Schopfer F.J., Baker P.R.S. and Freeman B.A, *Trends Biochem. Sci.* **2003**, 28(12):646-54
82. Hughes M.N., *Methods Enzymol.* **2008**; 436:3-19
83. Goldstein S, Merényi G., *Methods Enzymol.* **2008**, 436:49-61
84. Tsai, J.H.M., Hamilton T.P., Harrison J.G., Jablosky M., van der Woerd M., Martin J.C. and Beckman J.S., *J. Am.Chem.Soc.* **1994**,116:4115-4116
85. Eiserich J.P., Hristova M., Cross C.E., Jones A.D., Freeman B.A., Halliwell B., van der Vliet A., *Nature* **1998**, 39,1393–1397
86. Radi R., *Proc. Natl. Acad. Sci. U S A* **2004**, 101(12):4003-4008.
87. Pfeiffer S., Schmidt K., Mayer B., *J. Biol. Chem.* **2000**, 275(9):6346-52
88. De Caro J.D., Behnke W.D., Bonicel J.J., Desnuelle P.A., Roverly M., *Biochim. Biophys Acta.* **1983**, 3:253-62
89. Ischiropoulos H., Zhu L., Chen J., Tsai, M. Martin, J.C., Smith C.D. and Beckman J.S., *Arch. Biochem. Biophys.* **1992**, 298:431-437.

90. Souza J. M., Daikhin E., Yudkoff M., Raman C.S. and Ischiropoulos H., *Arch. Biochem. Biophys.* **1999**, 371,169-178.
91. Sacksteder C.A., Qian, W.J., Knyushko, T.V., Wang H., Chin, M.H., Lacan G., Melega W.P., Camp D.G., Smith R.D., Smith D.J., Squier T.C. and Bigelow, D. J., *Biochemistry* **2006**, 45:8009-8022.
92. Greenacre S.A. and Ischiropoulos H., *Free. Radic. Res.* **2001**, 34, 541-581.
93. Ohshima H., Friesen M., Brouet I., Bartsch H., *Food Chem. Toxicol.* **1990** 28(9): 647-52
94. Poole L.B., Nelson K.J., *Curr. Opin. Chem. Biol.* **2008**, (1):18-24.
95. Salsbury F.R, Knutson S.T., Poole L.B., Fetrow J.S., *Protein .Sci.* **2008**, 17: 299-312.
96. Biswas S., Chida A.S., Rahman I., *Biochem. Pharmacol.* **2006**, 71:551-564
97. Phalen T.J., Weirather K., Deming P.B., Anathy V., Howe A.K., van der Vliet A., Jonnsson T.J., Poole L.B., Heintz N.H., *J. Cell Biol.* **2006**, 175:779-789
98. Salmeen A., Barford D., *Antioxid. Redox Signal.* **2005**, 7:560-577.
99. Yang J., Groen A., Lemeer S., Jans A., Slijper M., Roe S.M., den Hertog J., Barford D., *Biochemistry* **2007**, 46:709-719.
100. Tonks N.K., *Nat. Rev. Mol. Cell Biol.* **2006**, 7:833-846.
101. Dafre A.S., Artenib N.S., Siqueirab I.R. and Netto C.A., *Neuroscience Letters* **2003**, 345 (1): 65-68
102. Canet-Avilés R.M., Wilson M.A., Miller D.W., Ahmad R., McLendon C., Bandyopadhyay S., Baptista M.J., Ringe D., Petsko G.A., Cookson M.R. *Proc. Natl. Acad. Sci. U S A* **2004**, 101(24):9103-9108.
103. Marcum J.L., Mathenia J.K., Chan R., Guttmann R.P., *Biochem. Biophys. Res. Commun.* **2005**, 334(2):342-8
104. Newman S.F., Sultana R., Perluigi M., Coccia R., Cai J., Pierce W.M., Klein J.B., Turner D.M., Butterfield D.A., *J. Neurosci. Res.* **2007**, 85(7):1506-14
105. Okamoto T., Akaike, T., Sawa T., Miyamoto Y., van der Vliet A. and Maeda H., *J. Biol. Chem.* **2001**, 276: 29596–29602.
106. Zhang H.J., Zhao W., Venkataraman S., Robbins M.E., Buettner G.R., Kregel K.C. and Oberley, L.W., *J. Biol. Chem.* **2002** , 277: 20919–20926.
107. Gruber C.W., Cemazar M., Heras B., Martin J.L. and Craik D.J., *Trends Biochem. Sci.* **2006**, 31: 455–464.
108. Li F., Sonveaux P., Rabbani Z.N., Liu S., Yan B., Huang Q., Vujaskovic Z., Dewhirst M.W., Li C.Y., *Mol. Cell* **2007**, 26: 63–74.
109. Riccio A., Alvania R.S., Lonze B.E., Ramanan N., Kim T., Huang Y., Dawson T.M., Snyder S.H., Ginty D.D., *Mol. Cell* **2006**, 21: 283–294.
110. Hu R.G., Sheng J., Qi X., Xu Z. Takahashi, T.T. and Varshavsky A. *Nature* **2005**, 437: 981–986.

## **2. BIDIMENSIONAL TANDEM MASS SPECTROMETRY FOR SELECTIVE IDENTIFICATION OF NITRATION SITES IN PROTEIN**

### **2.1 Introduction**

In this chapter is reported the development of a new high throughput method to detect nitration sites in proteins. The biological relevance of this PTMs identification (see section 1.4.1) makes extremely important the study of new tools that can enhance the Proteomics analytical efficiency toward this subject.

The strategy proposed may be classified as belonging to a class of general derivatization methods defined, by Amoresano et al. (1), with the acronym RIGhT (Reporter Ion Generating Tag). This approach is based on the labelling of the target residues with reagents capable to generate reporter ions in MS<sup>2</sup>/MS<sup>3</sup> experiments. The detection of the reporter is a very restricted selectivity criterion that is used to reduce the analytical complexity to a few numbers of species, resulting in an improved duty cycle and enhanced dynamic range achievable by the MS analysis. In operative terms, the use of a high selective MS replaces the off-line chromatographic steps (affinity and/or bidimensional chromatography) aimed at isolating the labelled peptides with the advantage of avoiding the time consuming analysis and the tremendous decreasing in sensitivity. For these features, considering that the analysis of nitrated protein has followed the history of Proteomics evolution, we can define the strategy presented in this chapter as a *third generation* of the Proteomics analysis.

#### **2.1.1 Proteomic identification of nitrated proteins: the state of the art**

Proteomics approach is largely applied to the identification of nitrated proteins in tissues (2-6). After that in 1996 Ye et al. set up the first immuno-detection method (7), many works were realized using the visualization of nitrated proteins by Western blotting, followed by the MS analysis of the *in situ* digested proteins, positive to the immuno-assay. However, by this approach un-equivocally localization of nitration sites may be achieved just obtaining the 3-nitrotyrosine-containing peptide sequences by MS<sup>2</sup> data. For 2DE fractionated proteins, the identification based on the fragmentation spectra was presented in only a limited number of works (8-9). This lack of data may be caused by the classical limitations of the 2DE technique (see 1.3.1), in particular the low quantity of protein extract analysable by iso-electric focusing (IEF), considering the sub-stoichiometric characteristic of such PTMs. In addition of the common 2DE limitations, also the MS and MS<sup>2</sup> analysis of nitrated peptides suffer from some technical hindrances that have to be considered. In fact, MALDI-TOF analysis, that is the main technology of the PMF strategy of the *first generation Proteomics*, was demonstrated to be useless in low-abundance nitrated proteins analysis. This because the photochemical decomposition of the 3-nitrotyrosine (NO<sub>2</sub>Tyr), induced by MALDI UV laser, causes the loss of one or two oxygen atoms from the nitro group and also the formation of 3-aminotyrosine (10). The post-source decomposition splits in more satellite peaks the MS signal, decreasing dramatically the analysis sensitivity. The nitration of tyrosine residues may also compromise an efficient MS<sup>2</sup> fragmentation. It was demonstrated that the neutral amino acid losses from the N- and C- termini (11) depends on the number and nature of basic amino acid residues in a given peptide ion. Moreover the rearrangement of doubly or higher charged peptide ions can lead to the neutral loss

of internal amino acids (12). These processes may give rise to complex MS<sup>2</sup> spectra with peaks that are not automatically assigned by common MS software, thus the manual interpretation of the MS<sup>2</sup> spectra may be necessary in order to obtain unambiguous assignment of peptide sequences. This problem become real when sub-stoichiometric modified peptides do not generate the traditionally expected  $b_n$  and  $y_n$  fragments in yields too low for satisfactory assignment. This situation was observed during the MS<sup>2</sup> analysis of 3-nitrotyrosine/Cu<sup>2+</sup> complexes (13). In fact, collision induced dissociation leads to the neutral loss of H<sub>2</sub>CO<sub>3</sub>. A mechanism was proposed by which CID leads the intra-molecular reduction to amino group of the aromatic nitro group with oxygen transfer to the carboxylate group.

The development of gel free methods is more appropriate for the identification of

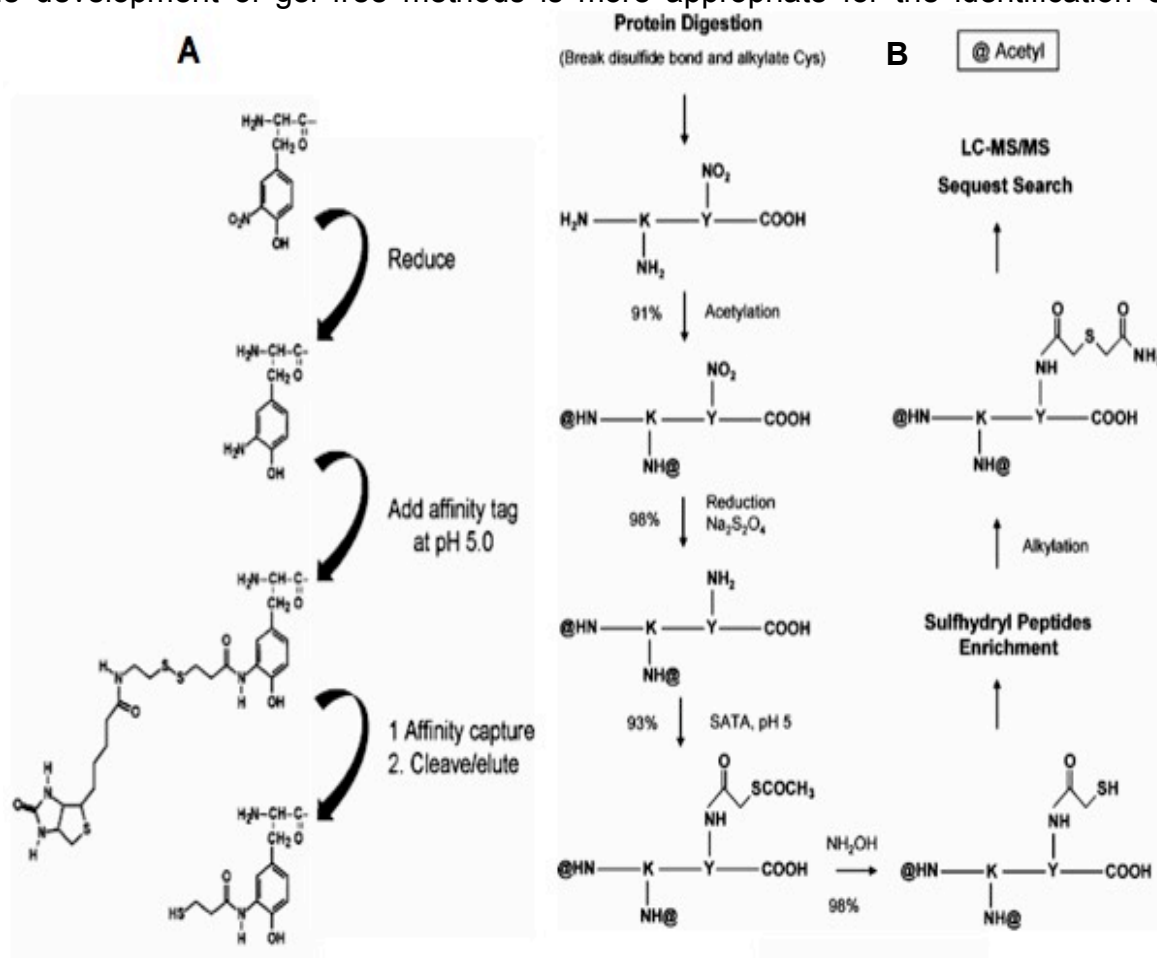


**Fig.2.1** Panel A shows the procedure suggested by Nikov et al. consisting in the conversion of 3-nitrotyrosine residue to its amine and the selective functionalization with a disulfide containing biotin tag using the peculiar 3-aminotyrosine 4.7 pKa. Panel B shows the procedure suggested by Zhang et al. also consisting in the 3-nitrotyrosine reduction to amine followed by the selective acylation with a thiol containing tag always using the peculiar 3-aminotyrosine 4.7 pKa

nitrated protein because it allows working with much higher amounts of nitrated proteins or peptides. By using multidimensional chromatography (SCX-RP)-MS<sup>2</sup> approach the rat neuroproteome was explored, identifying 31 sites of nitration in 29 different proteins (14). However, although this approach allows to overcome many limits of previously reported gel-based methods, the detection of lower abundant nitrated proteins remains problematic. For proteome analysis of these PTMs, a specific enrichment step before the MS analysis is highly advised. The unique method to directly enrich nitro-protein uses anti-nitrotyrosine based affinity

chromatography. However this strategy does not find good agreement, considering the quantity of papers published (15-16). This is probably due to the nitrotyrosine antibody lack of specificity and the difficulty related to the manipulation of proteins instead of peptides solutions. There are no effective enrichment methods for nitrated peptides, probably because of the poor chemical reactivity of the nitro group. However, different strategies were introduced based on the conversion of NO<sub>2</sub>Tyr nitro group in amine group, which is chemically reactive and hence can be used as a chemical handle to employ tagging groups. Nikov et al. reported a novel method for the identification of peptides containing nitrotyrosine residues in complex mixture (17). Before the reduction of nitrotyrosine free thiols were blocked with iodoacetamide. Then cleavable biotin tags were selectively anchored to the aminotyrosines, and the protein sample was digested. The biotinylated peptides were purified on a solid support, which presented streptavidin. Further, the elution with DTT consents to recover the nitrated peptides from the solid support and to directly analyze them by MALDI-TOF mass spectrometry. Zhang et al. introduced an improved enrichment strategy by hooking thiol group to nitropeptides (18). In practice, they reduced nitrotyrosine to aminotyrosine, which was derivatized with N-succinimidyl S-acetylthioacetate (SATA). Then by treatment with hydroxylamine the thio-ester group is converted to free thiol and this makes possible the purification using thiopropyl-sepharose beads. The enriched peptides were released and analyzed by LC-MS<sup>2</sup>, showing 6-10 times more nitrotyrosine-containing peptides than the global analysis of original samples. The nitro group reduction to 3-aminotyrosine was demonstrated to be useful also to improve MS analysis realizing LC-MS<sup>2</sup> method based on the Precursor Ion Scan of the 3-amino-tyrosine immonium ion (m/z 181.06) (19).

The state of the art traced in this paragraph shows the main problems related to the protein nitration analysis and how the technological improvements allow to enhance the performance of Proteomic approach. It emerges that, because of the high variability of matrices analyzed, it is not possible to define a general strategy allowing to detect nitrated proteins in any kind of biological samples. However, the availability of many tools, using different technologies and analytes physical-chemical properties, surely enhances the success probability of the research. Making a comparison between the strategies discussed above, it appears that the major problem is related to the sub-stoichiometric characteristic of the modification. In fact, the major improvements are achieved by the passage from gel-based techniques to nitro-peptides enrichment strategies using antibody or chemical derivatizations. However, it must be considered that many chromatographic steps are material and time consuming. Moreover, in the case of immuno-enrichment procedures, only SDS PAGE resolves the co-elution of the anti-body with the enriched protein mixture. Thus to avoid this problem, it may be interesting to develop a new strategy, using the chemical labelling features, not based on the chromatographic properties of modified peptides.

By a general view of the recently proposed Proteomics methods, it appears that scientific community tends to underestimate the separation features of the mass spectrometers, relegating them just to instruments for the peptides sequencing. In fact, just in a reduced number of works it is underlined that a mass spectrometer has discriminatory faculties that may be addressed to avoid the multi-chromatographic techniques (20-21). In addition atto-molar sensitivity of modern mass spectrometers is compatible with *in vivo* concentration of sub-stoichiometric PTMs, avoiding the enriching procedures.

### 2.1.2 The hybrid Triple Quadrupole/ Linear Ion Trap mass spectrometer

Triple-quadrupole (QqQ) analyzer consists in two resolving quadrupole mass filters (Q1 and Q3) separated by another one that is a collision cell (Q2). Instruments equipped with this technology are called ‘*beam-type*’ mass spectrometers because they are usually used with a continuous ion beam source. The beam-type feature is both the strength and the weakness of these instruments. In fact, when the mass filters are in scan mode, most of the ions are rejected, thus resulting in poor sample usage and low sensitivity (22). However, when the mass filters are not scanning, but they are set to transmit a single pre-selected ion, the efficiency and the sensitivity are very high. This characteristic, coupled with a high dynamic range, are the reasons that make the triple quadrupole system one of the most powerful tools for the analysis of complex mixtures (23). Moreover, QqQ optics also allow to perform very selective analysis such as precursor ion (PIS) and neutral loss (NL) scans that are not realizable with other mass spectrometers (24) (Fig.2.2). These specific scan modes lead to improve the detection of peptides with posttranslational modifications. For example in PIS mode, the Q3 is set to transmit a fragment ion, produced into the Q2, that is specific to a class of molecules while the first mass filter is scanning. By this approach it is possible to reduce the analysis only to the species of interest. A Proteomic application of this technique is achieved by tuning Q3 to the fragment  $m/z$  -79 from phosphorylated peptides  $MS^2$  loss of  $PO^{3-}$ . This method has been

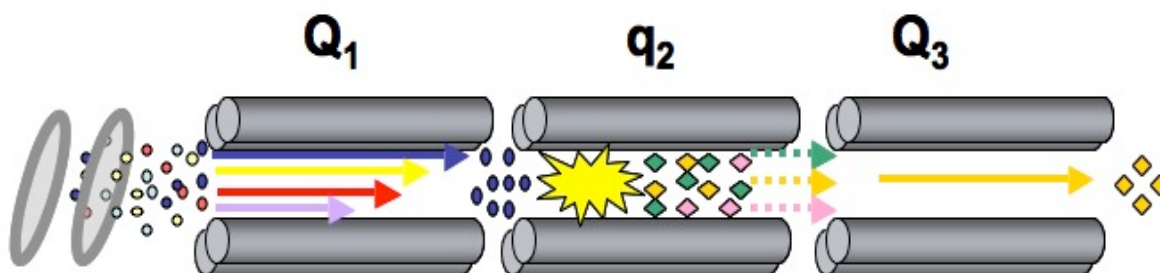


**Fig.2.2** Schematic operative representation of a triple quadrupole NL and PIS scan mode. Q1 scans in “DC/RF mode” the mass range, filtering sequentially the ions that are transferred to the q2. The second quadrupole is in RF only mode” and filled with neutral gas, thus the selected precursor ion is fragmented and the generated daughter ions are collimated and transferred by the RF field to successive analyzer. Q3 is fixed on a constant DC/RF value, with Unit resolution, consenting to reveal just the daughter ions having a given  $m/z$ . The fragment monitored during the analysis may be either constant following the same diagnostic moiety (PIS) or variable in function of the selected precursor following a fixed mass defect (NL)

demonstrated to enhance the identification of phosphorylated peptides about 100 folds if compared with more sensitive but less specific scan modes (25). The space separated  $MS^2$  characteristic of the triple quadrupole leads to record high quality fragmentation spectra. However, switching from the  $MS$  to  $MS^2$  mode changes the duty cycle from 100% to about 0.1 – 0.01% *per*  $m/z$ , drastically reducing the sensitivity. In addition the main limit of this optic is also the low resolution and the inability to perform  $MS^n$  experiment.

The ion-trap analyzers are fundamentally different from the beam-type instruments. Three-dimensional ion traps (IT) do not allow performing the selective scans discussed above. A single pulse of ions is introduced into the device, and trapped radially by an RF field. Mass spectrometers using an ion trap technology are more

sensitive instruments in comparison with triple quadrupole, because a full mass

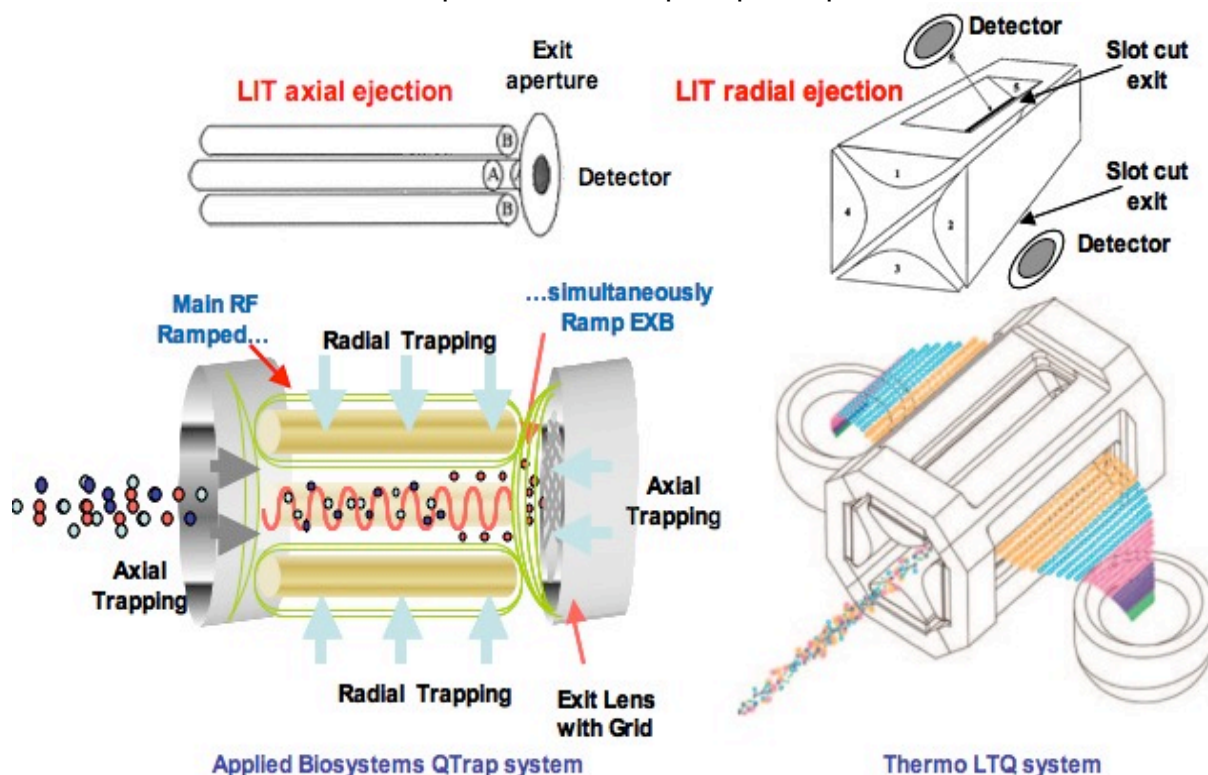


**Fig.2.3** Different types of LIT produced by Applied Biosystems and Thermo. Both the devices are characterized by the axial injection of the ions avoiding the end-cap interference found in the 3D-IT. Applied Biosystems equips their QTrap with an axial ejection LIT that may be rapidly converted in a classical quadrupole consenting to insert it in a triple quadrupole optic. Thermo-Finnigan equips their FT-ICR and Orbitrap with the more sensitive radial ejection LIT. The double detection and the emptying efficiency makes the Thermo LTQ a stand-alone analyzer

spectrum can be generated for each pulse of ions admitted. Moreover, several experiments of  $MS^n$  may be performed, providing detailed structural information of the analytes. However, IT has a limited number of ions trapping capacity, mainly for the three dimensional nature of the RF field, which confines trapped ions to a point at the center of the device, causing space charge effects. In addition to this limitation, IT has low ion injection efficiency caused by the interference generated by the RF alternating field around the end-cap hole. The development of linear ion trap (LIT) has opened to a new generation of mass spectrometer. LIT consists in a classical quadrupole at which is applied a stopping potential DC at the entrance and at the exit. In a different way from the IT, in the LIT ions are not confined axially by the RF potentials. Thus a linear oscillatory motion results along the axis of the quadrupole that leads to enhance ion storage and capacity. In addition the axial ion injection avoids the interference with the RF field improving the trapping efficiency. By using an auxiliary voltage the trapped ions are ejected radially (e.g. Thermo-Finnigan LTQ) through two slots cuts in the quadrupole rods. The presence of two detectors doubles the sensitivity of the analysis (26) (Fig.2.3). However the presence of two slots cuts long the z axis imposes to fabricate extremely precise devices. The storage space ion capacity is  $7 \times 10^6$ , resulting 10 folds greater than the IT. These features make the radial ejection LIT a stand-alone analyzer (27). Trapped ions may also be ejected axially (28). This is realized by the deformed fringing RF field near the quadrupole

exit, that converts the x, y motion, of the ions that are for a given RF at boundary stability conditions of Mathieu diagram, in axial motion. Thus the enhanced axial component of the motion leads ions to cross the DC barrier at the end of the quadrupole. Selective ion ejection is realized by changing RF potential that brings different  $m/z$  values at the boundary conditions. However, because the fringing field has short-range effect, just 20% of ions are ejected. The axial ejection, also if less sensitive than the radial ejection, makes possible to switch rapidly the LIT in a classical quadrupole. These features were used to project a hybrid mass spectrometer, commercialized by Applied Biosystems with the name QTrap, consisting in a triple quadrupole optic with the Q3 that is an axial ejection LIT (29). With this combination it is possible to perform all the selective scan modes of the triple-quadrupole instruments with the LIT sensitivity and high scan rate, allowing to carry out PIS and NL analysis at Proteomics scale. QqLIT geometry leads to improve  $MS^2$  quality of both the optics because the product ions scan is performed in hybrid manner. In practice the ions pass through Q1, which is tuned to transmit only the precursor ion of interest, and are accelerated into a high-pressure Q2 for the fragmentation. The fragments are then trapped in the LIT and then are scanned selectively. The lower sensitivity of the classical triple quadrupole  $MS^2$  analysis is improved by the higher LIT capacity. In addition the triple quadrupole space separated  $MS^2$  gives no peculiar ion traps low-mass cut off and enhances the dynamic range of the analysis. QTrap equipment and in particular the version 4000QTrap, that reaches LIT scan rate of 4000 amu/sec, also allows to perform chromatography compatible  $MS^3$  experiment. It is performed as the  $MS^2$  fashion but the useless fragments trapped in the LIT are discharged by the application of a radial RF, thus isolating the second precursor that is further fragmented. The space separated and high scan rate features of 4000QTrap lead to very rapid  $MS^3$  scan (0.3-0,5 sec) allowing to carry out this experiment in a LC/ $MS^2$  method.

### 2.1.3 Dansyl-Chloride: the RIGhT reagent

RIGhT approach is based on the analytes separation using the molecular structure features of selectively labelled peptides and the  $MS^2/MS^3$  fragmentation characteristics introduced by the reagent chosen.

RIGhT reagents have a peculiar structure consisting in a Reactive group toward the interesting residues, a Linker group that is loss as neutral moiety in  $MS^2$  experiment and a Reporter group that leads to generate stable fragment ions selectively detectable in  $MS^2$  experiment. For the development of a RIGhT

strategy to improve the identification of nitrated proteins, Dansyl Chloride was chosen as marker molecule. It is a primary amines reactive with all the structural features of a RIGhT reagent (Fig. 2.4). Once again, one of the ancient protein chemistry

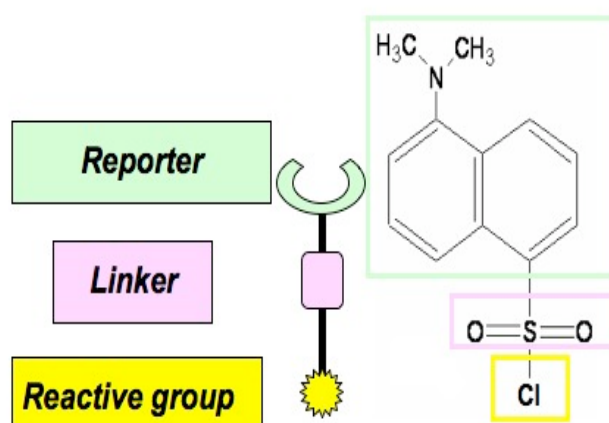
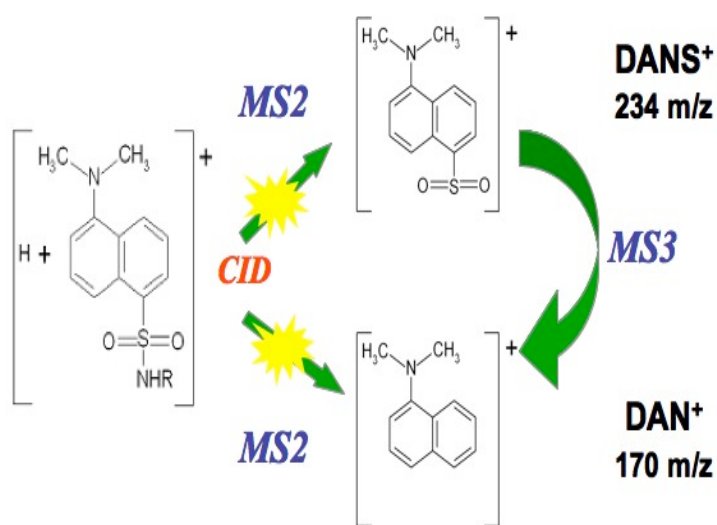


**Fig 2.4** Dansyl-chloride has the peculiar RIGhT reagent structure

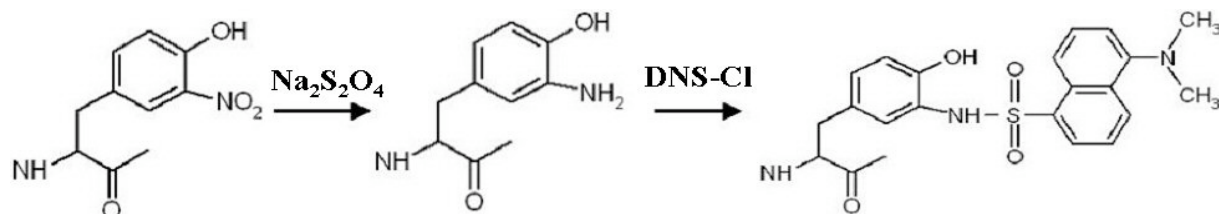
methods is used for the modern Proteomic techniques. In fact Dansyl Chloride chemistry was largely used for its fluorescence characteristics to detect proteins and peptides. Currently, we inherit from the past a relevant experience in the usage of Dansyl derivatives, in particular because by this class of reagents it was possible to



set up methods compatible with the biological concentrations, before the commercial availability of the mass spectrometers. After the introduction of these instruments at the end of the sixties, MS characteristics of dansyl derivatives were studied. In a work of 1968 Marino et al. showed the impact electronic fragmentation features of the dansyl derivatives (30). This knowledge was recently used by Amoresano et al (1) to set up a method to detect phosphoserine/threonine residues consisting in the

**Fig.2.5** Typical Dansyl-peptides CID fragmentations

selective modification of target residues with dansyl cysteamine followed by the detection and identification of the labelled peptides by exploiting the characteristic fragmentation pathway of derivatives. In fact in  $MS^2$  fragmentation, dansyl peptides give rise to two peculiar ions with 170  $m/z$  and 234  $m/z$ , in addition the last ion may be further fragmented in a diagnostic  $MS^3$  transition 234-170  $m/z$  (Fig. 2.5). These features were exploited by the use of an Applied Biosystems 4000QTrap mass spectrometer. By the coupling of this instrumentation and of the dansyl-derivatives characteristics, it was set up a high throughput LC- $MS^2$  method that it is based on Precursor Ion Scan (PIS) and  $MS^3$  experiments. PIS was chosen as survey scan for its selectivity and high scan rate characteristics. It consists in a Q1 scan across the full mass range, the ions separated are fragmented in the collision cell (Q2), finally the Q3 is set to transmit only the mass of the diagnostic fragment  $m/z$  170. Then the selected precursor ions



**Scheme 2.1** 3-dansyl-amino-tyrosine synthesis.

are submitted to a combined  $MS^2$  and  $MS^3$  experiment to specifically detect only those producing the transition 234-170 in  $MS^3$  mode, leading to the selective detection of the dansyl-peptides. This MS based “depletion” of un-desired peptides substitutes others chromatographic steps making the mass spectrometer a second dimension of the RP-LC separation.

Once again a look at the past allows to develop a new Proteomic strategy. In fact a dansyl chloride labelling procedure of nitrated proteins was developed by McIntyre in 1990 in order to selectively detect by fluorescence this post translational modification (scheme 2.1)(31). The most interesting feature of the proposed strategy is to perform at pH 5.0 the labelling reaction of 3-aminotyrosine formed by the precedent reduction of 3-nitrotyrosine residues. In fact in these pH conditions the newly generated aromatic amine is deprotonated ( $pK_a=4.7$ ) while the collateral reactions with N-term and Lysine primary amines are un-favored by the protonation. Moreover, the acid pH decreases the competitive aqueous hydrolysis of Dansyl chlorides (32). However, the strategy proposed by McIntyre was not optimized at Proteomics scale and the MS analysis was not afforded.

## **2.2 Materials and methods**

**Chemicals.** Tri(hydroxymethyl)aminomethane (Tris), 5-N,Ndimethylaminophtalene-1-sulfonyl chloride (dansyl chloride, DNSCI), ammonium hydrogen carbonate (AMBIC), and iodoacetamide, were purchased from Fluka, Tetranitromethane (TNM), bovine serum albumin (BSA), ethylenediaminetetraacetic acid (EDTA), sodium dithionite ( $Na_2S_2O_4$ ), guanidine, sodium acetate, trypsin, and dithiothreitol (DTT) were from Sigma (St. Louis,MO), Acetonitrile (ACN) was purchased from Baker (Phillipsburg, NJ). SDS-PAGE and western blot chemicals were purchased from Bio-Rad. Nitrotyrosine antibody was from Alexis. Trifluoroacetic acid HPLC grade was from Carlo Erba. All solvents were of the highest purity available from Baker. All other reagents and proteins were of the highest purity available from Sigma.

**In Vitro Nitration of BSA.** A BSA solution (10 mg/mL) in 200 mM Tris buffer (pH 8,0) was nitrated by addition of 350 mM TNM in acetonitrile using a Tyr/TNM ratio of 1/1 (mol/mol). The reaction mixture was stirred at room temperature for 30 min as previously described. 15 Nitrated BSA (N-BSA) was rapidly desalted by size exclusion chromatography on a Sephadex G-25M column (Amersham). Protein elution was monitored at 280 and 350 nm. The fraction containing the protein was manually collected, lyophilized, and stored at  $-20\text{ }^\circ\text{C}$ .

**Tryptic Digestion.** Aliquots of the BSA and N-BSA mixture were dissolved in denaturant buffer (guanidine 6 M, Tris, EDTA pH 8.0), reduced with DTT (10-fold molar excess on the cysteine residues) for 2 h at  $37\text{ }^\circ\text{C}$  and then alkylated with iodoacetamide (5-fold molar excess on the thiol residues) for 30 min at room temperature in the dark. Protein samples were desalted by the size exclusion cartridge PD-10 (Amersham), the elution was performed in AMBIC 10 mM. Protein elution was monitored at 280 and 350 nm. The fractions containing the protein were reunited, concentrated and digested by trypsin. Trypsin digestion was carried out using an enzyme/substrate ratio of 1/50 (w/w) either at  $37\text{ }^\circ\text{C}$  for 18 h.

**Reduction of Nitrotyrosine to Aminotyrosine.** Reduction of 3-nitrotyrosine to 3-aminotyrosine was carried out on aliquots of the modified peptide mixtures by using  $Na_2S_2O_4$  as previously reported (33). Before MALDI-TOF analysis, cleaning of the samples was performed using reversed-phase Zip-Tips C18 from Millipore (Billerica, MA).

**Synthesis of 3-Dansyl-amino-tyrosine.** The mixture of reduced BSA tryptic peptides was desalted by RP-HPLC on a reversed-phase C18 column (100 × 4.6 mm, 5 μm; Phenomenex). Peptide fractions were lyophilized and then dissolved in 100 mM sodium acetate pH 5.0 buffer, 0.9% sodium chloride. Samples were treated with a 18.5 ng /μL solution of DNS-Cl in ACN (1000-fold molar excess), and the buffered solutions were allowed to react at 65 °C for 16 h.

**Labelling of Bovine Milk Protein Extract.** A sample of commercially available bovine milk was reacted with a 100 mM solution of TNM for 30 min at room temperature. Modified milk proteins were purified by precipitation with the Amersham Clean Up kit and dissolved in denaturant buffer. Reduction of both the SH and nitro groups of the protein mixture was carried out in “one pot” using 20 mM DTT, 40 mM iodoacetamide, and a 200 mM solution of Na<sub>2</sub>S<sub>2</sub>O<sub>4</sub> in the dark for 30 min. The protein mixture was purified by size exclusion chromatography on a Sephadex G-25M column equilibrated and eluted with 50 mM AMBIC. Protein fractions were concentrated and then digested with trypsin as already described. The resulting peptide mixture was reacted with DNS-Cl as described above.

**Mass Spectrometry.** MALDI-MS experiments were performed on a Voyager DE-STR MALDI-TOF mass spectrometer (Applied Biosystems, Framingham, MA) equipped with a nitrogen laser (337 nm). Typically, 1 μL of the total mixture was mixed (1/1, v/v) with a 10 mg/mL solution of -cyano-4-hydroxycinnamic acid in acetonitrile/50 mM citrate buffer (2/3, v/v).

NanoLC-MS<sup>2</sup> and MS<sup>3</sup> experiments were performed on a 4000 QTrap mass spectrometer (Applied Biosystems) coupled to an 1100 nanoHPLC system (Agilent Technologies). Peptide mixtures were loaded onto an Agilent reversed-phase precolumn cartridge (Zorbax 300 SB-C18, 5 × 0.3 mm, 5 μm) at 10 μL/min with solvent A (0.1% formic acid, loading time 7 min). Peptides were then separated on a Agilent reversed-phase column (Zorbax 300 SBC18, 150 mm × 75 μm, 3.5 μm), at a flow rate of 0.2 μL/min using 0.1% formic acid, 2% ACN in water as solvent A 0.1% and formic acid, 2% water in ACN as solvent B. The elution was accomplished by a 5-65% linear gradient of solvent B in 60 min. A micro-ionspray source was used at 2.5 kV with liquid coupling, with a declustering potential of 50 V, using an uncoated silica tip (o.d. 150 μm, i.d. 20 μm, tip diameter 10 μm) from New Objectives (Ringoos, NJ). Spectra acquisition was based on a survey precursor ion scan for m/z 170,1. The Q1 quadrupole was scanned from m/z 400 to 1400 in 2 s with resolution “low”, and the precursor ions were fragmented in q2 using a linear gradient of collision potential from 30 to 70 V. Finally, Q3 was set to transmit only ions at m/z 170 with resolution “unit”. This scan mode was followed by an enhanced resolution experiment for the ions of interest and then by MS<sup>3</sup> and MS<sup>2</sup> acquisitions of the two most abundant ions. MS<sup>2</sup> spectra were acquired using the best collision energy calculated on the basis of m/z values and charge state (rolling collision energy). MS<sup>3</sup> spectra were performed on the fragment ion at m/z 234 and acquired using Q0 trapping, with a trapping time of 150 ms and an activation time of 100 ms, scanning from m/z 160 to 210. The entire cycle duration is 5.3 s.

## **2.3 Results and discussions**

BSA (1 mg) was nitrated with TNM, and the excess reagent was rapidly removed by size exclusion chromatography as described in the Materials and Methods

paragraph. TNM-induced modifications were determined by MALDI mapping analyses. Aliquots of the BSA and N-BSA mixtures were reduced with DTT and alkylated with iodoacetamide. Proteins were then digested by trypsin, and the resulting peptide mixtures were directly analyzed by MALDI mass spectrometry. Spectral analyses led to the 85% of BSA sequence coverage, and more important, 95% of tyrosine residues could be verified. Two mass signals recorded at  $m/z$  972.5 and 1524.8, respectively, did not correspond to any peptide within the BSA sequence. These values occurred 45 Da higher than the signals corresponding to the peptides 137-143 and 396-409, respectively, suggesting that they originated from the nitrated derivatives of these fragments. This hypothesis was corroborated by satellite peaks at -16 and -32 Da, revealing the typical photodecomposition pattern of nitrated peptides previously described to occur during the MALDI analysis of nitropeptides (10) (Figure 2.6 A). This finding indicated that Tyr137 and Tyr399 were partially converted into the corresponding  $\text{NO}_2\text{Tyr}$  residues following TNM treatment. These data were in perfect agreement with previous results on in vitro BSA nitration (10, 19). However, signals occurring at  $m/z$  927.5 and 1479.7 were attributed to the theoretical fragments,  $m/z$  137-143 and 396-409, respectively, were detected thus indicating that the nitration reaction was not quantitative.

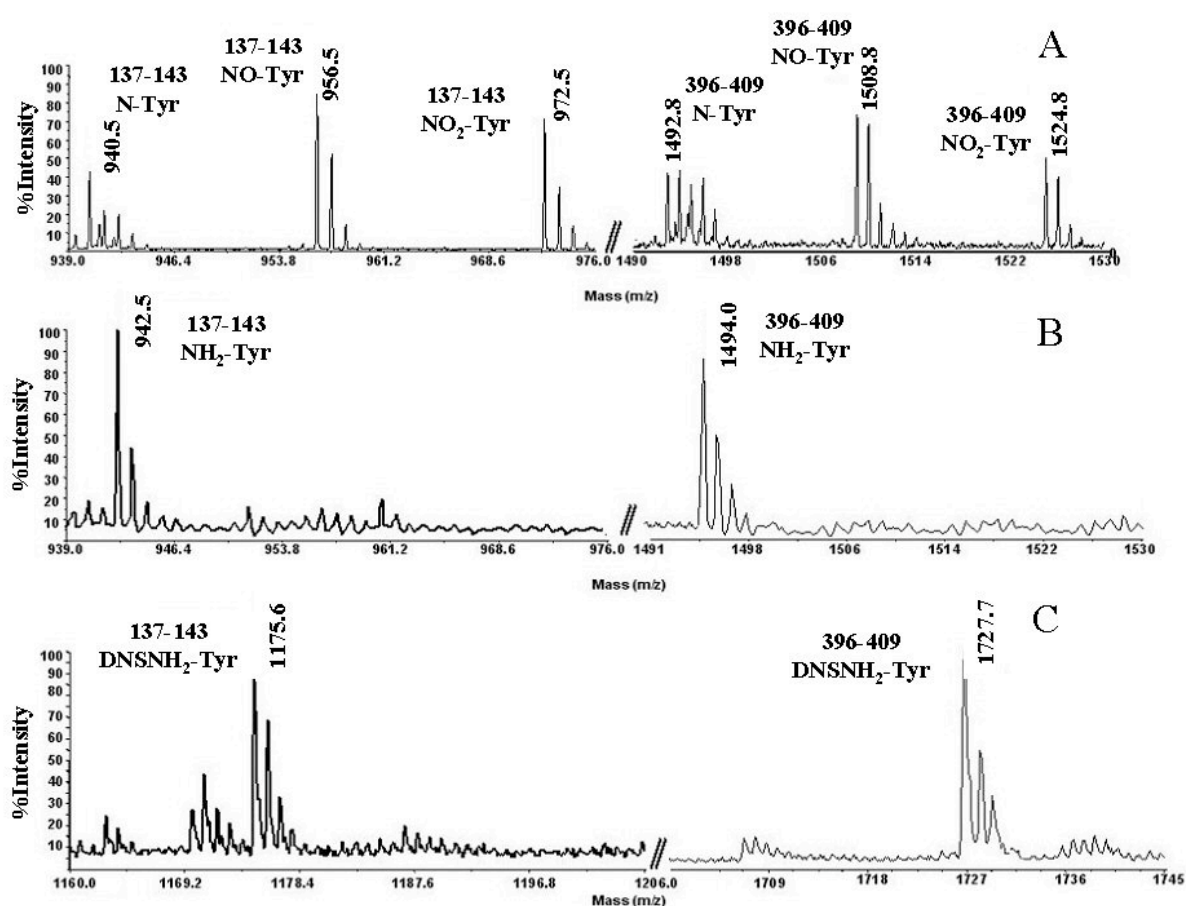


**Fig.2.6** In the **panel A** it is showed the MALDI-TOF spectrum enlargement of the nitrated BSA peptides 137-143 (972.5  $m/z$ ) and 396-409 (1524.8  $m/z$ ). The characteristic  $\text{NO}_2\text{Tyr}$  post source decomposition is observed by the presence of the satellite peaks at -16Da and -32Da. **Panel B** shows that the  $\text{NO}_2\text{Tyr}$  reduction by  $\text{Na}_2\text{S}_2\text{O}_4$  is complete, no  $\text{NO}_2\text{Tyr}$  signals are present in the MALDI-TOF spectrum enlargement. **Panel C** shows the MALDI-TOF spectrum enlargement of the newly formed 3-dansylamino tyrosine peptides.

**Synthesis of 3-Dansyl-Amino-tyrosine.** Conversion of nitropeptides into their 3-dansyl-amino derivatives was accomplished as indicated in Scheme 2.1. First, nitro groups were reduced by  $\text{Na}_2\text{S}_2\text{O}_4$  treatment, the peptide mixture was desalted by HPLC, and the extent of reduction was monitored by MALDI-MS. Mass spectral analysis showed the disappearance of the classical 3-nitrotyrosine photodecomposition pattern, indicating nearly quantitative reduction, and its replacement by two new signals at  $m/z$  942.4 and 1494.8, attributed to peptides  $m/z$  137-143 and 396-409, respectively, containing an amino-Tyr residue (Figure 2.6B). Aminotyrosine residues were chemoselectively labelled with DNS-Cl following the reported procedure. The reaction was carried out at pH 5.0 exploiting the different  $pK_a$  value of the 3-aminotyrosine (4.7) (33) which is partly deprotonated and is therefore amenable to react with DNS-Cl at variance with aliphatic (10.4-11.1) and N-terminal amino groups (6.8-8.0), which are largely protonated. The extent of reaction was monitored by MALDI-MS analysis showing the presence of two new signals at  $m/z$  1175.6 and 1727.8 occurring 233 Da higher than the 3-aminotyrosine-containing peptides (Figure 2.6C). These signals corresponded to the expected dansyl derivatives of the 3-aminotyrosine peptides. No modification at the N-terminus or Lys residues was detected.

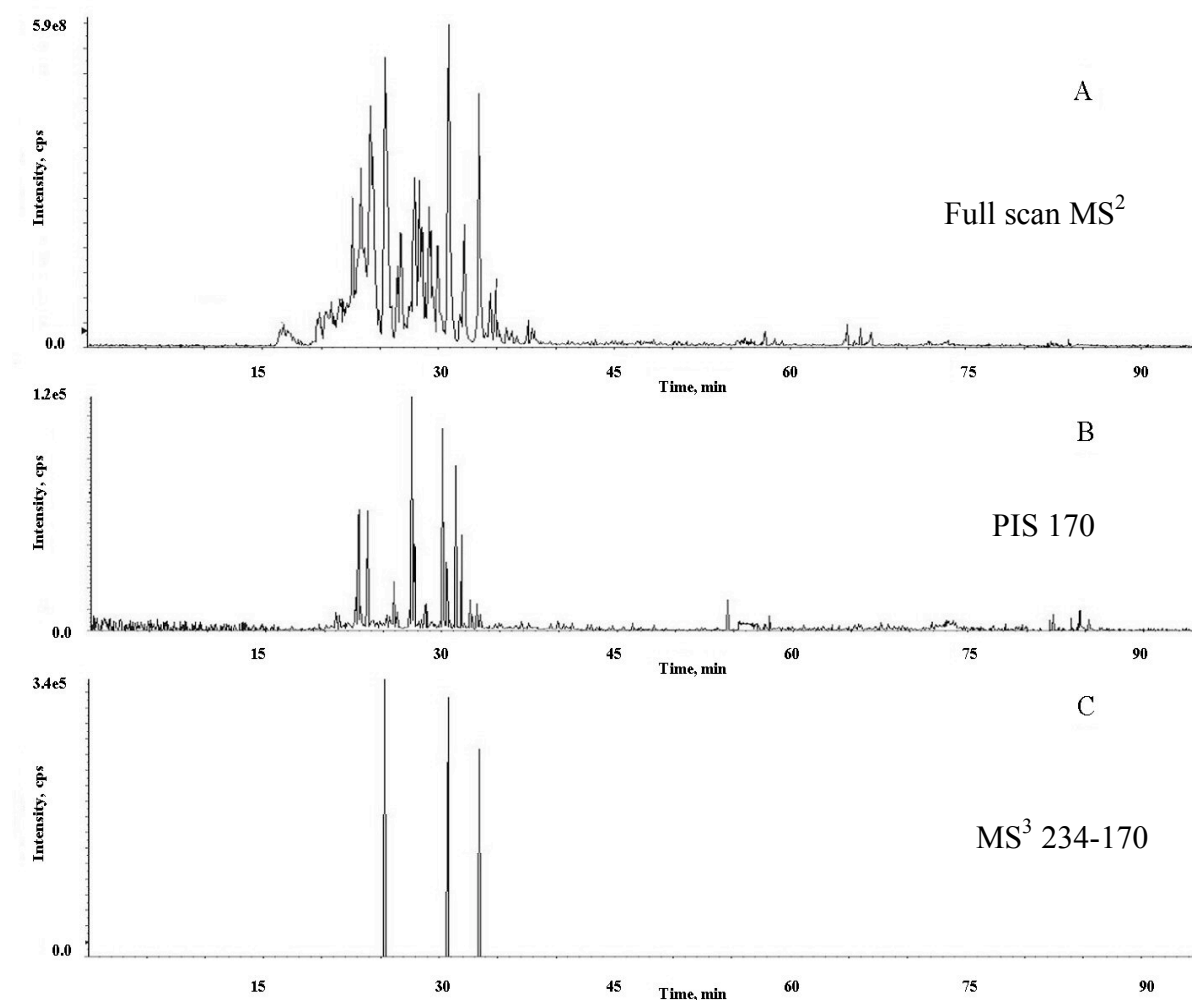


**Fig.2.7** In the **panel A** it is showed the total ion current of a full scan LC-MS<sup>2</sup> of a nitrated BSA/BSA trypsin digest. **Panel B**: PIS of nitrated BSA/BSA peptide mixture after dansyl labelling. About 73% of un-desired peptides are not analyzed. The MS<sup>3</sup> chromatogram in **panel C** shows that by the double selection criteria 100% of un-desired peptides are removed by the spectrometer.

**LC-MS/MS Analysis of 3-Aminodansyl-Tyr Peptides.** The exact location of the original nitro groups was assessed by LC-MS<sup>2</sup> analysis of the peptide mixture using a linear ion trap 4000 Q-Trap instrument and an experimental procedure that combines precursor ion scan with MS<sup>3</sup> scan mode as already described (1). In the precursor ion scan mode, only the precursor ions producing the m/z 170 fragment were detected. The selected precursor ions were then subjected to a combined MS<sup>2</sup> and MS<sup>3</sup> experiment to specifically detect only those ions originating the dansyl-specific m/z 234-170 transition in MS<sup>3</sup> mode as indicated in Figure 2.3. Figure 2.7 shows the LC-MS<sup>2</sup> traces corresponding to the various experiments. The chromatographic profiles reported in Figure 2.7B and 2.7C for the m/z 170 precursor ion scan and for the transition m/z 234/170 in MS<sup>3</sup> mode, respectively, showed a lower number of signals compared to the LC-MS<sup>2</sup> full scan profile (Figure 2.7A). Moreover, a significant increase in the signal/noise ratio could be achieved as the higher selectivity MS criteria were applied (Figure 2B and C). However, the precursor ion TIC exhibited a number of ions that are very unlikely related to 3-dansylamino-Tyr peptides (Figure 2.5B). In fact, the PIS of the fragment 170 m/z was realized with the Q3 in “unit” resolution characterized by a width of about 1 Da. Thus by this analysis a restrict number un-dansylated peptides may be also detected as that containing the N-Term couple Gly-Ile/Leu, Ala-Val, by the detection of their b<sub>2</sub> ions. However by this analysis 73% of unlabelled BSA peptides remain un-detected. The MS<sup>3</sup> selection criterion is more restrictive than the PIS. In fact, the MS<sup>3</sup> TIC (Figure 2.7C) showed the presence of only three peaks related to doubly charged ions at m/z 588.2, 792.9, and 986.8, resulting in 100% MS depletion of un-desired species. However the MS<sup>3</sup> is too slow to be used as unique survey scan, thus PIS is necessary for a first gas phase “fractionation” of the sample making the MS<sup>3</sup> scan compatible with chromatography. The corresponding MS<sup>2</sup> fragmentation spectra of peptides positive analysis led to the determination of the entire sequence of these species, identifying the fragments 137-143, 396-409, and 445-458, respectively, all of which contain 3-aminodansyl-Tyr residues. Moreover, modified Tyr residues could easily be detected at the level of Tyr137, Tyr399, and Tyr451, allowing for the exact identification of the original nitration sites. As an example, Figure 2.8B shows the MS<sup>2</sup> spectrum of the peptide m/z 396-409 carrying a dansyl moiety. The modified ion is stable during collision-induced dissociation, providing easily interpretable daughter ion spectra. Both the y and b fragment ions still retained the modifying group linked to the amino Tyr residue, thus denoting original nitration. As indicated in the spectrum, the mass difference between the b<sub>4</sub> and b<sub>3</sub> fragment ions is 411 Da corresponding to the 3-dansylaminotyrosine residue. It should be noted that the LC-MS<sup>2</sup> analysis revealed the occurrence of a further nitration site within the peptide m/z 448- 458 at level of Tyr451, which escaped previous MALDI analysis. Moreover, the daughter ion spectra of 3-dansylamino-Tyr-containing peptides showed some peculiar features. Besides the signals at m/z 170 and 234, typical of dansyl derivatives, a further signal at m/z 384 was always observed and assigned to the immonium ion of 3-dansylamino-Tyr. This stable fragment could then be used either as an alternative diagnostic fragment in the precursor ion scan or simply to confirm the presence of a 3-dansylamino-Tyr residue in the peptide sequence. Finally, a fragment ion related to the loss of the dansyl moiety as neutral group was always observed in the daughter ion spectra when the 3-nitrotyrosine residue is located at N-terminal position. In fact, the fragment ion at m/z 942.5 in Figure 2.8A belongs to the y series and occurs 233 Da lower than the molecular mass of the dansylated peptide m/z 137-143, showing the

neutral loss of the dansylated moiety. This kind of behavior is observed when the peptide N-Terminal amino acid is labelled.

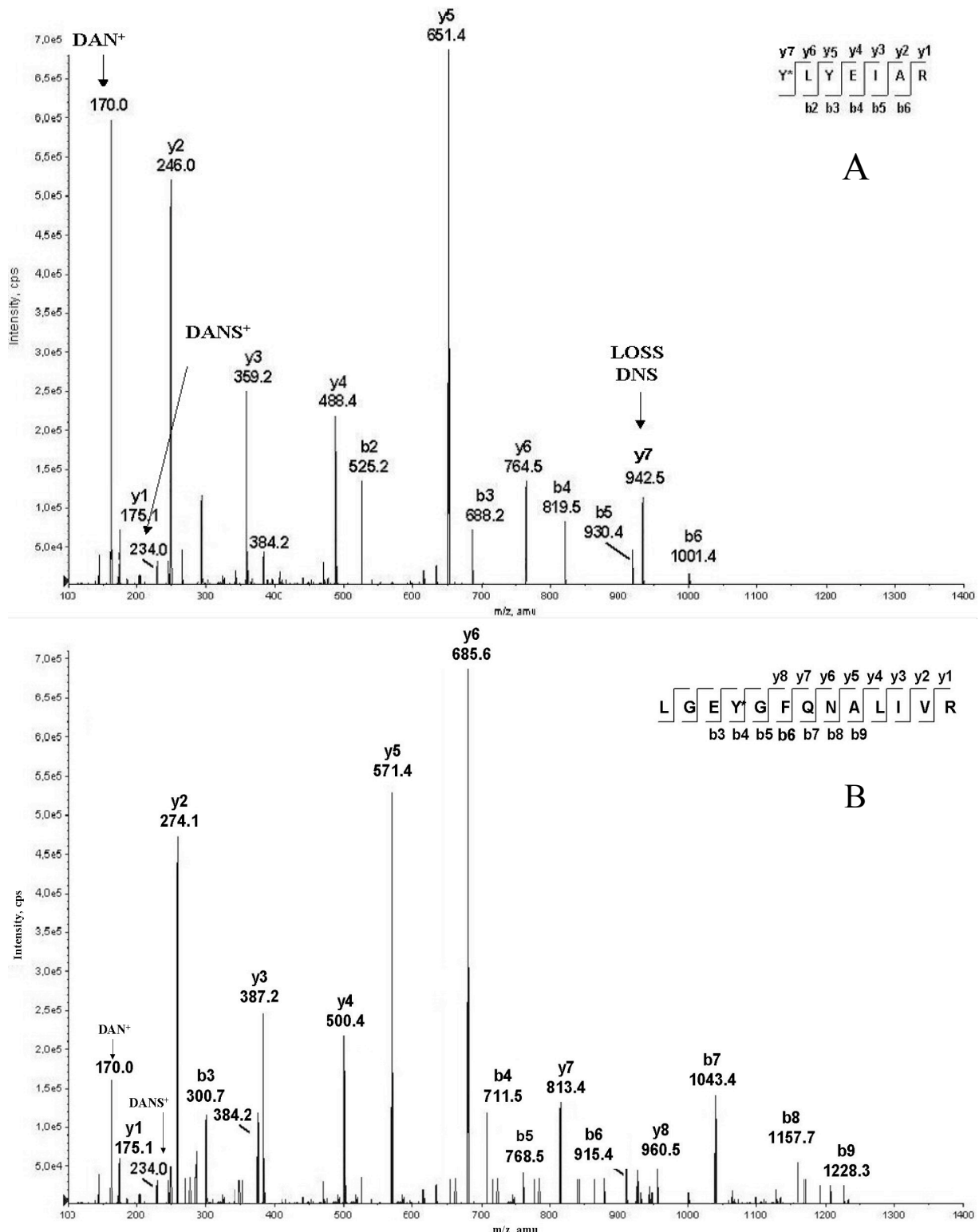


**Fig.2.8** MS<sup>2</sup> spectra relative to the nitrated BSA peptides 137-146 (panel A) and 396-409 (panel B)

**Location of BSA 3-Aminotyrosine-Containing Peptides in Complex Protein Mixtures.** The feasibility of the developed procedure to identify 3-nitrotyrosine

peptides in proteomics analysis was probed by mixing 100 µg of the mixture of BSA and nitrated BSA with 10 mg of the entire cellular extract from *Escherichia coli*. An aliquot of the modified proteome was fractionated by SDS-PAGE to demonstrate that BSA was indistinguishable from and in similar amount to other *E. coli* proteins. The total protein extract was then submitted to the procedure described above.

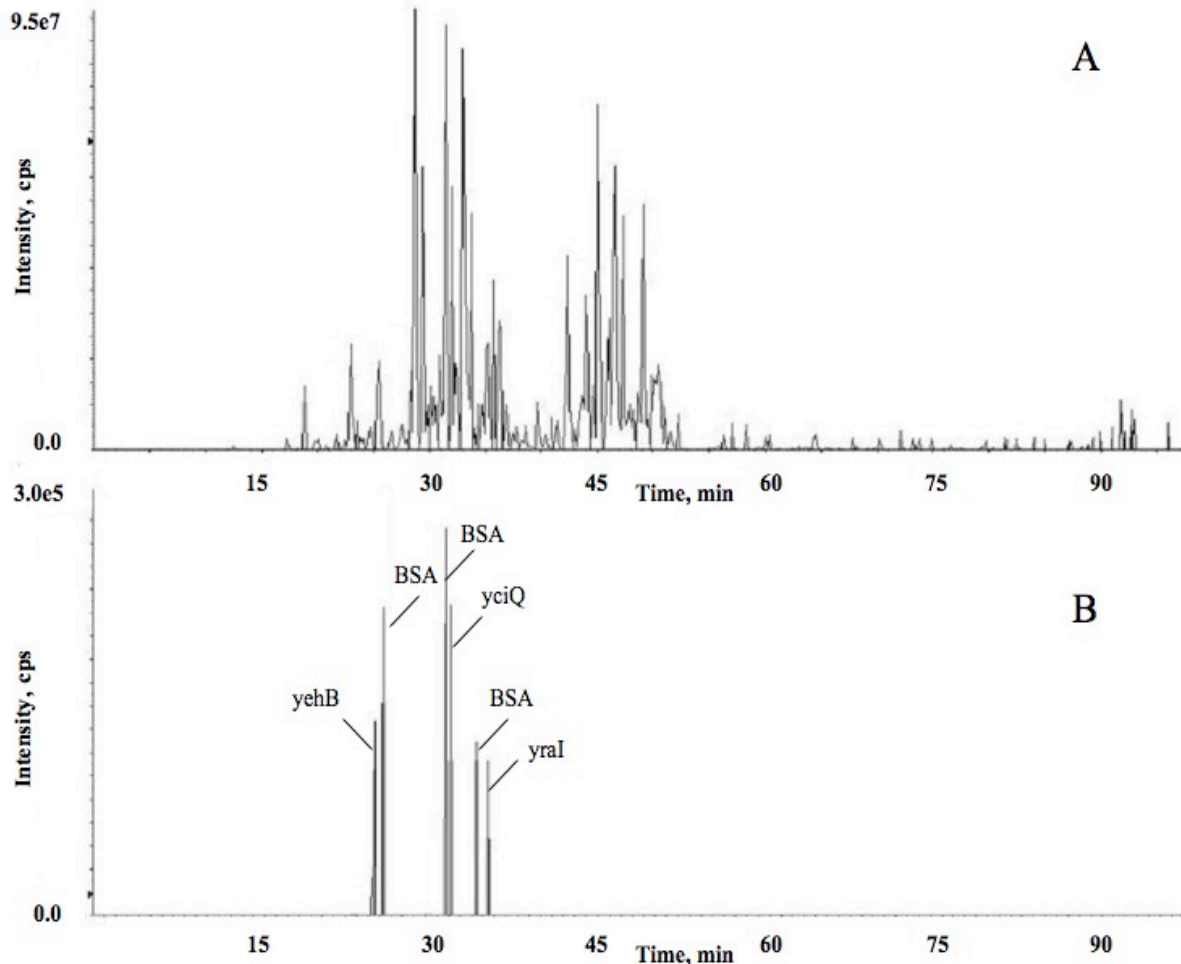


**Fig.2.9** Total ion current of PIS (**panel A**) and MS<sup>3</sup> (**panel B**) of *E.coli* protein extract spiked with nitrated BSA

Nitrotyrosines were reduced with dithionite, and the modified protein mixture was digested with trypsin. The newly generated amino-Tyr-containing peptides were labelled with dansyl chloride at pH 5.0, and an aliquot of peptide digest containing 50 fmol of nitropeptide mixture was submitted to the bidimensional tandem mass spectrometry procedure described above. Figure 2.7 shows the reconstructed ion chromatogram for the precursor ion scan (A) and the selective dansyl transition in MS<sup>3</sup> mode (B). As clearly indicated in the figure, the precursor ion scan mode still showed the occurrence of a large number of signals, most of which are not related to NO<sub>2</sub>Tyr -containing peptides. The further selection based on the MS<sup>3</sup> scan removed a large number of false positives leading to a simple ion chromatogram essentially dominated by six intense signals. Identification of nitrated tyrosine residues was carried out by taking advantage of the flexibility of the MASCOT software, a database search utility available on the net. First, a variable modification of 411.0 Da corresponding to 3-aminodansyltyrosine residues was introduced into the

Modification File within the MASCOT software. Second, the peak list used for database search only consisted in the MS<sup>2</sup> spectra of the peptide species that had generated a signal both in the precursor ion TIC and in the MS<sup>3</sup> ion scan. The MS<sup>2</sup> fragmentation spectra of the six signals observed in the MS<sup>3</sup> scan reported the occurrence of three NO<sub>2</sub>Tyr-containing peptides originated from the BSA sequence. In addition the other three signals detected correspond to nitrated *E.coli* peptides (Table 2.1).

**Labelling and Analysis of a Nitrated Protein Extract of Bovine Milk.** The proposed strategy was finally employed to identify 3-nitrotyrosine residues in a more complex sample, the entire bovine milk. Bovine milk was in vitro nitrated with TNM,

<i>Protein</i>	<i>Sequence</i>	<i>Scores</i>
yraI	MF-NO <sub>2</sub> Y <sup>139</sup> -RPAQHLK	24
yciQ	NQIKHGF-NO <sub>2</sub> Y <sup>10</sup> -R	35
yehB	IAAP-NO <sub>2</sub> Y <sup>134</sup> -R	30

**Table 2.1** *E.coli* nitrated peptides

with trypsin. The resulting peptide mixture was selectively labelled with dansyl chloride and directly submitted to LC-MS/MS analysis using the double selectivity criteria.

<i>Protein</i>	<i>Sequence</i>	<i>Score</i>
β-Casein	AVP-NO <sub>2</sub> Y <sup>105</sup> -PQR	40
β-Lactoglobulin	VLVLDTD-NO <sub>2</sub> Y <sup>115</sup> -KK	36
	V-NO <sub>2</sub> Y <sup>98</sup> -EELK	20
Vimentin	QQ-NO <sub>2</sub> Y <sup>275</sup> -ESVAAK	25
Claudin2	AKSEFNS-NO <sub>2</sub> Y <sup>224</sup> -SLTGYV	23
Homeobox protein Hox D-12	F-NO <sub>2</sub> Y <sup>101</sup> -TPDVAAGPEERGR	21

**Table 2.2** nitrated milk protein

nitration sites occurring in low-abundant proteins, such as Vimentin and Claudin 2.

## **2.4 Conclusion**

The major problem in the proteomic analysis of nitroproteins is the need to discriminate modified proteins, usually in very low concentrations, from the large amount of un-modified proteins. Moreover, biological relevant PTMs often occur at sub-stoichiometric level making even more difficult the identification of the 3-nitrotyrosine-containing proteins in the presence of a larger percentage of the corresponding *non*-nitrated form. Finally, precise localization of the nitration site is often required to fully describe the biological process. Existing methodologies

essentially rely on immunochemical techniques, whereby nitrated proteins can be detected by alignment of the western blots with the 2DE gels of the entire cellular

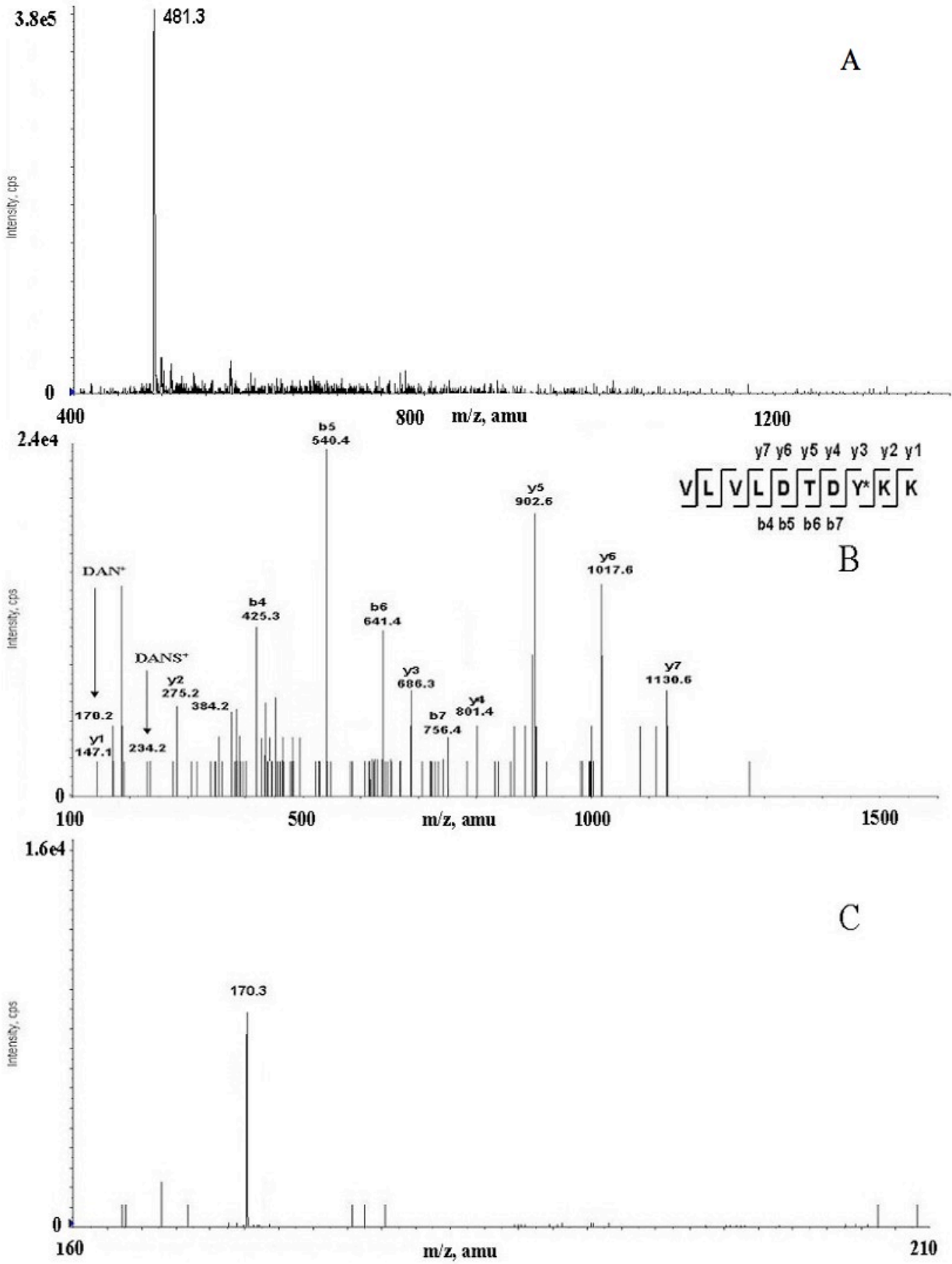


**Fig.2.10** In the **panel A** is showed the MS spectrum of  $\beta$ -lactoglobulin nitrated peptide detected in PIS mode as triply charged ion. In the **panels B** and **C** are showed respectively its MS<sup>2</sup> and MS<sup>3</sup> spectra

proteome (8-9). Alternatively, specific capture of 3-nitrotyrosine-containing proteins by immuno-affinity procedures (15-16) can also be employed. However, neither of these approaches completely fulfills the analytical requirements for nitro proteome analysis. However, the peptide mixture from the tryptic digest of the whole enriched nitroprotein bulk is still too complicated to be analyzed in a simple one-step process and 2D-HPLC, typically consisting of ion exchange and reversed-phase separations, in conjunction with tandem mass spectrometric methods had to be used (14). The strategy described in this chapter is based on a totally different approach involving dansyl chloride labelling and relies on the huge potential of MS<sup>n</sup> analysis. According to the so-called “gel-free procedures”, the analysis is carried out at level of peptides following tryptic digest of the whole protein mixture. However, discrimination between nitropeptides and un-modified peptides is achieved by taking advantage of the instrumental features of a hybrid (triple quadrupole/linear ion trap) mass spectrometer. Peptide analysis is carried out by LC-MS/MS, and the peptide ions of interest are discriminated by two selectivity criteria based on two subsequent tandem MS experiments, a precursor ion scan followed by MS<sup>3</sup> scan mode. This procedure can then be considered as a sort of “instrumentally driven” bidimensional selection. The proposed strategy consists in two simple chemical manipulation steps, namely, reduction of 3-nitrotyrosine residues to the corresponding NH<sub>2</sub>-Tyr derivatives and the chemoselective labelling with DNS-Cl at pH 5.0, exploiting the lower basicity of aromatic amines compared to the aliphatic ones.

Analysis of chemically nitrated BSA following tryptic digestion confirmed the ability of the bidimensional selection to simplify the peptide ion chromatogram, leading to selective identification of 3-nitrotyrosine-containing peptides. This experiment underlined the usefulness of the two selectivity criteria in that the precursor ion scan still showed the presence of non-nitrated peptide ions that were completely ruled out in the MS<sup>3</sup> scan mode. Moreover, since this combined MS approach provides only the daughter ion spectra of the nitrated peptides, this procedure always leads to the unambiguous localization of the nitrated Tyr residues. Because of its operational simplicity, avoiding long-lasting and time-consuming fractionation procedures, this new strategy seems to be well suited for large-scale proteomic profiling of nitration sites. Moreover, the general rationale of the method can in principle be extended to the detection of other PTMs. The high impact of the innovative “RIGhT” strategy presented in this chapter, is confirmed by the publication of the data showed above on a first class analytical chemistry journal (Amoresano A, Chiappetta G, Pucci P, D'Ischia M, Marino G., *Bidimensional tandem mass spectrometry for selective identification of nitration sites in proteins*, *Analytical Chemistry* (2007), 79(5):2109-17).

## **2.5 References**

1. Amoresano A., Monti G., Cirulli C., Marino G., *Rapid Commun. Mass Spectrom.* **2006**, 20:1400-1404.
2. Aulak, K. S., Miyagi M., Yan L., West K. A., Massillon D., Crabb J.W., Stuehr D. J., *Proc. Natl. Acad. Sci. USA* **2001**, 98:12056–12061.
3. Turko I.V., Li L., Aulak K.S., Stuehr D.J., Chang J.Y., Murad F., *J. Biol. Chem.* **2003**, 278: 33972–33977;.
4. Fiore G., Di Cristo C., Monti G., Amoresano A., Columbano L., Pucci P., Cioffi F.A., Di Cosmo A., Palumbo A., d'Ischia M., *Neurosci Lett.* **2006**, 394(1):57-62.
5. Rabbani N., Thornalley P.J., *Methods Enzymol.* **2008**; 440:337-59
6. Oberley T.D., Swanlund J.M., Zhang H.J., Kregel K.C., *J Histochem Cytochem.* **2008**, 56(6):615-27
7. Ye Y.Z., Strong M., Huang Z.Q., Beckman J.S., *Methods Enzymol.* **1996**, 269:201 – 209.
8. Zhan, X.; Desiderio, D. M., *Biochem. Biophys. Res. Commun.* **2004**, 325:1180–1186;.
9. Kanski J., Behring A., Pelling J., Schöneich C. *Am. J. Physiol. Heart Circ. Physiol.* **2005**, 288: H371–H381;.
10. Sarver, A., Scheffler N.K., Shetlar M.D.; Gibson B.W., *J. Am. Soc. Mass Spectrom.* **2001**, 12:439–448.
11. Martin D.B., Eng J.K., Nesvizhskii A.I., Gemmill A., Aebersold R., *Anal. Chem.* **2005**, 77:4870–4882.
12. Yagüe J., Paradela A., Ramos M., Ogueta S., Marina A.; Barahona F., López de Castro J. A., Vásquez J., *Anal. Chem.* **2003**, 75:1524–1535;.
13. Vaisar T., Heinecke J.W., Seymour J., Turecek F., *J. Mass Spectrom.* **2005**, 40:608–614;.
14. Sacksteder C.A., Qian W.J., Knyushko T.V., Wang H., Chin M.H., Lacan G., Melega W.P., Camp D.G., Smith R.D., Smith D.J., Squier T.C., Bigelow D.J. *Biochemistry* **2006**, 45 (26), 8009-8022.
15. Thomson L., Christie J., Vadseth C., Lanken P.N., Fu X., Hazen S.L., Ischiropoulos H., *Am J Respir Cell Mol Biol.* **2007**, 6(2):152-7
16. Zhan X., Desiderio D.M., *Anal Biochem.* **2006** 354(2):279-89.
17. Nikov G., Bhat V., Wishnok J.S. and Tannenbaum S.R., *Anal. Biochem.* **2003**, 320, 214-222.
18. Zhang Q., Qian W.J., Knyushko T.V., Clauss T.R., Purvine S.O., Moore R.J., Sacksteder C.A., Chin M.H., Smith D.J., Camp D.G., Bigelow, D.J. and Smith R.D. *J. Proteome. Res.* **2007**, 6, 2257-2268.
19. Petersson A.S., Steen H., Kalume D.E., Caidahl K. and Roepstorff P. *J. Mass Spectrom.* **2001**, 36, 616-625.
20. Cirulli C., Chiappetta G., Marino G., Mauri P., Amoresano A., *Anal. Bioanal. Chem.* **2008**, 392(1-2):147-59.
21. Seiwert B., Karst U., *Anal. Chem.* **2007**, 79(18):7131-8.
22. Johnson J.V. Jost R.A., Kelley P.A., Bradford P.E., *Anal. Chem.* **1990** 62, 2162–2172
23. Sabatine M.S., Liu E., Morrow D.A. Heller E., McCarroll R., Wiegand R., Berriz G.F., Roth F.P., Gerszten R.E., *Circulation.* **2005**, 112(25):3868-3675.
24. Niggeweg R., Köcher T., Gentzel M., Buscaino A., Taipale M., Akhtar A., Wilm M., *Proteomics* **2006**, 6(1), 41-53.

25. Annan R.S., Huddleston M.J., Verma R., Deshaies R.J., Carr S.A., *Anal Chem.* **2001**, 73(3):393-404
26. Schwartz J.C., Senko M.W., Syka J.E.P., *J. Am. Soc. Mass Spectrom.* **2002**, 13:659 – 669.
27. Douglas D.J., Frank A.J., and Mao D., *Mass Spec. Rev.* **2005**, 24: 1 – 29
28. Londrya F. A., and Hager J.W., *J Am. Soc. Mass Spectrom.* **2003** 14(10):1130-47
29. Hager J.W., *Rapid Commun. Mass Spectrom.* **2002**,16: 512-526
30. Marino G., Buonocore V. *Biochem. J.*, **1968** 110: 603-604
31. McIntyre J. C., Schroeder F., Behnke W. D., *Biochemistry* **1990**, 29: 2092-2101
32. Gross C., Labouesse B., *European J. Biochem.*, **1969** 7:463-470
33. Sokolovsky M., Riordan J.F., Vallee B.L., *Biochemistry* **1966** 5: 3582-3589.

### **3. QUANTITATIVE IDENTIFICATION OF PROTEIN NITRATION SITES BY USING iTRAQ REAGENTS**

#### **3.1 Introduction**

Patho-physiological events often alter the protein expression, including the posttranslational modifications status as for example tyrosines nitration in cells, tissues, or biological fluids. The ability to make relative quantitative estimations about protein abundance and their modification differences according to different conditions, is essential for identifying key molecular targets or candidate biomarkers involved in different diseases. However, the limitations of mass spectrometry based approach for protein nitration identification (see chapter 2) have even more impacts when quantitative estimations have to be performed. For this reason Proteomics approach is lacking of strategies to make the protein nitration profiling in different cell states. The results, discussed in the precedent chapter, showed that a very selective MS analysis may improve the dynamic range achievable by a mass spectrometer and enhance also the signal/noise ratio. However, dansyl chloride is not commercially available in C, N, O, S isotopic forms which prevents the development of a quantitative method. So far, the iTRAQ chemistry has been limited to primary amines. In this chapter it is reported a new strategy based on the use of iTRAQ reagents coupled to mass spectrometry analysis for the selective labelling and the “*quantitative detection*” of NO<sub>2</sub>Tyr residues. This method was proved to lead to the simultaneous localisation and quantification of nitration sites both in model proteins and in biological systems.

#### **3.1.1 Protein nitration quantification: state of the art**

Protein nitration quantification in biological samples is an analytical challenge. The main problem related to this kind of analysis is the low percentage of modified tyrosine residues that was measured to be NO<sub>2</sub>Tyr: tyrosine  $\approx$  1 ppm (1-2). This feature, coupled to the low mass increment of the modification (+45Da) and the diluted effect of protein iso-electric point decrease induced by Tyr nitration (3), makes it difficult to distinguish nitrated protein from the respective wild type by 2DE. Thus direct quantitative estimation based on spot intensity is not possible. In addition, the low quantity of nitrated peptides in biological samples leads to record low quality spectra. Therefore, if an accurate mass measurement coupled with short sequence coverage may sometimes allow to identify the nitration site, the quantitative analysis based on the MS signal intensity needs good quality of the peaks in terms of sharpness, signal/noise ratio and overlapping with isotope pattern of other signals. For these reasons, procedures allowing simultaneously to identify and quantify nitrated protein by classical Proteomics techniques, are not yet proposed. In fact the most important quantitative studies were addressed to the absolute estimation of the global level of NO<sub>2</sub>Tyr amino acid. Because NO<sub>2</sub>Tyr is considered as the best biomarker to detect oxidative damage *in vivo*, the first quantitative studies were addressed to develop clinical methods capable to correlate pathological states and concentration changes of basal free amino acidic NO<sub>2</sub>Tyr in biological fluids by absolute quantification. This was first accomplished by gas chromatography (GC) based techniques, performing analyses in Selected Ion Mode (SIM) and using an isotopically enriched 3-nitrotyrosine as internal standard (1, 2, 4). For the first time it

was possible to quantify NO<sub>2</sub>Tyr at biological levels with femto-nano molar sensitivity. Moreover it was also possible to estimate the ratio modified/unmodified free tyrosine *in vivo*. Further, the analysis was also extended to quantify the level of nitrated protein in biological samples (5). This was realized by the HCl hydrolysis of proteins to amino acid followed by the GC analysis of released tyrosine and nitrated tyrosine. For the sensitivity GC is considered as the “Gold standard” for the absolute quantification of NO<sub>2</sub>Tyr in biological fluids and tissues. Problems with the generation of NO<sub>2</sub>Tyr during sample processing, particularly during acid hydrolysis of proteins and derivatization of amino acids before the chromatographic separation, have been identified (6). Thornalley et al. (7) proposed the enzymatic hydrolysis of proteins with a cocktail of enzymes, however the recovery yield slightly decreased compared to acid hydrolysis (8). Although GC-MS analysis is a corroborated method to quantify NO<sub>2</sub>Tyr concentration, the required extensive silylation of amino acid enhances the complexity of the assay. Nitrated peptides and proteins were also detected by HPLC separation using different detectors. For example, derivatization of reduced NO<sub>2</sub>Tyr with fluorophore was used in order to make possible the selective detection by fluorescence (9). However, this approach is less sensitive and specific. Best results are obtained using an HPLC equipped with an electrochemical detector. In fact, NO<sub>2</sub>Tyr amino acid is detected in plasma with sensitivity comparable to that of GC, using the oxidation potential of 0,88V relative to the acetylated 3-aminotyrosine oxidation (10-11). Mass spectrometry was also coupled to HPLC for the absolute quantification of the global nitration extent in biological samples. In particular realizing ESI-MS<sup>2</sup> experiments based on the Multiple Reaction Monitoring (MRM) scan, using a triple quadrupole, or on the Single Reaction Monitoring (SRM), with an ion trap (12-13). MRM and SRM scans allow to detect only the parent ions that give peculiar MS<sup>2</sup> transitions, resulting in a very high duty cycle MS method improving the sensibility of the technique. Tyrosine (182 Da), nitrotyrosine (227 Da) and their isotopic internal standards (respectively 192 Da and 233 Da) were detected using the MS<sup>2</sup> neutral losses of ammonia (-17 Da) and formic acid (-46 Da). If all these methods for the global nitrated tyrosine estimation in biological fluids may be useful diagnostic tools, no functional information is provided by these strategies. In fact, more than NO<sub>2</sub>Tyr absolute measures, in order to understand the biological effect of the nitration, it is important to perform nitrated protein expression profiles in healthy/disease samples by using strategies leading to “quantitative identification”. Immunological approaches have been used to identify cellular sources of reactive nitrogen species and specific protein targets for modification (14-17). The use of 3-nitrotyrosine antibodies to perform ELISA analysis or western blot immuno-detection of 2DE fractionated protein, theoretically may allow at the same times to identify and to quantify the nitrated proteins. However, by using more accurate GC MS analysis, it was demonstrated that the immuno-detection based quantitative estimations were 10-100 folds overestimated (18). Isotope stable labelling techniques coupled to MS analysis would be an interesting approach that could lead to the quantification of identified nitro-peptides. However, none of the enrichment strategies summarized in the precedent chapter have proposed a “heavy” version of the tag used (19-20). As already cited in this paragraph (12-13) and demonstrated in the chapter 2 (21), high selective MS methods (MRM, SRM, PIS/MS3) allow to enhance the signal-noise ratio of free or peptide-bound nitrated tyrosine in low concentration. On this basis, we tried to set up a quantitative method based on the dansyl chloride strategy showed before. This was performed by using a deuterated heavy form of DNS-Cl. However a high percentage of modified peptides showed a deleterious deuterium effect causing a not perfect co-



peptide mixture are pooled and analyzed in the same LC-MS<sup>2</sup> run.

All the peptides with the same sequence, but carrying different versions of the tag will be chromatographically indistinguishable and identical in mass. Labelled peptides with the same sequence are also identical in MS mode, thus enhancing the sensitivity of the analysis because the MS signal is generated by the contribution of four samples. In addition because for any peptide a unique MS signal appears, the resulting spectra is not complicated by the analysis of four samples in the same time and this feature is very important for the duty cycle of LC-MS<sup>2</sup> method. Upon fragmentation, the reporter group is detached, creating signals in the “quite” low mass range region (114-117 Da) of the MS<sup>2</sup> spectrum. The balance group is lost as neutral moiety, so the remaining peptide backbone is unmodified and can generate backbone fragments that are identical in m/z for all samples, resulting in improved S/N ratios because all differentially coded samples contribute to MS<sup>2</sup> spectrum. Quantitative estimations are done calculating the peak area of the reporter ions, which ratios respect the original contribution of each peptide from the starting sample. Recently, an octu-plex iTRAQ kit has been proposed thus allowing the simultaneous analysis of eight different samples (23) Moreover, iTRAQ labelling coupled with pulsed Q dissociation technique has been recently proposed for protein quantification by ion traps avoiding the classical low mass cut off (24).

### **3.2 Materials and Methods**

#### **Chemicals**

Bovine serum albumin (BSA), tetranitromethane (TNM), ammonium bicarbonate (AMBIC), guanidine, dithiothreitol (DTT), trypsin, iodoacetamide (IAM) and triethyl ammonium carbonate (TEAB) were purchased from Fluka. Tris(hydroxymethyl)aminomethane, sodium dithionite as well as the MALDI matrix  $\alpha$ -ciano-4-idrossicinnamic acid were purchased from Sigma. iTRAQ reagents were furnished by Applied Biosystems. Methanol, trifluoroacetic acid (TFA) and acetonitrile (ACN) are HPLC grade type from Carlo Erba, whereas the other solvents are from Baker. Gel filtration columns PD-10 are from Pharmacia, the HPLC ones from Phenomenex, whereas the pre-packed columns Sep-pak C-18 are from Waters.

#### **BSA nitration.**

An aliquot of 200  $\mu$ g BSA was dissolved in Tris 200 mM pH 8.0 buffer and was added to a 830 nmol/ml solution of TNM in ACN in a molar ratio 1:10 BSA/TNM. The reaction was carried out under agitation for 30 min at room temperature. The mix of BSA and nitrated BSA (N-BSA) was then desalted by size exclusion chromatography on a SEPHADEX G-25M column; the elution was carried out with Tris 300 mM and the fractions analyzed through UV spectrometry at 220 and 280 nm wavelength. Positive fractions were collected and dried.

#### **Reduction and carboxamido-methylation of BSA.**

BSA and N-BSA mixture were dissolved in denaturation buffer (guanidine 6 M, Tris 0.3 M, EDTA 10 mM, pH 8.0). Reduction was carried out by using a 10:1 DTT/cysteine molar ratio. After incubation at 37°C for 2 h, iodoacetamide was added to perform carboxamidomethylation using an excess of alkylating agent of 5:1 respect to the moles of thiolic groups. The mixture was then incubated in the dark at room temperature for 30 min. The alkylation reaction was stopped by addition of formic

acid, in order to achieve an acidic pH. The product was purified by size exclusion chromatography. The elution was performed with TEAB 50 mM pH 8.0.

**BSA digestion.** Protein digestion was carried out in TEAB 50mM pH 8.0 buffer using trypsin at a 50:1 protein : trypsin mass ratio. The sample was incubated at 37°C for 16 h. Then the sample was dried.

**Acetylation of peptide mixture.** Peptide mixture was dissolved in 30% TEAB 500mM pH 8.0, 70% ACN. Acetylation was performed by using acetic acid N-hydroxy-succinimide ester in molar ratio 500:1 reagent / peptides. The reaction was carried out for 1 h at room temperature.

**Nitro groups reduction.** Reduction of nitro groups to amino groups was performed by adding  $\text{Na}_2\text{S}_2\text{O}_4$  at 100:1  $\text{Na}_2\text{S}_2\text{O}_4/\text{NO}_2\text{Tyr}$  molar ratio. The reaction was carried out at room temperature for 10 min under stable stir. The product was purified by SEP-PAK RP-LC with C18 column. Peptides were eluted using 80% ACN, 20% formic acid 0.1%. Fractions were collected and lyophilized.

**Bacterial strains, growth conditions and protein extract preparation** Escherichia coli K12 strain was grown in aerobic conditions at 37°C in LB medium. After 16 h, bacteria were harvested by centrifugation and resuspended in Buffer Z (25 mM HEPES pH 7.6, 50 mM KCl, 12.5 mM  $\text{MgCl}_2$ , 1 mM DTT, 20% glycerol, 0.1% triton) containing 1  $\mu\text{M}$  phenyl methyl sulfonyl fluoride. Cells were disrupted by sonication. The suspension was centrifuged at 90,000 x g for 30 min at 4°C. After centrifugation the protein concentration of the extract was determined with Bradford assay.

**iTRAQ selective labelling.** Sample was dissolved in TEAB 500mM pH 8.0 and then was divided in two tubes and each of these was differentially labelled with alternatively iTRAQ reagent 114 and iTRAQ reagent 117, following iTRAQ protocol furnished by Applied Biosystem.

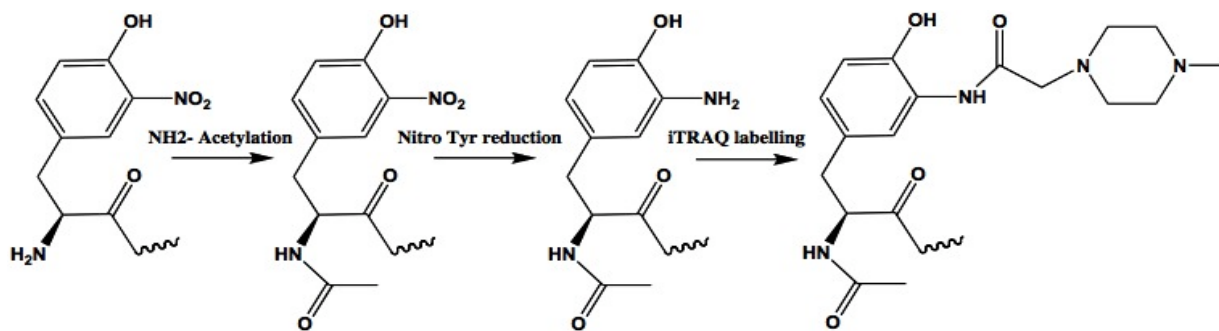
**Labelling of Bovine Milk Protein Extract.** A sample of commercially available bovine milk was reacted with a 10 mM solution of TNM for 30 min under agitation at room temperature. Modified milk proteins were purified by precipitation with the Amersham Clean Up kit and dissolved in denaturant buffer. Reduction was carried out by using a 10:1 DTT / cysteine molar ratio. After incubation at 37°C for 2 h, iodoacetamide was added to perform carboxamido methylation using an excess of alkylating agent of 5:1 respect to the moles of thiolic groups. The mixture was then incubated in the dark at room temperature for 30 min. The alkylation reaction was stopped by addition of formic acid, in order to achieve an acidic pH. The protein mixture was purified by size exclusion chromatography on a Sephadex G-25 M column equilibrated and eluted with 50 mM TEAB. Protein fractions were concentrated and then digested with trypsin as already described. The resulting peptide mixture was acetylated and the nitro groups were reduced using a 200 mM solution of  $\text{Na}_2\text{S}_2\text{O}_4$  for 30 min. The protein mixture was then reacted with ITRAQ as described above.

**nanoLC Mass Spectrometry.** Peptide mixture, obtained as previously described, was analysed by LCMS<sup>2</sup> analysis using a 4000Q-Trap (Applied Biosystems) equipped with a linear ion trap coupled to an 1100 nano HPLC system (Agilent

Technologies). The mixture was loaded on an Agilent reverse-phase pre-column cartridge (Zorbax 300 SB-C18, 5x0.3 mm, 5  $\mu$ m) at 10  $\mu$ L/min (A solvent 0.1% formic acid, loading time 7 min). Peptides were separated on a Agilent reverse-phase column (Zorbax 300 SB-C18, 150 mm X 75 $\mu$ m, 3.5  $\mu$ m), at a flow rate of 0.2  $\mu$ L/min with a 5 to 65% linear gradient in 60 min (A solvent 0.1% formic acid, 2% ACN in water; B solvent 0.1% formic acid, 2% water in ACN). Nanospray source was used at 2.3 kV with liquid coupling, with a declustering potential of 20 V, using an uncoated silica tip from NewObjectives (O.D. 150  $\mu$ m, I.D. 20  $\mu$ m, T.D. 10  $\mu$ m). Spectra acquisition was based on a survey Precursor Ion Scanning for the ion m/z 114 and 117. It was performed over a mass range of m/z 400-1400 with Q1 set to low resolution and Q3 set to unit resolution. Precursors were collided in Q2 with a collision energy ramp of 25 to 65 V across the mass range. Spectra acquisition was based on a survey Precursor Ion Scan. A positive ion Enhanced Resolution Scan was performed at 250amu/s to determine the charge state of the ion. Enhanced Product Ion (EPI) scans ( $MS^2$ ) were performed at 4000 amu/s and collision voltages were calculated automatically by rolling collision energy and it performed a maximum of one repeat before adding ion to the exclusion list for 60 s. Once this duty cycle was completed, the polarity was switched back and the cycle repeated. The entire cycle duration, including fill times and processing times was less than 5.3 s. Data were acquired and processed using Analyst software (Applied Biosystems) and processed by using MASCOT in house software.

### **3.3 RESULTS AND DISCUSSION**

Molecules modified by oxidation, nitration and nitrosilation can act as cellular biomarkers. Identification of the specific targets of protein oxidation was generally accomplished by the detection and quantification of  $NO_2$ Tyr using 2-DE and Western blot techniques followed by mass spectral identification of candidate proteins (25). However, these procedures generally led to the identification of nitrated proteins but the fine localization and quantification of the nitration sites in complex protein mixture still remain a challenging task. In the precedent chapter, it was showed a strategy leading to the selective detection of nitrated tyrosine residues by using dansyl chloride labelling coupled to advanced mass spectrometry experiments (21). The proposed strategy has showed to be specific, sensitive, simple and fast. Because no heavy form of dansyl chloride is commercially available, quantitative analysis of complex protein mixtures cannot be addressed directly. However the improvements given by selective MS analysis could make possible the “quantitative identification” of nitrated proteins. For its structural features it was found iTRAQ as “RIGHt” reagent to achieve this result. The idea proposed is outlined in the Scheme 1. According to the so-called “gel-free procedures”, the analysis is carried out at peptide levels following tryptic digest of the whole protein mixture. This approach was first applied to bovine serum albumin as model protein. Two hundred  $\mu$ g of BSA were nitrated using TNM as described in materials and methods section. Then the resulting BSA and N-BSA mixture was reduced, alkylated and hydrolyzed using trypsin. The peptide mixture was then analyzed via MALDI-MS to verify the extent of nitration.



**Scheme 1**

**Scheme 3.1.** Strategy for selective labelling of 3-nitrotyrosine residues.

BSA is a protein of about 66 kDa, showing 20 tyrosine residues along its sequence. However mass spectral analyses demonstrated that *in vitro* nitration was limited to only few tyrosine residues, namely the ones exposed in the structure of the protein and thus more sensitive to nitration. Nitrated peptides were identified by MALDI mapping procedure, by comparing the experimental peptides masses with the theoretical values on the basis of amino acid sequences. As already reported a  $\Delta M$  of +45 was attributed to the modified peptide, due to introduction of a nitro-group (26). Figure 1 (panel A and B) showed partial MALDI-MS spectrum of the tryptic BSA and N-BSA mixture. As an example, the signals occurring at  $m/z$  972.5, 1524.8 showed molecular masses 45 Da higher than the theoretical ones. These signals were attributed to the peptides 137-143, 396-408, having the Tyr residue been modified by a nitro group. As a whole, the MALDI-MS analysis showed the occurrence of four signals exhibiting a mass increment of 45 Da. These signals were attributed to the nitro-peptides 137-143, 396-408, 322-334, 444-457 (at  $m/z$  972.5, 1524.8, 1612.9, 1770.8, respectively) As further proof, these signals exhibited the characteristic pattern of nitrated peptides, due to photodecomposition of nitrated tyrosine residues by MALDI source (26).

In the previous chapter, the selective labelling of 3-nitrotyrosine residues was essentially based on a reduction step and conversion to 3-aminotyrosine residues followed by specific dansylation at pH 5.0. A similar approach was attempted here. However, iTRAQ labelling does not permit to exploit the low pKa value (3) of such amine to obtain a selective labelling, as observed for the dansyl-chloride strategy. Only a small percentage of primary aromatic amine modification by iTRAQ was observed. This behavior may be explained by the faster rate of hydrolysis of both the iTRAQ N-hydroxysuccinimide-ester group and the formed aminotyrosine-iTRAQ derivative in mild acidic conditions (27).

Thus, it was necessary to set up a double step procedure. First of all, lysine residues and N-terminus primary amine were protected to facilitate specific labelling of the 3-nitrotyrosine residues. Blocking can be easily performed under mild conditions by a variety of reagents that are commercially available. In fact, several strategies to introduce  $\text{NH}_2$ - labels have been described (28-29). Generally, it is not possible to reliably control the selectivity of the reaction, because the  $\epsilon$ -amino group of lysine is readily and stably modified by reagents that target the N-terminus (30-31). Blocking the N-terminus and the lysine side chain can be done either prior or after the enzymatic digestion of the sample. By blocking the lysines after digestion, we retained the ability to use trypsin as enzyme for proteolytic cleavage.

Preliminary acetylation experiments were performed by using acetic anhydride as reagent and peptide mixture obtained from trypsin digestion of myoglobin, as model. MALDI-MS analysis performed on the resulting peptide mixture showed that the acetylation reaction was not quantitative. Thus, we decided to use acetic acid N-hydroxy-succinimide ester as reagent since it has been shown to lead to an efficient lysine acetylation (32). The yield of the reaction was monitored by MALDI-MS. As an example Figure 3.2 reports the partial MALDI-MS spectrum of the acetylated myoglobin tryptic mixture. The signal at  $m/z$  1649.2 was attributed to the peptide fragment 18-23 carrying an acetyl group, fully modified. No signal related to the unmodified peptide was observed thus indicating that the acetylation was quantitative.

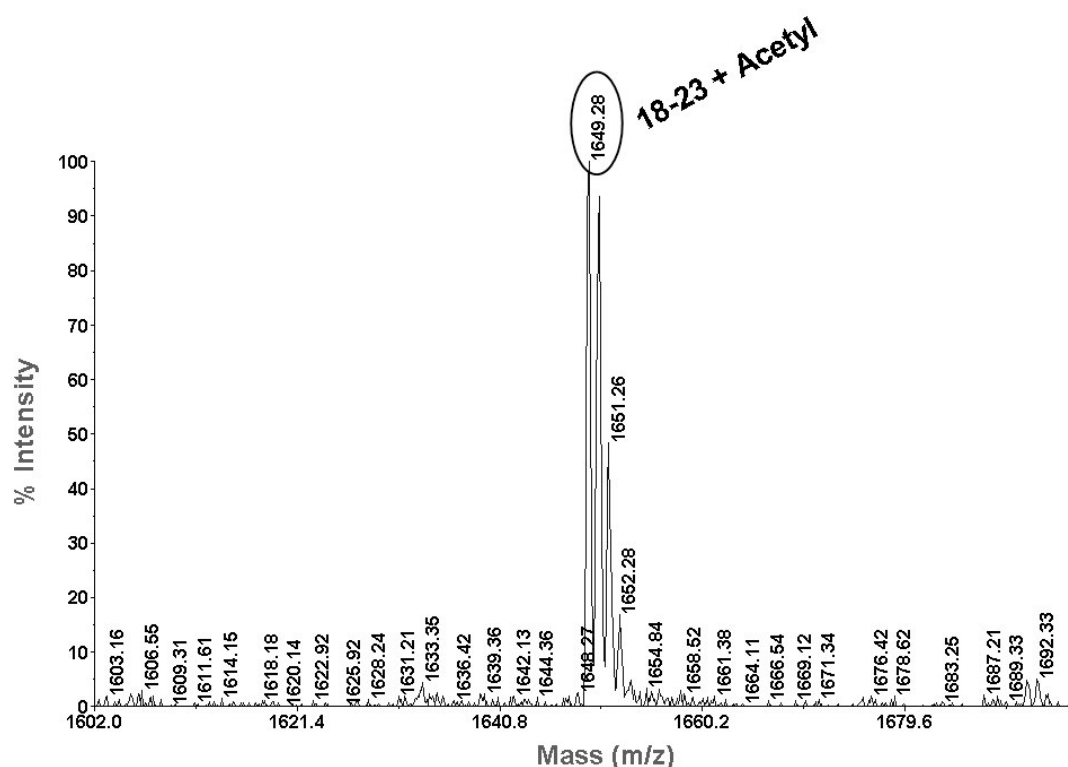


**Figure 3.2.** Detail of MALDI-MS spectrum of acetylated myoglobin showing peptide 18-23 with acetylated N-terminus; there are no evidence in the spectrum for non acetylated form of the same peptide.

Thus, nitrated peptides were subjected to the acetylation using acetic acid N-hydroxy-succinimide ester as described in material and methods section. All the successive analyses revealed that every peptide detected had the N-term amine and eventually the  $\epsilon$ -amino group of lysine protected. Only after the acetylation step it was possible to reduce the nitro-group of 3-nitrotyrosine residues to an amino group, susceptible to iTRAQ addition. Conversion of nitropeptides into their amino derivatives was accomplished by  $\text{Na}_2\text{S}_2\text{O}_4$  treatment. The peptide mixture was desalted by sep-pak C18 cartridge and the extent of reduction was monitored by MALDI-MS.

As for quantitative analysis, labelling reaction was carried out on the newly generated amino groups by following the default protocol. iTRAQ technology (trademarked by Applied Biosystems), allows quantitative analysis of protein expression through the use of isobaric tags, enabling the quantitation of four (22) to eight complex protein samples (23) in a single multiplexed analysis.

As an example to illustrate the possibility to use iTRAQ labelling strategy for selective quantitative analysis of 3-nitrotyrosine residues and at the same time to reduce the costs, we decided to carry out our methodology just on a duplex. Thus we analyzed only two samples and we choose iTRAQ 114 and iTRAQ 117 as labelling reagents. After the labelling, the resulting samples, N-BSA(114) and N-BSA (117), were pooled in molar ratio 1:1 and 1:4 respectively. The two mix (1:1 and 1:4) were then submitted to LC-MS<sup>2</sup> analysis in PIS mode, by using a 4000QTrap coupled with a 1100 nano HPLC system, thus allowing the simultaneous identification and quantification of differentially labelled peptides in a single chromatographic run. Thus, we set up an experiment by using a precursor ion scan (PIS) for the iTRAQ reporter ions at m/z 117.1. Moreover, in order to demonstrate that the choice of the fragment to monitor nitrated peptides in PIS mode is un-relevant, because of the isobaric characteristic of the iTRAQ, we decided to analyze the same sample in two separate chromatographic runs, the first in PIS of ion 114.1 and the second in PIS of ion 117.1.

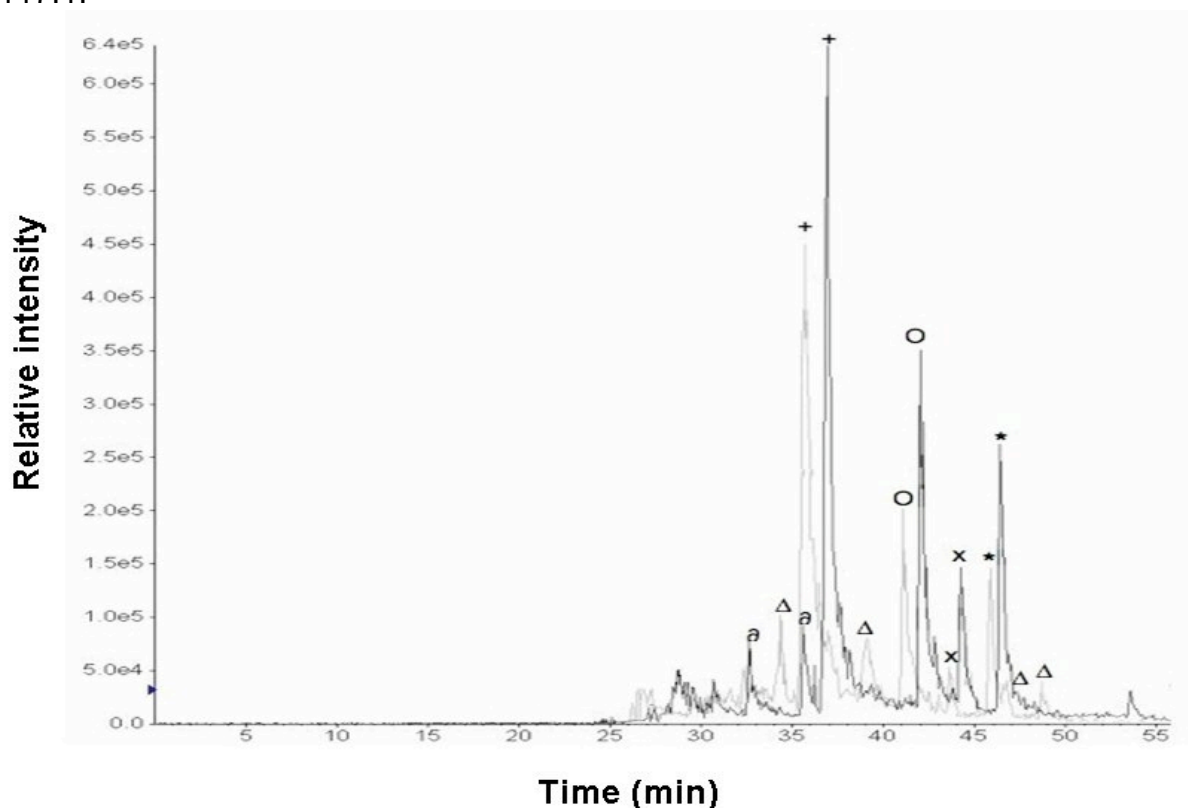


**Figure 3.3.** Overlapped chromatograms of nitrated BSA recorded by PIS analysis of ions 114 (grey line) and 117 (bold line) respectively. The chromatogram of PIS 114 is shifted back of 1 minute to have a better comparison of signals. The symbols +, O, X, \*, are referred to BSA nitrated peptides 137-143, 396-408, 444-457, 322-334, respectively. The symbols Δ, ∂ are referred to BSA un-specific peptides detected in PIS of 114 and PIS of 117 respectively.

As shown in the Figure 3.3, the two chromatographic profiles are quite identical and super imposable, differing just in the total ion current intensity that reflects the original ratio 1:4 between the two samples. In fact, it should be noted that PIS ion current is recorded from the fragment generated in MS<sup>2</sup> and no memory is retained about the intensity of the parent ion. To gain information about the sequence of the peptide and the site of nitration, a second stage of mass analysis is performed in which the precursor ion is selected by the first mass analyzer and fragmented. Differentially labelled peptides were indistinguishable during a single step of MS analysis due to

typical characteristics of iTRAQ reagents. During MS<sup>2</sup>, labelled peptides produce fragmentation spectra that allow the identification of the protein. Moreover, MS<sup>2</sup> produces fragmentation at the sites modified by the iTRAQ reagent yielding the reporter ions (m/z 114 and 117) that are visible as separated peaks in the low mass region of the MS<sup>2</sup> spectrum. The ratios of the areas of these peaks were then used to perform a relative quantitative analysis (33-34). Figure 3.4 shows the reconstructed ion chromatogram of the 1:1 N-BSA sample analyzed by precursor ion scan of 117 (A) and a classical full scan MS (B).

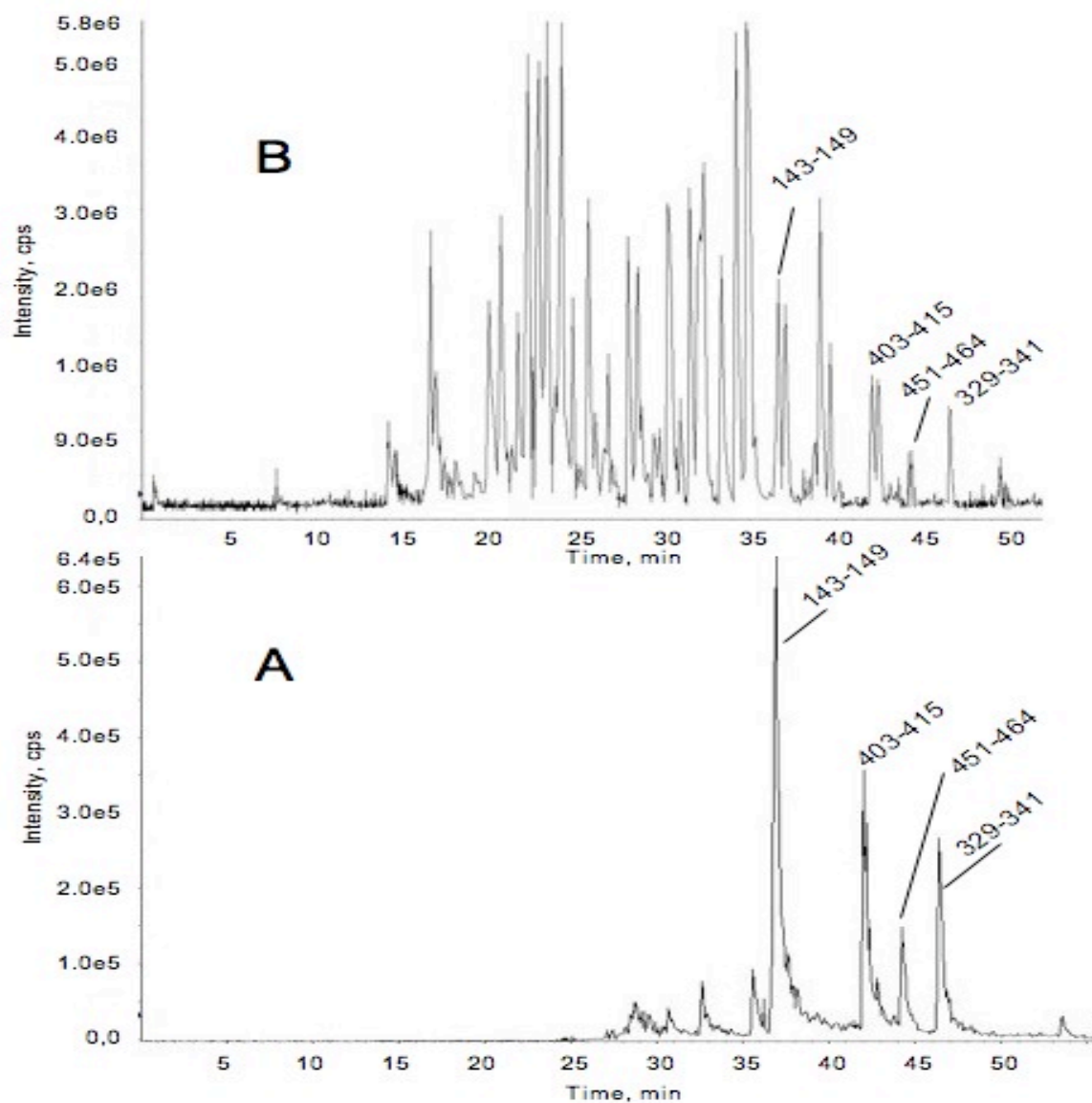


**Figure 3.4.** *Panel A* Chromatogram of nitrated BSA recorded in PIS 117. *Panel B* Chromatogram of nitrated BSA recorded in a full scan MS mode.

As clearly shown, the PIS analysis led to reduce the number of un-desired signals, improving also the duty cycle of the method and the sensitivity toward nitro-peptides enhancing signal/noise ratio. However, others signals appear in the chromatogram not related to nitrated peptides. This effect might be generated by the presence of different fragment ions in the region 113-114 or 116-117, many of which generated after the acetylation step (Table 3.1). For this reason we used the 114 and 117 iTRAQ reagents, in order to have the worst condition of selectivity and demonstrate the feasibility of the proposed methodology. An accurate manual analysis of MS<sup>2</sup>

spectra revealed that many false positive were selected for the presence of  $m/z$  114 fragment whose intensity would be negligible on the quantitative estimation (Figure 5). To enhance the selectivity of the analysis made by the 4000QTrap, we also tried to introduce an  $MS^3$  event as done in dansyl-based strategy (21). In particular we tried to fragment the  $MS^2$  ion at  $m/z$  145 and monitor the loss of CO giving rise to the peculiar reporter ions of iTRAQ in  $MS^3$  mode. A preliminary experiment revealed that  $MS^3$  spectra exhibited a very poor intensity caused by the low yield of ion fragment at  $m/z$  145 in  $MS^2$  mode. Thus, we found that to enhance the selectivity of LC/ $MS^2$  analysis good results were obtained increasing the signal threshold of PIS using the great difference in signal intensity between the iTRAQ reporter ions and others mentioned previously (Table 3.1).

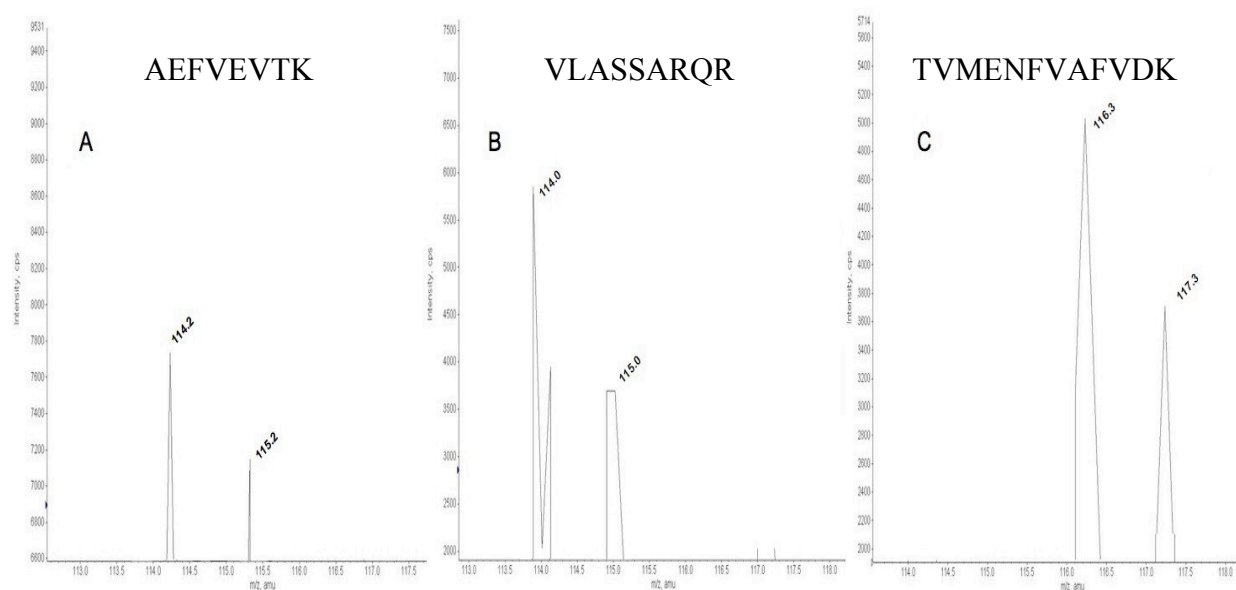


**Figure 3.5.**  $MS^2$  spectra enlargement of characteristic iTRAQ  $m/z$  region of non specifically detected BSA peptides. **Panel A** peptide AEFVEVTK was detected in PIS 114 due the presence of an acetylated  $b_1$  ion of alanine residue at  $m/z$  114.2. **Panel B** peptide VLASSARQR was detected in PIS114 mode because of the presence of an acetylated immonium ion of valine at  $m/z$  114.0. **Panel C** peptide TVMENFVAFVDK was detected in PIS 117 mode because of the presence of an acetylated immonium ion of threonine at  $m/z$  116.3 or its isotope.

In these operative conditions, we inferred that our LC/ $MS^2$  method for the 4000QTrap analysis resulted to be a good compromise between selectivity and sensitivity that are fundamental parameters in nitro-proteome analysis because of the sub-stoichiometric characteristic of protein nitration. In fact we want to underline that, without any chromatographic nitro-peptide enrichment, just using the mass spectrometer gas phase fractionation features, we had eliminated about 96% of BSA un-desired peptides detected with a classical LC/ $MS^2$  approach. Furthermore if eventually, in a borderline case, the detection of a false positive may complicate the analysis, the sample may be re-analyzed inverting the diagnostic iTRAQ reporter ion monitored by PIS analysis. Indeed un-specific ions detected in PIS of 114 were not detected in PIS of 117 and *vice versa*. Identification of nitrated tyrosine residues was carried out by taking advantage of the flexibility of the in house MASCOT software. The software was properly modified by adding in the “modification file” the value of  $\Delta M$  159 for iTRAQ labelled amino-tyrosine residue. For Mascot analysis it was necessary to set the software supplying key information, e.g. proteolytic enzyme, fixed modifications, variable modifications, sample taxonomy, eventually missed cleavage, etc. The data obtained from  $MS^2$  analysis in PIS mode were exploited

Interfering ions	Mass	Peptides	Scan
(Ac)b1 Ala	114.1	(Ac)ADE(Ac)K(Ac)KFWGK(Ac)	PIS 114
(Ac)b1 Ala	114.1	(Ac)AEFVEVTK(Ac)	PIS 114
(Ac)Immonium Val	114.1	(Ac)VLISSARQR	PIS 114
(Ac)Immonium Val	114.1	(Ac)VH(Ac)KECCHGDLLECADDR	PIS 114
(Ac)Immonium Thr	116.1	(Ac)TCVADESHACCEK(Ac)	PIS 117
(Ac)Immonium Thr	116.1	(Ac)TVMENFVAFVDK(Ac)	PIS 117

**TABLE 3.1.** Un-labelled BSA peptides and their precursor detected in PIS 114 and PIS 117 mode.

both to identify nitration sites by using SwissProt database and to perform quantitative analysis.

Nitration sites Y137, Y406, Y457, Y337 were identified by the detection and by MS<sup>2</sup> spectra interpretation from MH<sup>2+</sup> ions at m/z 564.8, 841.0, 963.5, 885.3, respectively. As an example the MS<sup>2</sup> spectrum of modified peptide 137-143 is shown in Figure 3.6A. The derivatized product ions were identified from either the corresponding *b<sub>n</sub>* or *y<sub>n</sub>* product ion series. By using the Analyst software tool for calculation of peaks area (Applied Biosystems), it was possible to compare the areas signals relative to reporter ions at m/z 114 and 117. As an example, for the MS<sup>2</sup> spectrum mentioned above a ratio of 1.1 + 0.2 was calculated.

Figure 3.6B showed the MS<sup>2</sup> spectrum relative to the peptide 444-457 for the mixture 1:4 molar ratios between N-BSA labelled with iTRAQ 114 and N-BSA labelled with iTRAQ 117. In this case nitration site was detectable from *y* ions and the area ratios for the reporter ions at m/z 117 and 114 resulted to be 4.1 + 0.4, thus providing an accurate measurement of the relative abundance of each nitrated peptide. Moreover, the presence of an intense iTRAQ-labelled amino tyrosine immonium ion at 292.1 m/z could be detected in both spectra (Fig. 3.6). This ion might be used as an indication for the occurrence of a nitration site in the peptide.

### Analysis of complex mixtures

In a proof of principle, to investigate the feasibility of applying the method to proteomic analysis, a model system was constituted by adding 5 ng of protein mix containing BSA and N-BSA to 30 mg of an *E.coli* entire soluble protein extract. Aliquots of mix of BSA and N-BSA, as control, and *E.coli* extract spiked with BSA mix were fractionated by SDS-PAGE and submitted to a western blot analysis using anti-nitrotyrosine antibody as indicated in Figure 3.7. The analysis showed that the amount of N-BSA was quite impossible to differentiate from the other bacterial proteins. Moreover, in lane D is possible to appreciate that the sample used could be considered similar to a “dirty” N-BSA *E. coli* protein extract, thus being a good candidate for the nitro-proteome study. The total protein extract was then submitted to the procedure described above. The mixture was hydrolyzed with trypsin and lysine residues were protected by acetylation. Nitrotyrosines were then reduced with dithionite, and the newly generated amino Tyr-containing peptides were submitted to the iTRAQ labelling protocol, using 114 iTRAQ molecule.

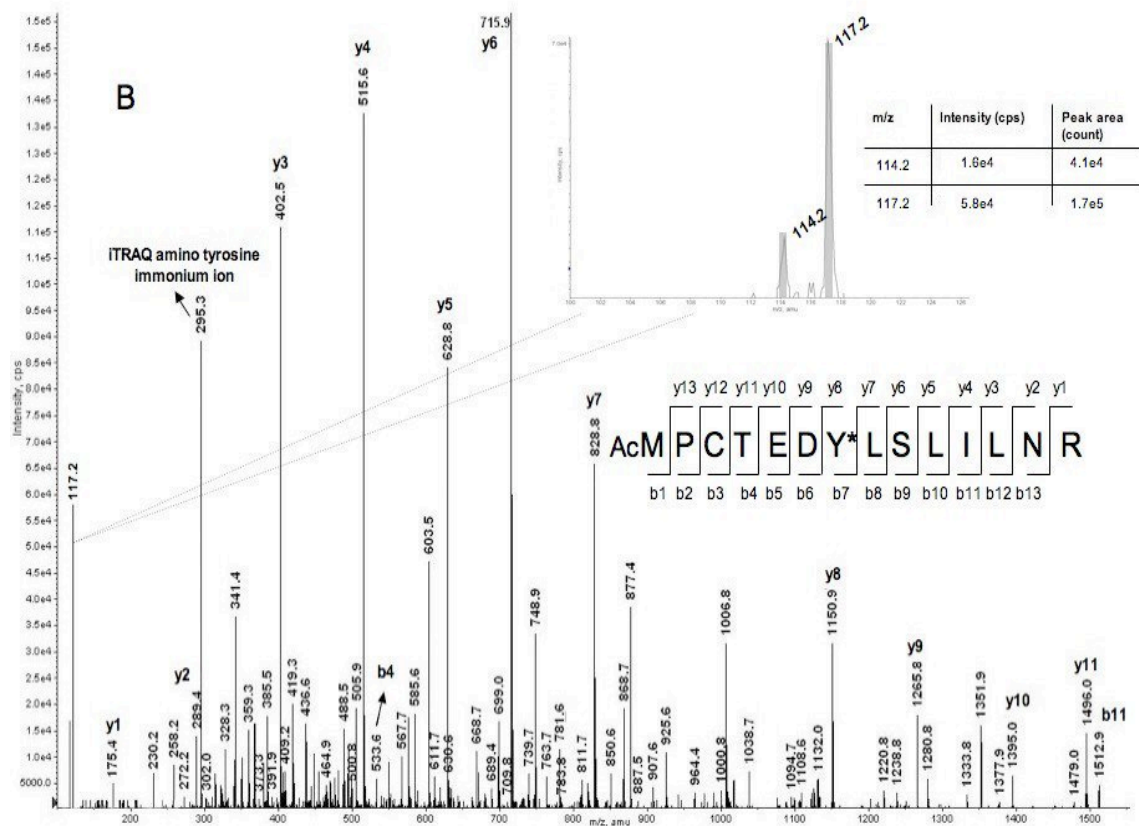
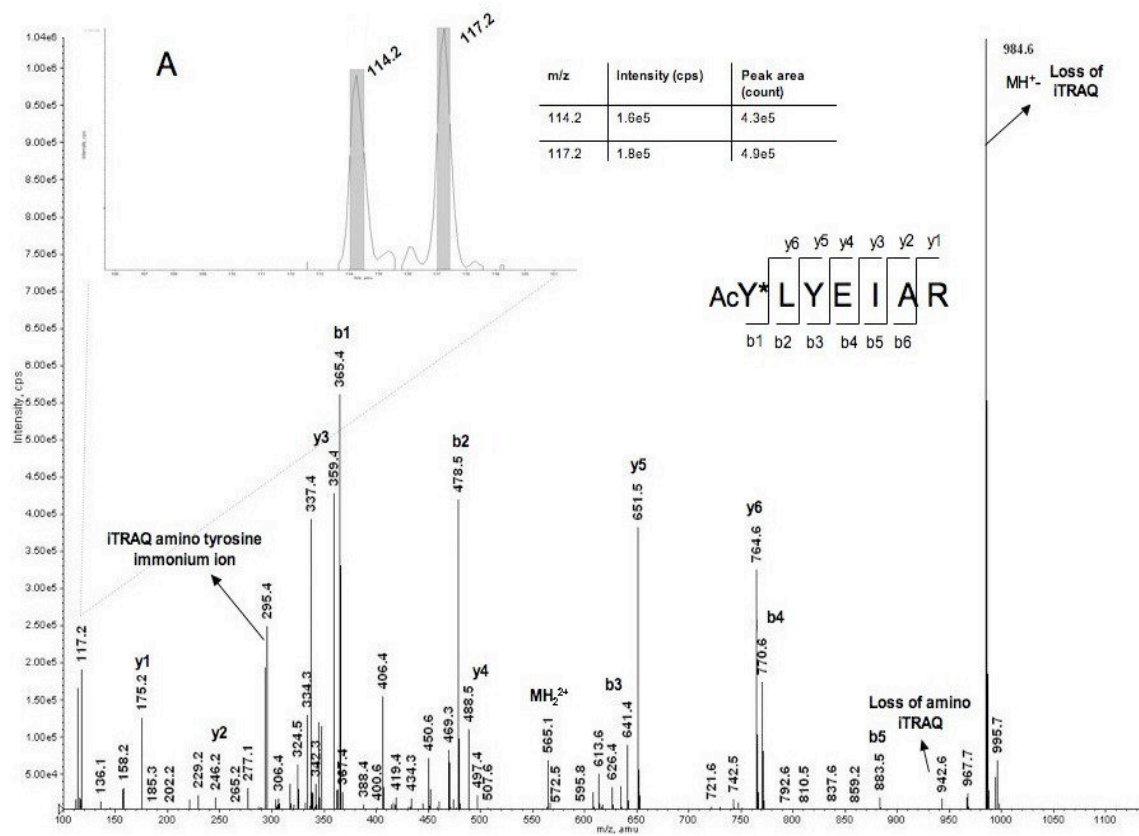


**Figure 3.6. Panel A** MS<sup>2</sup> spectrum of nitrated BSA peptide 137-143 labelled by iTRAQ reagent in 1:1 ratio. **Panel B** MS<sup>2</sup> spectrum of nitrated BSA peptide 444-457 labelled by iTRAQ reagent in 1:4 ratio. Spectra enlargement showed iTRAQ signals allowing quantitative estimation.

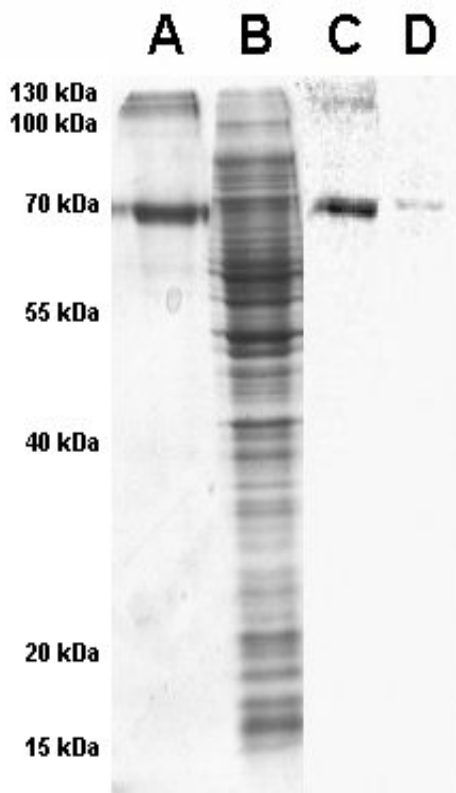


**Figure 3.7.** SDS-PAGE and western blot analyses of *E.coli* protein digest spiked with nitrated BSA (lane B) where N- BSA band was indistinguishable by the others. Lane A: Standard mix of BSA and N-BSA as control. Lanes C and D :western blot analysis by using anti-nitrotyrosine antibody of control and *E. coli* samples, respectively.

After the labelling reaction, LC-MS<sup>2</sup> analysis of the mixture was performed by using the 4000QTrap, as already described. Figure 3.8 shows a three-dimensional graphic, defined as Counter Plot, representing LC-MS<sup>2</sup> parameters, namely elution time, m/z and ion counts expressed in greyscale intensity. This graphical view, obtained by the Analyst software tool, showed the duty cycle and sensitivity improvement of the strategy proposed. A full scan MS analysis of N-BSA spiked with an entire digest of *E.coli* protein extract is reported Figure 3.8A. As clearly shown in figure, this MS analysis is not competitive for such complex peptide mixture. Indeed, due to the large time spent by the spectrometer analyzing the most abundant peptides, only 3 of 4 nitrated peptides present in the mixture were detected. The high selectivity of the optimized PIS analysis (Fig. 3.8B) greatly reduced the number of analyzed species, leading to a real increase in sensitivity. Protein Identification of nitrated proteins was

carried out using the modified MASCOT software as described above. These peptides corresponded to the same peptides previously detected in the analysis of homogeneous nitrated BSA. Thus, our results underscored the ability of the proposed selective labelling strategy to discriminate nitropeptides from their unmodified counterparts in a complex matrix. The proposed strategy was finally employed to identify unknown 3-nitrotyrosine residues in a complex sample as the entire bovine milk. Bovine milk was in vitro nitrated with TNM and the extent of nitration was monitored by SDS-PAGE and western blot analysis as described above. Figure 3.9 (lane A) showed that the high difference of milk protein abundance in the sample reflected the high dynamic range features of the proteomic analysis. In addition the immuno-detection (lane B) showed the low extent of protein nitration thus indicating that this model system could be suitable for the proteomic analysis. The entire milk protein extract was then dissolved in denaturant buffer, and cysteine alkylation and nitro groups reduction were performed “one pot” as described in the Materials and Methods section. Two protein samples were then desalted and digested with trypsin. The resulting peptide mixtures were acetylated, differentially labelled with iTRAQ reagents (114 and 117) and mixed in molar ratios of 1:1 and 1:4. The samples were then selectively analyzed by nano-LC/MS<sup>2</sup> in PIS mode for the reporter ion at m/z 117.

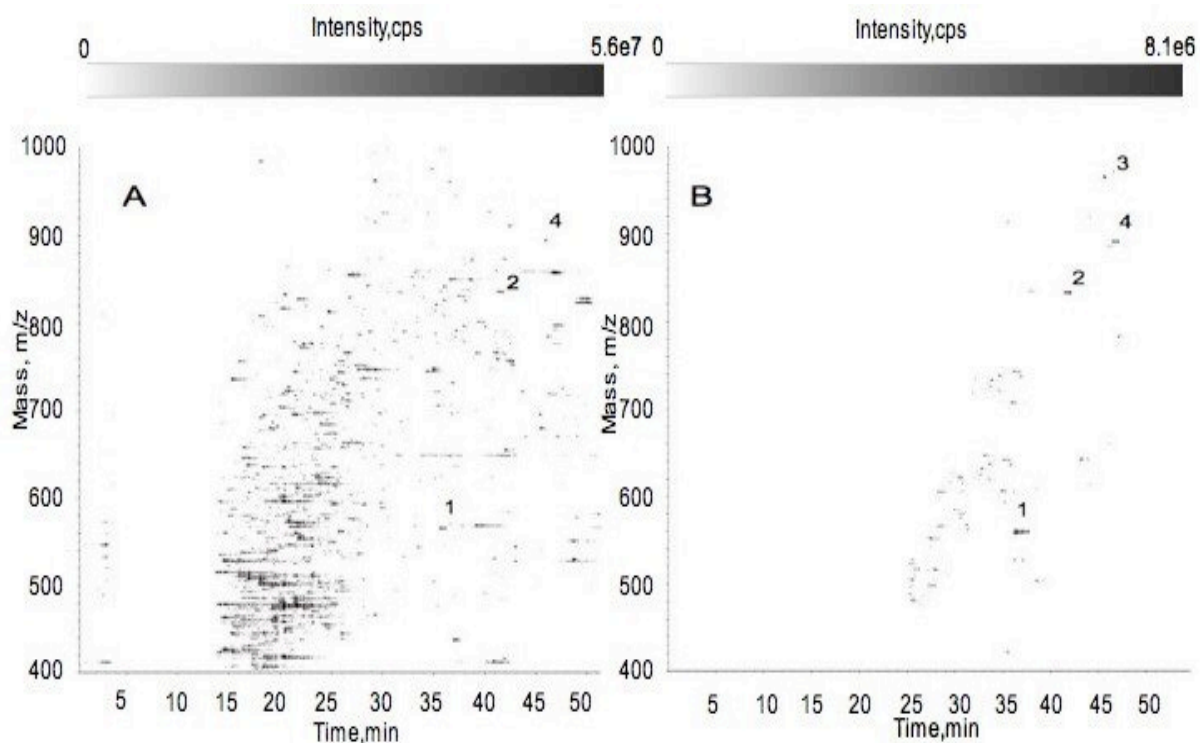


**Figure 3.8.** Counter plot representation of a whole *E.coli* protein digest spiked with nitrated BSA analyzed, by a classical full scan MS (Panel A) and PIS (Panel B) after iTRAQ selective labelling.

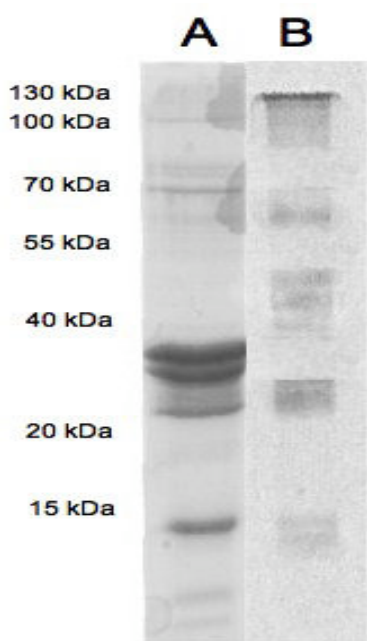


**Figure 3.9.** SDS-PAGE (lane A) and western blot analysis by using anti-nitrotyrosine antibody (lane B) of *in vitro* nitrated milk proteins.

Identification of nitrated milk proteins was carried out using the modified MASCOT software as described. The results obtained were mediated on triplicate analyses and are summarized in the Table 3.2. As indicated in the table, besides the high-abundant milk proteins ( $\alpha$ -casein and  $\beta$ -lactoglobulin), this procedure was also able to assess the nitration sites occurring in low-abundant proteins, like Vimentin and Integrin thus demonstrating the feasibility of this strategy for the identification of protein nitration in proteomics. Concerning for the quantifications, we realized the quantitative estimation of 7/9 nitrated peptides. In fact, the spectra of the two lower abundant proteins, although let us to unequivocally identify the nitration site, were too weak to make an accurate quantitative measure all over the signals. Figure 3.10 the MS<sup>2</sup> spectrum of a nitrated peptide within  $\alpha$ -casein is shown. It is interesting to note that the occurrence of an acetylated threonine residue at N-terminal position does not affect the quantitative estimation.

### **3.4 CONCLUSIONS**

The iTRAQ approach has been successfully applied to a variety of prokaryotic and eukaryotic samples including *Escherichia coli*, yeast, human saliva, human fibroblasts and mammary epithelial cells to identify and

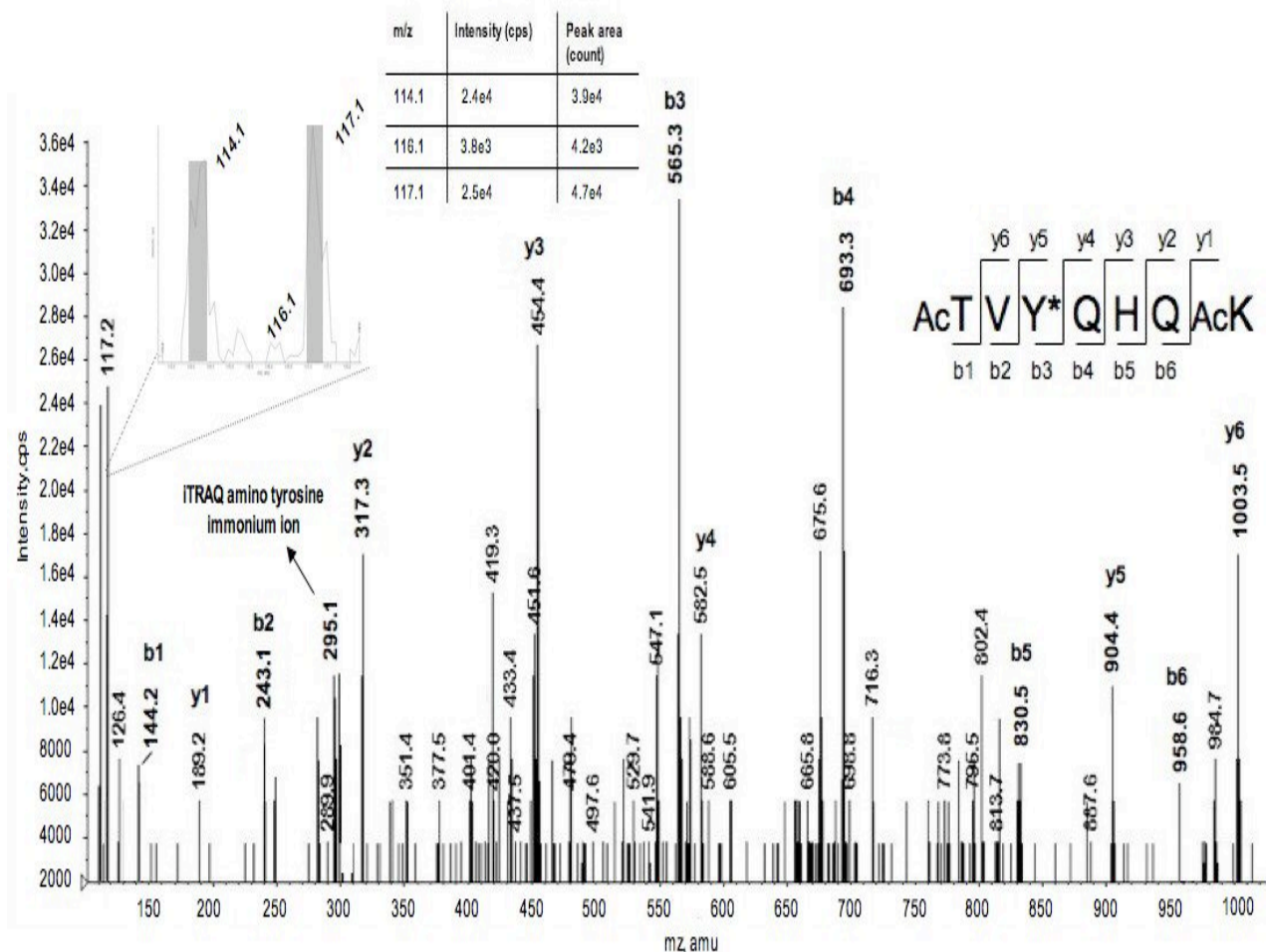


**Figure 3.10** MS<sup>2</sup> spectrum of  $\alpha$ -Casein nitrated peptide TVYQHQK detected in an *in vitro* nitrated milk proteins extract. In the spectrum enlargement of iTRAQ mass region, the characteristic signals of the reporter ions and a signal at m/z 116.1 of acetylated threonine immonium ion are visible.

quantify the proteins in these samples (35-36). Zhang et al. (37) combined the iTRAQ labelling approach with immunoprecipitation to quantify tyrosine phosphorylated peptides epithelial cells.

However, iTRAQ has been also applied to identify and quantify protein level in shotgun proteomics approach (38-39). This work represents the first innovative application of iTRAQ labelling strategy to the analysis of post-translational modification. In particular we addressed the analysis of protein nitration, thus providing a powerful analytical method to identify nitrated protein, localize tyrosine nitration sites and to quantify the extent of protein nitration in a single experiment.

The newly developed procedure was successfully tested on complex biological systems (manuscript in preparation), to assess its feasibility for proteomic investigation of nitroproteins. Here the strategy proposed, taking in account the availability of linear ion trap to select specific labelled peptides giving rise to diagnostic MS<sup>2</sup> product ions, resulted to be of interest in the selective detection of protein nitration. Moreover, because of its operational simplicity, avoiding long-lasting and time-consuming fractionation procedures, this new strategy seems to be well suited for the large-scale quantitative profiling of nitration sites. Because of the cost of iTRAQ kits, it is preferable to integrate the previously proposed method to selectively identify nitration sites on a screening scale and further select the samples

<b>m/z OBSERVED</b>	<b>SCORE</b>	<b>SEQUENCE</b>	<b>RATIO 114/117</b>	<b>PROTEIN ACC. NUMB.</b>
740.2	59	(Ac)VLVDTY*K(Ac)K(Ac)	4.1±0.1 1.2±0.2	Beta-Lactoglobulin P02754
796.5	49	(Ac)DMPIQAFLLY*QEPVLPVVR	3.8±0.4 0.9±0.2	Beta-Casein P02666
573.5	44	(Ac)TVY*QHQQ(Ac)	4.3±0.2 1.2±0.3	Alpha-s1-Casein P02663
568.8	42	(Ac)Y*LYEIAR	3.9±0.1 0.8±0.3	Albumin bovine P02769
426.8	36	(Ac)ADLIAY*LK(Ac)K(Ac)	4.1±0.4 1.3±0.2	Cytochrome c P62849
716.3	34	(Ac)STRTVSSSSY*R	4.1±0.4 1.2±0.4	Vimentin P48616
617.4	30	(Ac)AY*PTPARSK(Ac)	4.2±0.7 1.4±0.3	Glycoprotein hormones alpha chain P01217
565.9	29	(Ac)HFHLY*GR	5.2±1.6 1.8±0.9	Integrin alpha-L P61625
559.8	29	(Ac)LELY*LPK(Ac)	7.1±3.4 1.8±1.2	Plasma serineprotease inhibitor Q9N212

**TABLE 3.2.** Nitrated milk Proteins detected by the selective iTRAQ labelling strategy coupled with a selective PIS-MS analysis

to be of interest for quantitative analysis. The strategy reported here was set up with a 4000QTrap mass spectrometer, however this approach may be realized also using others mass spectrometer optics, with opportune modifications. For example, Niggeweg et al showed the possibility to perform PIS compatible with chromatographic separations coupled to a QTOF (40). Moreover, it would be very interesting to evaluate possible improvements, in terms of selectivity and quantitative estimation, by measuring with high resolution and accuracy (< 10 ppm) iTRAQ reporter ions. This may be accomplished by a Thermo LIT/Orbitrap performing MS<sup>2</sup> experiments in Higher Energy Collision Induced Dissociation (HCD) (24). The optics and the electronics of this instrument leads to perform analysis in an operation mode called "Parent Ion Mapping" that may be considered as reconstructed PIS. However, the feeling is that, because of the higher duty cycle of a triple quadrupole based PIS, eventual improvement would have real effectiveness in an off-line LC-MALDI/MS<sup>2</sup> analysis more than in a classical LC-ESI-MS<sup>2</sup>. The use of iTRAQ reagents for the selective detection and quantification of nitration sites in proteins was recognized to be a valid Proteomic tool. Indeed, the data showed in this chapter were published on a first class Proteomic journal (Chiappetta G, Corbo C, Palmese A, Marino G, Amoresano A, *Quantitative identification of protein nitration*, Proteomics (2008) in press)

### **3.5 References**

1. Leeuwenburgh, C., Hardy, M. M., Hazen, S. L., Wagner, P., Oh-ishi, S., Steinbrecher, U. P., *J. Biol. Chem.* **1997**, 272: 1433–1436.
2. Schwedhelm E., Tsikas D., Gutzki F.M., Froulich J.C., *Anal. Biochem.* **1999**: 276:195–203.
3. Sokolovsky M., Riordan J.F., Vallee B.L., *Biochem. Biophys. Res. Commun.* **1967**, 2: 20-25.
4. Tsikas D., *J. Biochem. Biophys. Methods* **2001**, 49: 705–731.
5. Frost M.T., Halliwell B., Moore K.P., *Biochem. J.* **2000**, 345: 2453– 458.
6. Yi D., Ingelse B.A., Duncan M.W. and Smythe G.A., *J. Am. Soc. Mass Spectrom.* **2000**, 11: 578–586.
7. Thornalley P.J., Battah S., Ahmed N., Karachalias N., Agalou S., Babaei-Jadidi R., *Biochem. J.* **2003**, 375: 581–592
8. Delatour T., Fenaille F., Parisod V., Richoz J., Vuichoud J., Mottier P. and Buetler T., *J. Chromatogr. B* **2007**, 851: 268–276.
9. Kamisaki Y., Wada K., Nakamoto K., Kishimoto Y., Kitano M., Itoh T., *J. Chromatogr. B Biomed. Appl.* **1996**, 685:343–347.
10. Shigenaga M.K., Lee H.H., Blount B.C., Christen S., Shigeno E.T., Yip H. and Ames, B.N., *Proc. Natl. Acad. Sci. USA* **1997**, 94: 3211–3216.
11. Nuriel T, Deeb R.S., Hajjar D.P. and Gross S.S., *Methods Enzymol.* **2008**, 441: 1–17.
12. Althaus J.S., Schmidt K.R., Fountain S.T., Tseng M.T., Carroll R.T., Galatsis P. and Hall E.D., *Free Radic. Biol. Med.* **2000**, 29: 1085–1095.
13. Nicholls S.J., Shen Z., Fu X., Levison B.S. and Hazen S.L., *Methods Enzymol.* **2005**, 396: 245-266
14. Zheng L., Nukuna B., Brennan M.L., Sun M., Goormastic M., Settle M., Schmitt D., Fu X., Thomson L, Fox P.L., Ischiropoulos H., Smith J.D., Kinter M. and Hazen S.L., *Clin. Invest.* **2004**, 114: 529–541.
15. Vadseth C., Souza J.M., Thomson L., Seagraves A., Nagaswami C., Scheiner T., Torbet J., Vilaire G., Bennett J.S., Murciano J.C., Muzykantov V., Penn M.S., Hazen S.L., Weisel J.W. and Ischiropoulos H., *J. Biol. Chem.* **2004**, 279: 8820–8826.
16. Ceriello A., Mercuri F., Quagliaro L., Assaloni R., Motz E., Tonutti L. and Taboga C., *Diabetologia* **2001**, 44: 834–838.
17. Khan J., Brennan D.M., Bradley N., Gao B.R., Bruckdorfer R. and Jacobs M., *Biochem. J.* **1998**, 330: 795–801.
18. Rabbani N., Thornalley P.J., *Methods Enzymol.* **2008**, 440: 337-359
19. Nikov G., Bhat V., Wishnok J.S. and Tannenbaum S. R., *Anal. Biochem.* **2003**, 320: 214-222.
20. Zhang Q., Qian W.J., Knyushko T.V., Clauss T.R., Purvine S.O., Moore R.J., Sacksteder C.A., Chin M.H., Smith D.J., Camp D.G., Bigelow D.J. and Smith R.D., *J. Proteome. Res.* **2007**, 6: 2257-2268.
21. Amoresano A., Chiappetta G., Pucci P., D'Ischia M., Marino G., *Anal Chem.* **2007**, 79: 2109-2117.
22. Ross P.L., Huang Y.N., Marchese J.N., Williamson B., Parker K., Hattan S., Khainovski N., Pillai S., Dey S., Daniels S., Purkayastha S., Juhasz P., Martin S., Bartlet-Jones M., He F., Jacobson A., Pappin D.J., *Mol. Cell. Proteomics* **2004**, 3: 1154-1169

23. Ow S.Y., Cardona T., Taton A., Magnuson A., Lindblad P., Stensjö K., Wright P.C., *J. Proteome Res.* **2008**, 7: 1615-1628.
24. Bantscheff, M., Boesche, M., Eberhard, D., Matthieson, T., *Mol. Cell. Proteomics* **2008**, 7(9):1702-13.
25. Tyther R., Ahmeda A., Johns E., Sheehan D., *Proteomics* **2007**, 7: 4555-4564.
26. Pettersson A.S., Steen H., Kalume D.E., Caidahl K., Roepstorff P., *J. Mass Spectrom.* **2001**, 36: 616-625.
27. Jencks W.J., *Acc.Chem.Res.* **1976**, 9: 425-432.
28. Geng M., Ji J., Regnier F.E., *J. Chromatogr. A* **2000**, 870: 295-313.
29. Brancia F.L., Oliver S.G., Gaskell S.J., *Rapid Commun. Mass Spectrom.* **2000**, 14: 2070-2073
30. Zhang X., Jin Q.K., Carr S.A., Annan R.S., *Rapid Commun. Mass Spectrom.* **2002**, 16: 2325-2332.
31. Zappacosta F., Annan R.S., *Anal. Chem.* **2004**, 76: 6618-6627.
32. Scholten A., Visser N.F., van den Heuvel R.H., Heck A.J., *J. Am. Soc. Mass Spectrom.* **2006**, 17(7): 983-994.
33. Skalnikova H., Rehulka P., Chmelik J., Martinkova J., Zilvarova M., Gadher S.J., Kovarova H., *Anal. Bioanal. Chem.* **2007**, 5:1639-1645.
34. Gafken P.R., Lampe P.D., *Cell Commun. Adhes.* **2006**, 5-6: 249-262.
35. .Hardt M., Witkowska H.E., Webb S., Thomas L.R., Dixon S.E., Hall S.C., Fisher S., *J.Anal. Chem.* **2005**, 77: 4947-4954.
36. Cong Y.S., Fan E., Wang E., *Mech. Ageing Dev.* **2006**, 127: 332-343.
37. Zhang Y., Wolf-Yadlin A., Ross P.L., Pappin D.J., Rush J., Lauffenburger D.A., White F.M., *Mol. Cell Proteomics* **2005**, 9 1240-1250.
38. Aggarwal K., Choe L.H., Lee K.H., *Brief. Funct. Genomic Proteomic* **2006**, 5: 112-120.
39. Jorrín J.V., Maldonado A.M., Castillejo M.A., *Proteomics* **2007**, 7: 2947-2962.
40. Niggeweg R., Köcher T., Gentzel M., Buscaino A., Taipale M., Akhtar A., Wilm M., *Proteomics* **2006**, 6(1): 41-53.

## 4. IMPROVED LC-MALDI-MS<sup>2</sup> ANALYSIS BY PEPTIDES DANSYLATION

### 4.1 Introduction

The effects of the peptide dansylation in the MALDI-TOF ion mode are showed. As described in chapter 1, MALDI-MS was one of the first tools developed for the Proteomic-scale studies to perform the PMF approach thanks to its high resolution and accurate mass measurement. Structural information may be also obtained using the classical MALDI-TOF instruments by the fragmentation spectra generated by the *Post Source Decay* (PSD) decompositions of the analytes. However, an effective MALDI-MS<sup>2</sup> high throughput method it is also amenable since the commercialization of MALDI-TOF spectrometers. The effects of peptide dansylation on MALDI-MS analysis were already presented by Parker et al. (1). However, no considerations on the fragmentation characteristics of the dansyl-peptides and the application of this technique to the Proteomic wide-scale were done.

#### 4.1.1 MALDI-TOF mass spectrometer

The main features of MALDI-TOF mass spectrometry have been already briefly discussed in the paragraph 1.2.1a. The main limitation of this technique relies in the lacking of satisfactory fragmentation spectra that can give fundamental peptide primary sequence information. The use of a single analyzer MALDI-TOF equipped with a reflector device allows the acquisition of peptide product ions spectra generated by the metastable fragmentation using the PSD technique (2) whose principle are summarized in Figure 4.1.

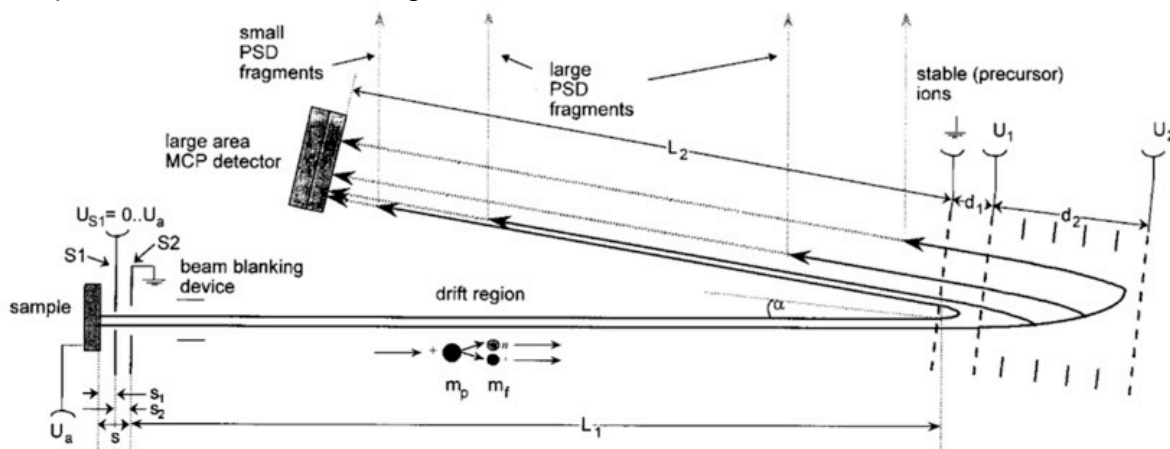


**Fig.4.1** Schematic representation of PSD experiment by using a MALDI-TOF instrument

The ions generated in the source by the pulsed laser irradiation are accelerated in the field free region of the TOF. At this stage ions have acquired higher internal energy by many processes (laser absorption, collisions, thermal heating, etc.) that may cause the uni-molecular metastable fragmentation on time scale shorter than the flight time. Because the ion decay occurs between the source and the reflectron, after the initial acceleration the precursor and the daughter ions travel the TOF with the same velocity but with different kinetic energies, arriving to the deflecting mirror at the same time. In this region the trajectory of precursor and product ions are differentiated both geometrically by the different curvature angle and timely by the different acceleration impressed at the exit of the reflector, thus a fragmentation

spectra may be recorded. However, to record one single complete product ion spectra several steps have to be acquired by ramping the reflectron potentials. This because the ion reflector is able to analyze ion masses with sufficient resolution only within a certain range of kinetic energies. In fact, after the decay the fragment ions lose their kinetic energy. Thus in every step, besides the resolved fragment ions corresponding to the appropriate kinetic energy range, the low mass range contains also un-resolved fragments, that should be further focalized. In order to analyze these lower mass ions, the potentials of the reflector have to be decreased in steps until all product ions have been focalized on the detector with sufficient mass resolution. Finally, all the PSD spectrum sections have to be concatenated by the computer and mass calibrated. Also if MALDI-PSD technique leads to obtain peptide structural information with simple MS equipment, the product ion spectra are characterized by poor sensitivity and relatively low mass accuracy and resolution. All these limits were definitively overcome by the TOF/TOF optic, as showed in figure 4.2, composed by two field free regions separated by a collision cell. The principles of the fragmentation in TOF/TOF instruments are slightly different to that of the classical MALDI-TOF devices.

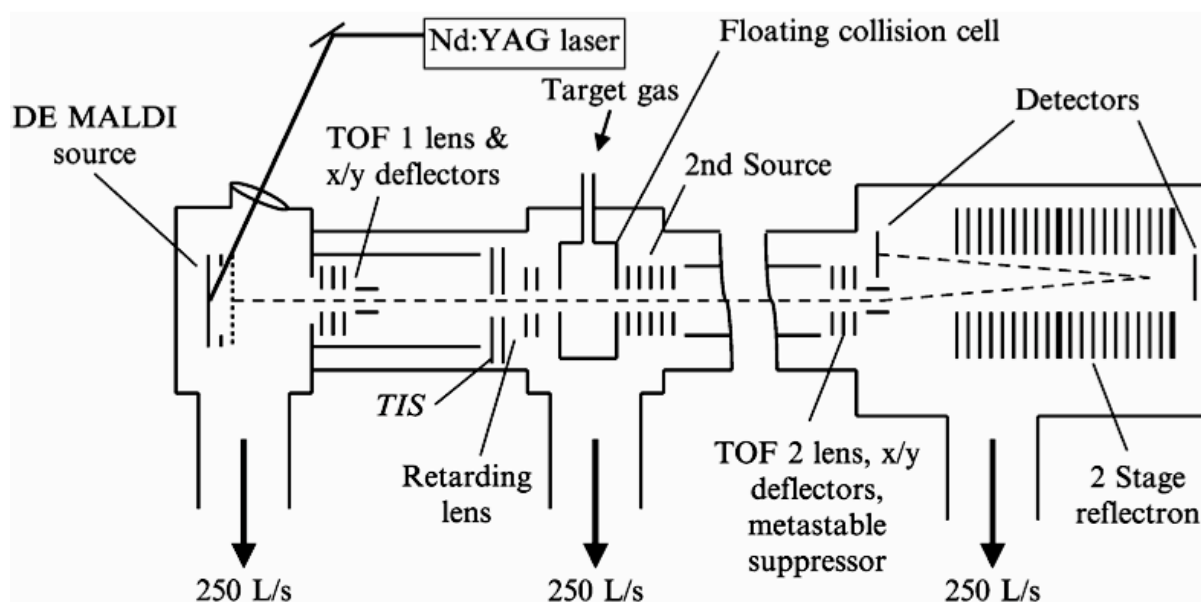


**Fig.4.2** Schematic representation of the Applied Biosystems 4800 MALDI-TOF/TOF mass spectrometer

Because of the ions dissociation is induced by the laser excitation, 20-30% higher intensity is used in MS<sup>2</sup> mode. After the delayed extraction the ions pass through the first field free region undergoing the post source decay cited above. At the end of the first TOF a *Timed Ion Selector* (TIS) leads to isolate the precursor and its product ions that flight at the same velocity. This is realized by opening and closing a deflecting gate, calculating their arrive time. Inside the collision cell the precursor may be further fragmented filling the region with neutral gas (CID ON mode). In this case richer spectra similar to the beam type instruments are obtained, characterized by the presence of both *b* and *y* ions, immonium ions and internal fragments. The presence of the collision cell is certainly one of the main improvements introduced by the TOF/TOF optics, increasing the low fragmentation efficiency of the PSD technique. However, in many cases the PSD mode gives rise to good spectra leaving the collision cell empty by the gas (CID OFF mode). Because the most intense

fragment peak is 1-2% of the precursor signal (3), the latter is removed by a metastable suppressor device in order to overcome the suppression of the daughter ion signals, eliminating the eventual metastable ions that would be generated in the second TOF. Before their entrance in the second TOF, ions are newly accelerated within one single range of kinetic energy. This event leads to finally separate in the second TOF the fragment ions that assume different velocities in function of their mass with the same kinetic energy. In practice, the second TOF plays the role deputed to the reflectron in the classical PSD experiments realized with MALDI-TOF instruments, resulting an increased resolution and accuracy of the MS<sup>2</sup> spectra. Since the ions do not arrive with the same kinetic energy to the reflectron, it has not been ramped to focalize the fragments. The MALDI-TOFTOF mass spectrometer is equipped with extremely modern materials and electronic components leading to enhance the laser pulse rate and power and also the ion transfer efficiency consenting to realize hundreds of MS<sup>2</sup> spectra *per* hour in a totally automated mode. This feature finally leads to couple off-line a MALDI spectrometer to a chromatographic separation by using a automated spotter that deposits drops of column eluate and matrix on a MALDI-plate. Thus, the chromatographic peptide separation, being fixed on the plate, may be analyzed several times by the MALDI-TOFTOF mass spectrometer, resulting in a very robust LC-MALDI/MS<sup>2</sup> technique.

#### **4.1.2 Enhanced MALDI-MS analysis by peptide modification: state of the art.**

It is widely accepted that the MALDI-MS development is one of the events that played a key role in the implementation and the appraisal of the proteomics approach, finally becoming nowadays a routinely used technique. Despite the ionization mechanisms are not yet completely understood, it is retained that the ionization efficiency is highly dependent by the peptide structure and the amino acid composition. This phenomenon is supported by the evidence that the MS signal intensities do not reflect the effective relative concentration of the peptides, In particular, the presence of basic sites and hydrophobic groups (4) leads to enhance the yields of the ionization process. In addition, it has also been postulated that the UV-adsorbing group, as aromatic moiety, are capable to favorite desorption/ionization, aiding the laser energy transfer to the analyte (4-5).

Hence, in order to increase the MALDI-MS analysis, many studies based on the chemical peptides modification with "MALDI-active" groups were realized. For instance, it was found that lysine C-terminated peptides have a lower ionization efficiency than the arginine C-terminated ones (6) because of the weaker gas phase basic feature of the  $\epsilon$ -amine group (7). Brancia et al. set up the conditions for lysine conversion to homoarginine by guanidination with *o*-methylisourea, leading to increased relative intensity of labelled peptides and also a higher recovery of the undetected ones (8). It was further demonstrated that the permanent cationic tag, sequestering the "mobile proton", suppresses the PSD fragmentation (9). On the contrary, the introduction of a strongly acid sulfo-group in peptide N-Terminal position decreases the MS signal intensity by the addition of a negative charge. However, for a singly charged peptide the presence of a "second" mobile proton enhances the PSD fragmentation (10). A combination of the two labeling procedures was performed to improve the results by using different cumarin aromatic derivatives (5, 9, 11). Other UV-adsorbing groups were evaluated demonstrating the importance of the energy transfer assistance in the MALDI techniques (12-13). The features of peptide N-Terminal labeling with the fluorescent dansyl chloride reagent were first

evaluated by Park et al. (1). They found that the characteristic protein MALDI-MS fingerprint changed by using this reagent because of usually un-detected peptides are revealed with higher signal intensities. However, some classical peptides are not detected after the dansylation. By this complementary an improved PMF identification and protein coverage resulted, undergoing to the database analysis a combined peak list generated by the labeled and un-labeled spectra. More recently it was also demonstrated that the dansylation improve the MALDI ionization and fragmentation in TOFTOF instruments of glycosylated peptides whose analysis is many times problematic (14).

## **4.2 Materials and Methods**

**Chemicals.** Tri(hydroxymethyl)aminomethane (Tris), 5-N.Ndimethylaminophthalene-1-sulfonyl chloride (dansyl chloride, DNS-Cl), sodium carbonate and iodoacetamide (IAM) were purchased from Fluka. Bovine serum albumin (BSA), ethylenediaminetetraacetic acid (EDTA), trifluoroacetic acid (TFA), guanidine, trypsin. and dithiothreitol (DTT), alpha-cyano-4-hydroxycinnamic acid (HCCA) were purchased from Sigma (St. Louis.MO). All the solvents were of the highest purity available from Baker. All other reagents and proteins were of the highest purity available from Sigma.

**Protein digestion.** Aliquots of the BSA were dissolved in denaturant buffer (guanidine 6M, Tris 300mM, EDTA 10 mM, pH 8.0) to a final concentration of 0.1 $\mu$ g/ $\mu$ L (2.0 pmol/ $\mu$ L), reduced with DTT (10-fold molar excess on the cysteine residues) for 2 h at 37 °C and then alkylated with IAM (5-fold molar excess on the thiol residues) for 30 min at room temperature in the dark. Protein samples were desalted by the size exclusion cartridge PD-10 (Amersham). The elution was performed in Na<sub>2</sub>CO<sub>3</sub> 100 mM pH 8.8. Protein elution was monitored at 280 and 350 nm. The fractions containing the proteins were pooled, concentrated and then digested. Trypsin digestion was carried out using an enzyme/substrate ratio of 1:50 (w/w) either at 37 °C for 18 h or by microwave heating putting the tube in a water-bath and warming for 1 minute in a domestic microwave oven at 700W.

**Bacterial strains growth conditions and protein extract preparation.** *Escherichia coli* K12 strain was grown in aerobic conditions at 37°C in LB medium. After 16 h bacteria were harvested by centrifugation and re-suspended in Buffer Z (25 mM HEPES pH 7.6, 50 mM KCl, 12.5 mM MgCl<sub>2</sub>, 1.0 mM DTT, 20% glycerol, 0.1% triton) containing 1  $\mu$ M phenyl methyl sulfonyl fluoride. Cells were disrupted by sonication. The suspension was centrifuged at 90.000 x g for 30 min at 4°C. After centrifugation the protein concentration of the extract was determined with Bradford assay.

**Peptide dansylation.** To 50  $\mu$ L of the BSA peptide mixture (2.0 pmol/ $\mu$ L) were added 50 $\mu$ L of a solution 5 ng/  $\mu$ L (18.5 nmol/ $\mu$ L) of DNS-Cl in ACN resulting in a approximate reactive excess of 1:10000. The reaction was carried out either for 45 min at 75 °C or warming the tubes in a water bath and warming for 5 min in a domestic microwave oven at 700 W.

**MALDI-MS<sup>2</sup> analysis.** Peptide mixtures in Na<sub>2</sub>CO<sub>3</sub> were diluted 10 folds in TFA 0.1% and then 0.5  $\mu$ L of the resulting solutions were charged on a 4800ABI plate and co-crystallized with 1 $\mu$ L of a solution 4mg/mL of HCCA in 70%ACN 30%. The spectra

were automatically acquired first in MS mode than the 25 most intense peaks with a minimum signal/ratio 100 were selected as precursor for the further MS<sup>2</sup> analysis. The MS spectra were recorded using a fixed laser intensity of 2100, for 1200 shots. The fragmentation spectra were acquired using a laser at 3500, for 2400 shots, with an acceleration voltage of 2kV, CID OFF and the metastable suppressor ON.

**LC-MALDI-MS<sup>2</sup>.** NanoLC-MALDI-MS<sup>2</sup> experiments were performed on a 4800 TOFTOF mass spectrometer (Applied Biosystems) coupled to an Ultimate 3000system (Dionex). Peptide mixtures were loaded onto an Dionex reversed-phase pre-column cartridge (C18 PepMap 100, 15 × 1 mm, 5 μm) at 20 μL/min with solvent A (0.1% formic acid, 2% ACN in water) for a loading time of 5 min. Peptides were then separated on a Dionex reversed-phase column (C18 PepMap 100, 150 mm × 75 μm, 3.5 μm), at a flow rate of 0.2 μL/min using solvent A, 0.1% formic acid, 10% water in ACN as solvent B. The elution was accomplished by a 0-50% linear gradient of solvent B in 35 min. The elutes were continuously mixed with a solution of HCCA 5 mg/mL with a flow of 436nL/min by a T junction. One hundred eighty spots were collected depositing the mixture (one each 10 sec) on a 4800ABI plate. The resulting plate was analyzed in MS and in MS<sup>2</sup> mode by the 4800 TOFTOF mass spectrometer. The MS method consists in a previous MS analysis of all the spots generating a list of precursor that are successively fragmented in MS<sup>2</sup> mode. The MS spectra were recorded using a fixed laser intensity of 2100, for 1200 shots. The 7 more intense peaks with a minimum signal/noise of 100 were selected as precursor for the successive MS<sup>2</sup> analysis. The fragmentation spectra were acquired using a laser at 3500, for 2400 shots with an acceleration voltage of 2kV, CID OFF and the metastable suppressor ON.

**Protein identification.** The MS and MS<sup>2</sup> data were used for the database analysis. By using the Applied Biosystems GPS tool, peak lists were generated, selecting MS signals with a signal/noise ratio 50 for the PMF analysis and signal/noise 30 for the MS<sup>2</sup> data. The created peak lists were submitted to MASCOT software using as research parameters: other mammalia and *Escherichia coli* as taxonomy respectively for the analysis of BSA and the *E.coli* protein extract. Cysteine carboxamidomethylation was selected as fixed modification and Lysine N-Terminal dansylation and Methionine oxidation were selected as variable modifications. The MS mass tolerance was set 75 ppm for the MS and 0.6 Da for the MS<sup>2</sup>. The instrument window was set on "MALDI-TOFTOF".

### **4.3 Results and discussion**

In order to improve the MALDI-MS<sup>2</sup> analysis by peptide dansylation, different reaction conditions were evaluated. To this aim Albumin Bovine (BSA) was chosen as standard protein. BSA aliquot was reduced, carbamidomethylated and digested by trypsin both classically by over night incubation at 37 °C and by microwave (MW) warming for 1 min of reaction time. An aliquot of the resulting peptide mixtures obtained were reacted with dansyl chloride both at 75 °C for 45 minutes and by MW warming for 5 minutes. The four different labeled samples, and the un-labeled classical and microwave BSA digests, used as controls, were analyzed in triplicate in MS mode by an Applied Biosystems 4800MALDI-TOFTOF by spotting 0.5 μL of the peptide solutions on the plate.

	<i>S/N 20</i>		<i>S/N 50</i>		<i>S/N100</i>		<i>MS<sup>2</sup> confirmed</i>
	<i>Match</i>	<i>Un-match</i>	<i>Match</i>	<i>Un-match</i>	<i>Match</i>	<i>Un-match</i>	
<i>Classical digestion (mean peptides)</i>	63.0	57.0	64.5	56.0	44.5	20.3	26
<i>Microwave digestion (mean peptides)</i>	65.0	35.0	65.0	27.5	47.0	14.0	34
<i>Classical digestion-classical dansylation (mean peptides)</i>	52.0	49.3	50.6	48.0	38.0	28.0	24
<i>Microwave digestion - classical dansylation (mean peptides)</i>	69.0	29.0	69.0	27.3	48.5	18.3	28
<i>Microwave digestion - microwave dansylation (mean peptides)</i>	70.6	29.3	69.7	30.0	48.3	12.6	31

**Table 4.1** shows the number of peptides identified by PMF averaged on three analyses using different parameter for the peak list generation

However, it must be underlined that the equivalent of dansylated mixture on the plate are two fold less abundant than the un-labeled one. This is due to the fact that the dansylation conditions generally consist in the 50% dilution of the sample with a solution of the reactive in ACN. Normalizing the final volume by a drying step is not advisable since the concentrated salts and un-reacted reagent may interfere with the correct crystallizations. As the final goal of this work is to set up a LC-MALDI/MS<sup>2</sup> based strategy the BSA samples were not desalted by ZIP-TIP chromatography, but diluted 10 folds in TFA 0.1% before to be spotted. Finally, 100 fmol *per* spot for the BSA sample and 50 fmol for the dansylated BSA were estimated to be analyzed. In order to develop a high throughput method it is important to set up an automatic MS<sup>2</sup> routine based on MS data. To set up the MS method, the analysis of a standard protein is performed. In practice for each spot the mass spectrometer first records an MS spectrum then a prefixed number of ions, which have generated an MS signal over a signal-noise ratio threshold, is selected and fragmented. Therefore, to perform an automatic MS<sup>2</sup> method it is important to define the optimal signal/noise ratio (S/N) to discriminate what ions detected in MS have to be further fragmented. This parameter is also important for the generation of the peak-lists that are further submitted to MASCOT software. In fact, the database searching consists in a hybrid search using both the MS and the MS<sup>2</sup> data. Thus, for each sample previous

analyzed, three peak-lists are generated including ions having MS signals with S/N of 100, 50 and 20 and submitted to PMF analysis using MASCOT software.

	<i>Identified peptides</i>	<i>Total score</i>	<i>Coverage</i>
<i>Classical digestion</i>	16	680	37%
<i>Microwave digestion</i>	23	1193	49%
<i>MW digestion diluted</i>	14	436	28%
<i>Classical digestion-classical dansylation</i>	8	104	12%
<i>Microwave digestion -classical dansylation</i>	15	399	22%
<i>Microwave digestion-microwave dansylation</i>	16	441	23%
<i>Combined research MW digest +MW digest-MW dansylation</i>	32	1625	57%

**Table 4.2** shows the results obtained by the automatic MALDI-MSMS analysis of the samples. The reported data are the mean values obtained by three separated experiments.

The variable dansyl modification of peptide N-terminal, lysine, tyrosine and histidine were considered. However in contrast with Park et al. (1) the aromatic amino acids were not found modified. The results resumed in the table 4.1 show that using the minimum value 20 S/N there are no relevant increments of the identified BSA peptides, however an increased number of un-assigned signals is observed. The value 50 S/N leads to enhance the matched signals in comparison to the higher 100 S/N. Also if the number of un-matched peptides is increased, it was chosen the threshold of 50 S/N for the subsequent peak-list generation for PMF analysis. The ions previously detected as related to BSA are fragmented in CID OFF mode and the spectra are manually interpreted. It is observed that maximum 34 peptides detected in MS and assigned by PMF to BSA resulted to be confirmed by MS<sup>2</sup> data (Tab.4.1). This result depends on the poor quality of fragmentation spectra related to the less abundant ions species generated in the MALDI source. Thus, although the high sensitivity and accuracy of such MS technique allows also to the weaker MS signals to be relevant for the PMF identification, the MS<sup>2</sup> analysis is restricted to a fewer number of peptides characterized by higher MALDI ionization efficiency. Also the collisional induced fragmentation (CID ON mode) of the less intense ions was explored without any relevant improvement. Since the number of peptides giving satisfactory MS<sup>2</sup> spectra is on average lower than the number of peptides having S/N higher of 100 (Table 4.1), this value is chosen as selection criteria for the MS<sup>2</sup> analysis. Thus using these parameters for the mass spectrometry experiments and

the database searching, all the samples are routinely analyzed in MS<sup>2</sup> by a MALDI-TOF/TOF without limits in the number of peptides to fragment *per spot*. As showed in table 4.2 the maximum of peptides fragmented and identified *per spot* is 22. Thus, in order to preserve the crystals by an excessive usage, leaving part of the sample intact for successive analysis, the MS<sup>2</sup> method is modified limiting the number of peptide to fragment *per spot* at 25. By the automated analysis a lower number of peptides is identified with respect to the manual mode. This it should be considered quite logical as in manual mode each peptide is fragmented with specific and optimized parameters. Moreover, the manual interpretation of the spectra may lead to the correct assignation of the sequence also when, in some borderline cases, MASCOT leads to ambiguous output. From the analysis of data in table 4.2, it appears that by classical digestion 16 unique BSA peptides are meanly detected leading the 37% of sequence coverage and total score of 680. The peptides recovery is improved if it is realized in a microwave field, indeed 23 unique peptides are meanly detected with 48% of sequence coverage and 1232 of score. This result appears also by PMF analysis where a larger number of hypothetical BSA peptides are considered. In fact as showed in Table 4.1, MW digested BSA is always identified with a larger number of peptides independently by the S/N used. This trend is also observed for dansylated peptides. Indeed, it appears that better results are obtained by microwave digestion of the sample, leading also to reduce drastically the time of analysis as demonstrated by other works (15-16). However, no significant labeling yield improvements are observed carrying out the dansylation reaction in microwave field. In fact the MW digested BSA dansylated both by classical warming and by microwave activation, 15 and 16 unique peptides are respectively identified in MS<sup>2</sup> with 22% and 23% of sequence coverage and score 399 and 441. Therefore, for further experiments only the procedure consisting in the protein digestion and peptides dansylation by MW heating will be taken in consideration. In fact, this protocol improved the hydrolysis yield and the whole procedure duration is reduced to about 1h with respect to 20h of the classical approach.

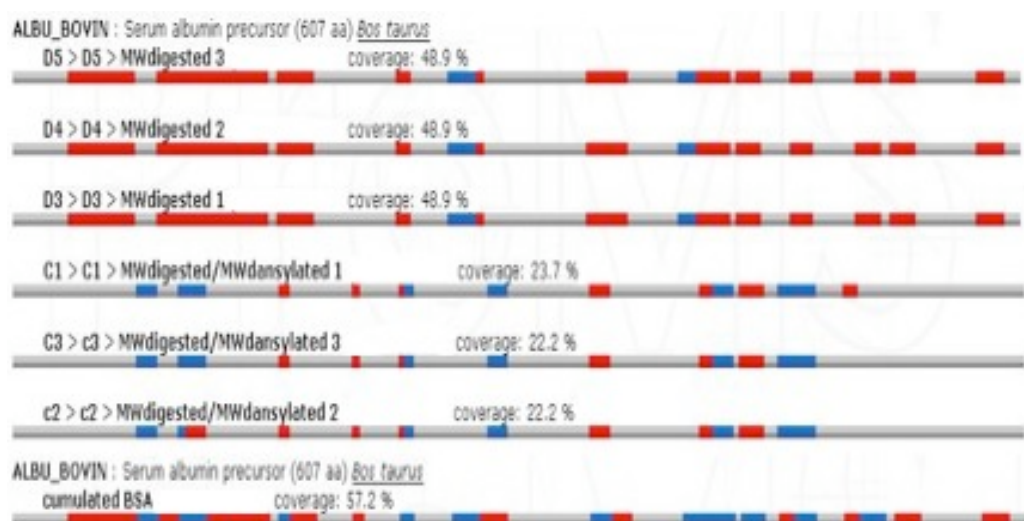


**Fig. 4.3** MyProms representation of the MS<sup>2</sup> data for MW digested BSA labelled and un-labelled with DNS-Cl.

In all the reaction conditions, it was observed that the side chain Lysine modification is not always quantitative. Therefore in some cases the same peptide is detected twice, both in the N-Terminal and in N-terminal/Lysine modified forms. Park et al. (1) demonstrated that after the peptide dansylation, the peculiar mass fingerprint of a protein changes. In fact, by the analysis of dansylated mixtures peptides not usually identified by the classical procedure are detected and *vice-versa*. For that reason the PMF identification is improved if the generated peak lists of the two analyses are combined and used for a unique data base searching. This behavior was also verified with MS<sup>2</sup> data by using the software MyProms (17), a tool that allows to store, to compare and to manage MASCOT searches. As shown in figure 4.3 the separated database searches for the dansylated and un-labeled peptide mixtures lead to identify BSA respectively with a maximum score of 458 and 1211 and maximum sequence coverage of 23% and 49%. By the combined peak list of this couple of data, the analysis is improved in fact it results a total score of 1625 and sequence coverage of 57%. It is interesting to underline that the statistic relevance of the incremented number of MS<sup>2</sup> data leads to high enhancement of the probabilistic score also if it is related to short increase of sequence coverage. In fact, when common peptides are found in their modified and un-modified forms, the best score is used for the calculations.

**Understanding the effects of peptides dansylation.** By analyzing data in tables 1 and 2 it should be noted that after the dansylation fewer peptides are above the selection criteria for fragmentation. This results in lower scores and coverages. However as already reported the un-labeled sample is more concentrated, so an aliquot of this sample is diluted in 50% ACN in order to evaluate if the induced modification may suppress the MALDI ionization. By the automatic MALDI-TOF analysis of the diluted BSA microwave digest, 14 peptides were detected with total score of 436 and sequence coverage of 28%. It confirms that the high differences, in terms of total number of fragmented peptides, observed after the peptide dansylation has to be attributed to the dilution effect and on contrary the dansylation leads to detect a larger number of peptides in MS<sup>2</sup>. Thus, it is possible to use the diluted sample as control also to understand other effects of peptide dansylation on MALDI-MS<sup>2</sup> technique. Besides the dilution, the sequence coverage, obtained from the un-labeled sample analysis, is higher although a lower number of peptides were used. To understand this behavior, a larger number of peptides have to be evaluated and to this aim all the control peptides identified by a PMF analysis and not identified by the automatic MS<sup>2</sup> routine were manually fragmented, as previously done for the dansylated mixture. The results are summarized in the Table 4.3. It is reinforced the evidence that the dansylation changes the ionization profile of MALDI-MS. In fact, according to Park et al., some peptides are detected and others not anymore detected after the dansylation. Moreover, it is observed that many peptides are not automatically fragmented because their relative signal intensity is too low, thus resulting in a change of the ionization hierarchy. For example the peptides m/z 1652.7 (DNS)-SLHTLFGDELCK and m/z 1672.7 (DNS)-RHPEYAVSVLLR were efficiently manually detected and sequenced after the dansylation but they were not automatically fragmented. If we exclude the common identified peptides contributing equally to the sequence coverage, we obtain 23 unique peptides for the control, 21 of which having molecular weight within m/z 1795.8 - 3511.7. Instead, for the dansylated sample 18 unique peptides are found within m/z 714.4 - 1696.8. This trend shows that dansylation improves the recovery of peptides in the low mass

	MASS	SEQUENCE	SCORE	MASS	SEQUENCE	SCORE
<b>COMMON PEPTIDES</b>	712.3	SEIAHR		945.3	*SEIAHR	
	927.4	YLYEIAR	32.3	1160.5	*YLYEIAR	26.5
	1001.5	ALKAWSVAR	35	1467.6	*AL*KAWSVAR	35
	1419.7	SLHTLFGDELCK	78.3	1652.6	*SLHTLFGDELCK	
	1439.7	RHPEYAVSVLLR	42	1672.7	*RHPEYAVSVLLR	
	1639.8	KVPQVSTPTLVEVSR	54.6	1712.8	*LGEYGFQNALIVR	86
	1479.8	LGEYGFQNALIVR	41.6	1800.7	*DAFLGSFLYEYSR	88.5
	1567.7	DAFLGSFLYEYSR	40	1957.8	*MPCTEDYLSLILNR	87.5
	1724.8	MPCTEDYLSLILNR	51.6	2105.9	**KVPQVSTPTLVEVSR	89.6
	2004.8	VASLRETYGDMADCCEK	26.5	2237.9	*VASLRETYGDMADCCEK	52
<b>UNIQUE PEPTIDES</b>	1193.6	DTHKSEIAHR	33	714.3	*FGER	
	1305.7	HLVDEPQNLIK	61.5	778.3	*VASLR	24.5
	1795.7	DDPHACYSTVFDKLLK		805.3	*QRLR	
	1880.9	RPCFSALTPDETYVPK	27	842.3	*AFDEK	
	1907.9	LFTFHADICTLPDTEK	56	882.3	*IETMR	18.3
	1927.7	CCAADDKEACFAVEGPK		891.3	*QEPER	
	2045.0	RHPYFYAPPELLYYANK		939.3	*CASIQK	
	2113.9	VHKECCHGDLLECADDR	60	922.3	*AWSVAR	20
	2148.0	LKPDNTLCDEFKADEKK		1022.4	*LVTDLTK	
	2247.9	ECCHGDLLECADDRADLAK		1051.4	*ATEEQLK	
	2277.1	LFTFHADICTLPDTEKQIK	51.5	1139.5	*IETMREK	24
	2405.2	LFTFHADICTLPDTEKQIKK		1247.6	*QTALVELLK	
	2487.1	YNGVFQECQAEDKGACLLPK		1301.4	*QNCDQFEK	28.5
	2492.2	GLVLIAFSQYLQCCPFDEHVK		1371.4	*CCTESLVNR	18
	2541.2	QEPERNECFLSHKDDSPDLPK	55.2	1524.6	*ECCDKPLEK	
	2612.2	VHKECCHGDLLECADDRADLAK	19.3	1608.7	**KQTALVELLK	
	2872.3	CCTKPESERMPCTEDYLSLILNR		1632.7	*CCT*KPESER	39
	3000.4	CCTESLVNRRPCFSALTPDETYVPK	13	1676.6	*YICDNQDTISSK	41
	3038.3	EYEATLEECCAADDPHACYSTVFDK		1696.8	*TCVADESHAGCEK	70
	3038.3	EYEATLEECCAADDPHACYSTVFDKLLK				
	3279.5	EYEATLEECCAADDPHACYSTVFDKLLK				
	3308.5	TVMENFVAFVDKCCAADDKEACFAVEGPK				
	3511.7	SHCIAEVEKDAIPENLPPLTADFAEDKDVCK				

**Table 4.3** shows the results of the automatic and manual MS<sup>2</sup> analysis of the MW digested/dansylated sample and for the diluted MW digested sample (control). For the manually fragmented peptides were not reported the MASCOT score because they are strongly dependent by the ad hoc parameters used to obtain good spectra. When the same peptide is detected in different dansylated form it is reported that ones with a better score or spectrum. Amino acids labeled with a star are dansylated

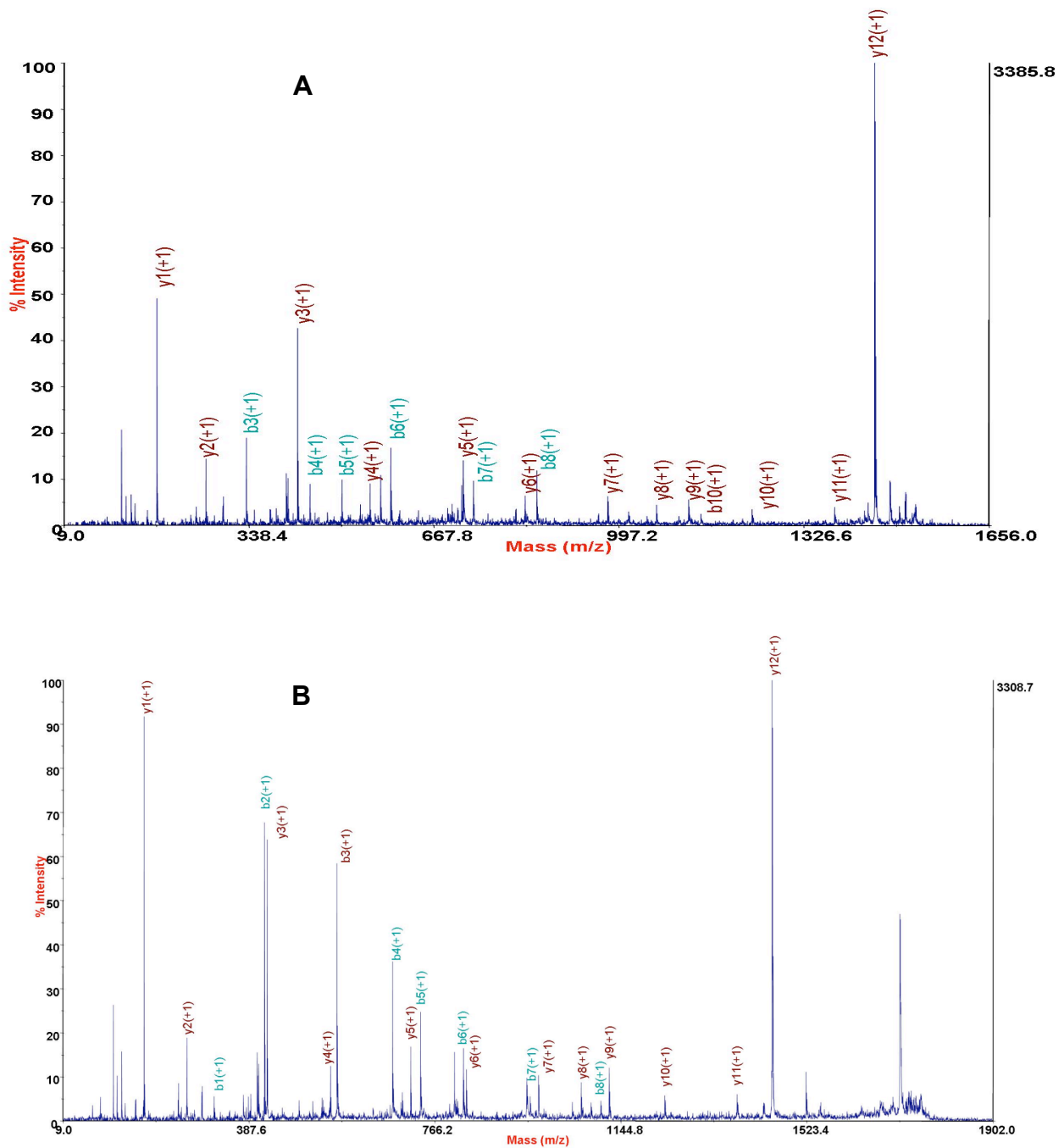


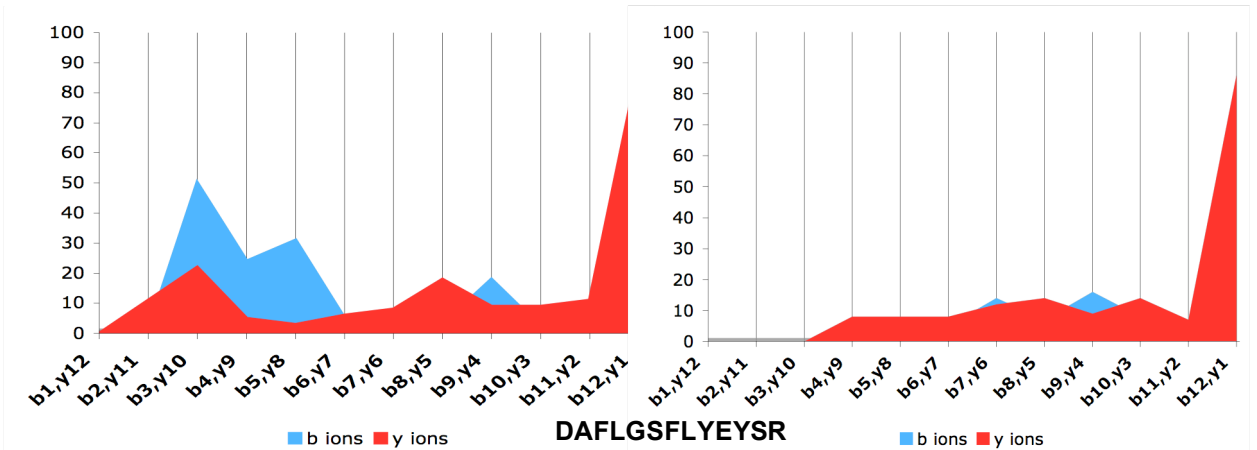
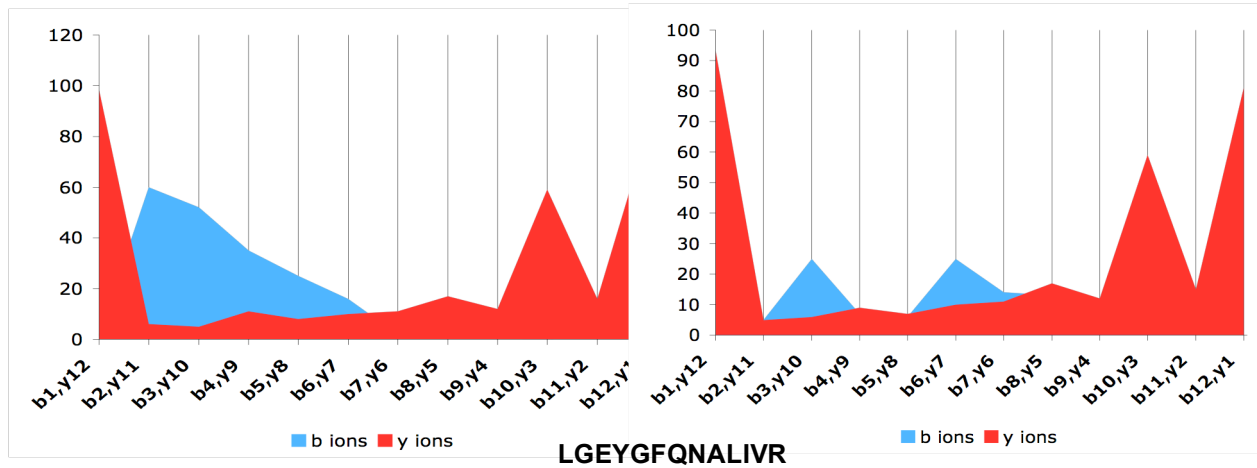
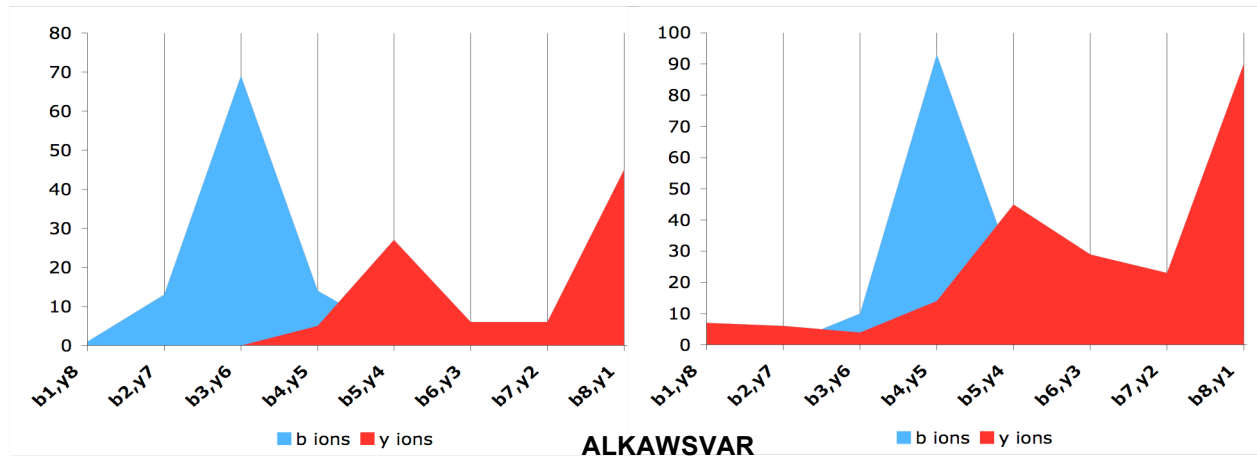
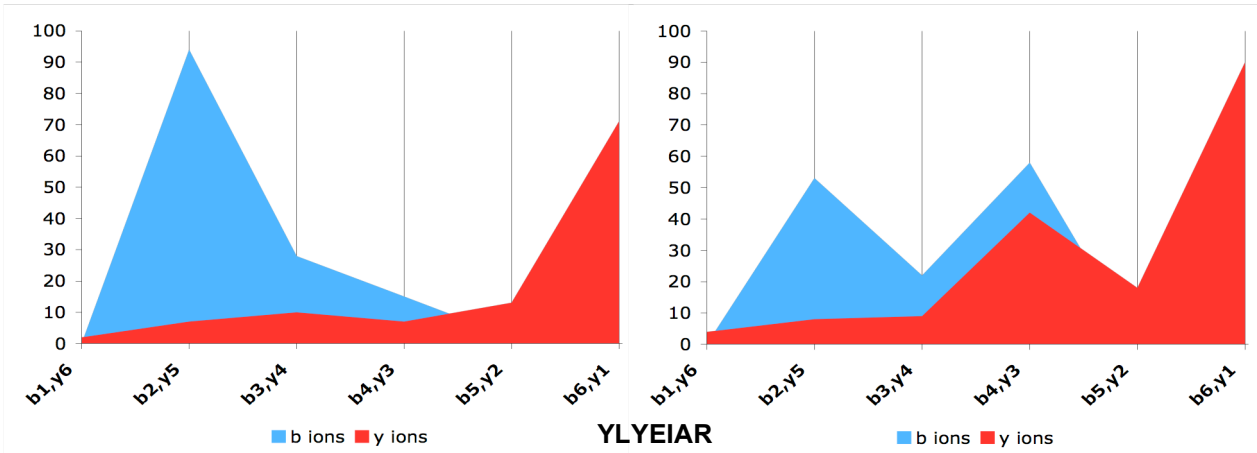
**Fig.4.4.** MS<sup>2</sup> spectra of the BSA peptide DAFLGSFLYEYSR dansylated (panel A) and un-dansylated (panel B)

range and decreases the ionization of the heavier, thus confirming the complementary characteristic of the double analysis. This result leads to understand the higher sequence coverage of the control sample also with less detected peptides. Park et al. (1) suggested that the dansylation of the strong basic lysine ε-amine in some cases might suppress the peptide ionization. However, this conclusion was achieved by using MS data only by comparing a few numbers of peptides with multiple modification sites. By using a larger number of MS<sup>2</sup> data the nature of the

observed effects may be better clarified. Among 23 peptides disappeared after the dansylation and 21 of them contained a C-Terminal Lysine. In fact the conversion of the  $\epsilon$ -amine (pKa 10.5) to sulfonamide decrease drastically its affinity toward the protonation. In addition the basic group introduced by the dansyl moiety is an aromatic tertiary amine (pKa 4.0) (4) that does not give the same contribution to the ionization as the C-Terminal lysine does (5-6). However, the detection of arginine C-terminal peptides with internal labeled lysine residues confirms that the basic properties of the C-terminal are very important for an efficient MALDI ionization. This behaviour can be observed for the peptides m/z 1467.6 (DNS)-AL(DNS)-KAWSVAR and m/z 1632.7 (DNS)-CCT(DANS)-KPESER (Tab.4.3). On the contrary, the decreased peptide N-Terminal basicity (pKa 8-9) is less relevant than the presence of a di-methylamino-naphtalene group in the same position.

In conclusion the peptide dansylation has two opposite effects in the MS mode.

A positive increased energy transfer due to the UV- absorbing naphtalene group that in the case of the BSA leads to identify 18 peptides not detected by the classical approach. This effect appears to be not linked to the peptide sequence. A negative suppressing effect when the C-Terminal basicity is loss by the modification. Obviously, these effects may be modulated by the peptide sequence and dansyl-lysine is detected when other basic sites are present in the sequence. This is the case for the peptide (DNS)-VASLRETYGDMADCCE(DNS)-K (not reported in the Tab. 4.3) whose N-Terminal and lysine were found both labelled. As concerning the MALDI-MS<sup>2</sup> features of dansyl-peptides it is interesting to underline that they are in most cases identified with higher score than the corresponding un-labeled one in the control (Tab. 4.3). This MASCOT score evaluation is made only considering the common 7 peptides that were automatically fragmented, under the same operative conditions. The reasons of this result are verified analyzing the respective fragmentation spectra of the peptides detected both in the control and the dansylated peptide mixtures. It appears that the fragmentation pattern of dansylated peptides exhibit in PSD mode enhanced *b*-type ions that may lead to a better sequence determination (Fig.4.4). The nature of fragmentation improvement has to be attributed to the fluorescent moiety in N-terminal position. These results are in perfect agreement with previous works where a fluorescent modification of N-Terminal amino acid induced a better generation of *b* series ions (5, 11-13). To better understand this effect, the values of the relative intensity of the *b* ions and their complementary *y* ions are evaluated for the automatically fragmented peptides. By the comparison of these values it is possible to monitor the trend of a singly-charged ion to preferentially give rise to *b* or *y* fragment ions. The values obtained are graphically represented in figure 4.5 where the relative intensities are reported as function of the relative ions. The curves obtained, blue for the *b* series and red for the *y* series, give a snapshot of how the peptide sequence is covered by MS<sup>2</sup> experiments performed with a MALDI-TOF/TOF. It appears, by the larger extent of the red curve, that the generation of *y* ions it is generally a preferential event. This is in agreement with the evidence that for a mono-charged tryptic peptide the probability that the charge is retained at the C-Terminal position is higher (20). Moreover, it is observed that the *y*-type ions intensities are higher for the first members of the series, then they decrease for the higher mass range. This heterogeneous intensity distribution effect may be attributed to the hybrid charge-directed/charge-remote fragmentation of tryptic peptides (cfr. par. 1.2.1)(19). In fact, following the mobile-proton model, the charge is transferred in the gas-phase by the basic sites to the vicinal amide-bond leading to its destabilization and further fragmentation. This event is statistically retired along the



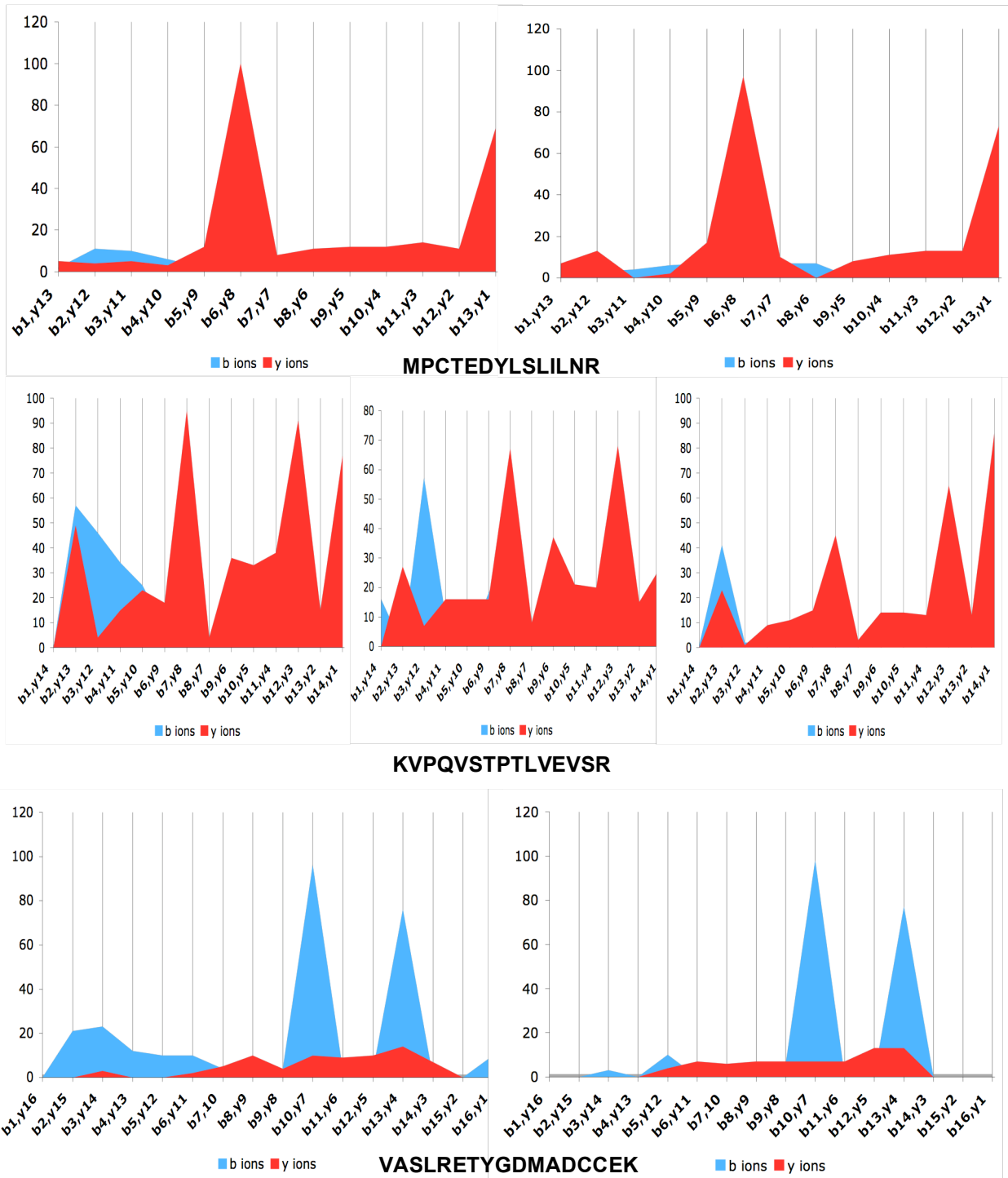


**Fig.4.5** graphic representation of ion intensities in function of the different  $b_n$  and  $y_n$  fragments. The resulting red curve is related to the  $y$ -type ions and the blue curve is related to the  $b$ -type ions

peptide chain, generating a population of isomer ions. However the charge localization of the arginine or lysine basic-group reduces the proton mobility to the amino acid near the C-Terminal position, with consequent destabilization of the amide bond in the N-Terminal region. The peptide DAFLGSFLYEYSR (fig 4.4 and 4.5) has a strong  $y_{12}$  for the presence of the aspartic acid in N-Terminal position that favors the vicinal amide bond protonation, providing a supplementary mobile proton. However, the enhanced  $y$ -type ion generation is thought to be caused by a

charge remote mechanism (21). Also the peptide KVPQVSTPTLVEVSR has high mass range  $y$  series ions characterized by strong intensities. This is probably due to the presence of an N-Terminal lysine residue that may enhance the charge-directed/charge-remote fragmentation of the N-Terminal peptide region.

This conclusion is enforced considering the bi-dansylated form of this peptide that was automatically fragmented leading to perform a comparison with the un-dansylated and mono-dansylated forms (see figure 4.4). The side-chain dansylation of the N-Terminal lysine decreases the intensity of the  $y$ -type ions mainly in the range  $y_8$  to  $y_{14}$ , confirming that the localization of a proton in N-Term position plays an important role in the charge directed- fragmentation. Obviously, the loss of the N-Terminal lysine charge localization affects mainly the  $b$ -type ions whose intensity results drastically decreased. The double dansylation of the peptide ALKAWSVAR has not the same drastic effect probably due to the internal position of the lysine and also the shorter length of the peptide. However, also in this case the  $y$  ions decrease in proximity of the dansylated lysine. The absence of the mono-dansylated form does not lead to make wider observation as previously done. As showed in figure 4.4, the N-Terminal amine dansylation does not influence the normal intensity distribution of  $y$  series. In fact, the red curves related to the dansylated and control peptides, remains unchanged, showing the typical decreasing intensity at the higher members of the series. Moreover, the blue curve, related to the  $b$ -type ions, appears greater for the labelled peptides than the un-modified one, confirming the starting observation that the N-Terminal amine dansylation increases the  $b$  ions generation. In addition, by the graphical representations of figure 4.4, others conclusion may be done. The  $b$  series of the un-modified peptides has the intensity distribution not complementary to the  $y$  series curve, but the higher values are mainly concentrated in the middle of the series. This may be due to the absence of the charge localization in the N-Terminal position making the  $b$  ion generation highly dependent on the charge directed fragmentation. Thus, the  $b$ -type ion generation is more probable at the central peptide-bond cleavages, where the amide protonation is still possible and the C-Terminal basicity has less sequestering power caused by the distance. Therefore, the N-Terminal region of a peptide remains not well covered by the  $MS^2$  analysis. N-Terminal dansylation, beside increasing the  $b$ -type ion intensity, appears to change the  $b$  series intensity distribution, shifting the higher values to the N-Terminal region and thus leading to a better sequence coverage by the  $MS^2$  data. This effect may be rationalized considering a double effect that the dansyl-moiety may give to the peptide fragmentation. In fact the UV-adsorbing dansyl naphtalene group may transfer the energy adsorbed by the laser radiation to the vicinal peptide bonds promoting the local destabilization without the introduction of a new mobile proton. In addition the dansyl moiety stabilize also the charge retention both introducing a second amine group and by the aromatic delocalization. The results obtained in this work perfectly agree to Renner and Spiteller (1985), where dansylated peptides were analyzed by Fast Atom Bombardment (FAB) MS (22)

**Complex protein mixture analysis.** In order to validate the results obtained on the standard protein and to evaluate the feasibility of peptide dansylation on large scale proteomic approach, a soluble protein extract of *E.coli* is reduced and alkylated in denaturant conditions. Then the protein mixture is desalted by size chromatography eluting in  $Na_2CO_3$  (see Materials and Methods paragraph). Finally, *E.coli* proteins are digested by trypsin in MW field. The resulting peptide mixture is divided in two aliquots, one of which is directly analyzed by LC-MALDI/ $MS^2$ . The second aliquot is

dansylated in MW field as described above (cfr. par.4.2), then dried to eliminate the ACN, re-suspended in 1% of formic acid and finally analyzed by LC-MALDI/MS<sup>2</sup>. It is expected 400 fmol of both un-dansylated and dansylated peptide mixtures are injected. The MS<sup>2</sup> data are used for the database research both by separate and combined peak lists. The results obtained are resumed in the Table 4.4. It appears that the improvements in the sequence coverage, score and complementary peptide recovery, evidenced by Park et al.(1) by PMF and then confirmed for the MALDI-MS<sup>2</sup> technique in the first part of this work, are kept un-varied also at Proteomic-scale. In fact, of the 22 identified proteins 6 were found only by dansylated peptides and 8 only by control ones. The others 8 proteins identified both by labelled and un-labelled peptides show an increased MASCOT score and higher sequence coverage. Again, peptides found both in the un-labelled and labelled forms have higher score in their dansylated form. As an example, the peptide ELANVQDLTVR of the RNA polymerase subunit alpha (RPOA) was identified with 80 as Score value in the dansylated form and 37 when is un-modified.

Protein	Mascot score	Score before dansylation	Numb. Peptides	Dansylated peptides	Coverage (%)	Coverage before dansylation
RPOA	433.4	280.0	9	4	28.3	17.3
RBSB	288.2	156.0	5	2	17.6	12.8
DNAK	188.4	87.0	5	3	9.2	3.8
EFTS	185.0	68.0	5	3	15.2	4.3
TIG	182.0	182	3	0	10.0	10.0
EFTU	169.4	105.2	6	2	18.8	9.9
RS1	111.9	87.0	3	1	7.5	5.6
RL10	108.4	54.3	2	1	9.7	9.7
CH60	103.6	47.7	2	0	6.4	6.4
RL18	91.2	0	3	3	19.7	0
RL9	68.6	31.7	2	1	12.8	7.6
ENO	56.0	0	2	2	2.8	0
SLYD	54.7	54.7	1	0	4.6	4.6
DBHA	50.3	50.3	2	0	32.2	32.2
RL2	46.2	0	1	1	3.3	0
CSPC	43.0	43.0	1	0	24.6	24.6
YJGF	41.0	0	2	2	17.2	0
CH10	33.8	33.8	1	0	14.4	14.4
TNAA	32.6	0	1	1	1.7	0
RL25	32.3	32.3	1	0	8.5	8.5
HNS	30.4	0	1	1	5.8	0
DINJI	30.1	30.1	1	0	8.1	8.1

**Table 4.4** *E.coli* proteins identified by LC-MALDI/MS<sup>2</sup> by the dansyl based method

#### **4.4 Conclusion**

The strategy described in this chapter aims to improve the identification power of the LC-MALDI/MS<sup>2</sup> by using the peptide dansylation. Peptide MALDI-MS features of this modification were first evidenced by Park et al (1). In fact, they found a complementarity between the protein peptide fingerprint of the labelled and un-labelled trypsin digests, which was used to enhance the sequence coverage and the MASCOT score. In the proposed work this behavior was confirmed and applied to gel free high-throughput and automated nanoLC-MALDI/MS<sup>2</sup> technique. Moreover, the global strategy has been also improved introducing the microwave-based chemistry

for the protein digestion and the peptide modification, resulting in a more efficient and very fast procedure (1h). The reaction conditions and the MS methods were first set up using BSA as standard protein. This experiments lead to understand that the complementarity of the detection concerns the peptide size and the presence of C-terminal lysine. In fact, large part of newly detected dansyl peptides is in the lower m/z region. This feature leads to cover short regions of the protein sequence, that are normally un-detected, that however, may be post-translational modified and escape mass spectral analysis in the classical approach. The observation of Park et al. that the side chain dansylation of C-Terminal lysine may, in some cases, decrease the peptide ionization was confirmed by using a larger number of MS<sup>2</sup> data. However, this feature does not invalidate the power of the strategy that is based on the use of MS data of modified and un-modified peptide mixtures. The large number of evaluated peptides led also to understand the effect of peptide dansylation on the peptide fragmentation in a MALDI-TOFTOF instrument. It was observed that in CID experiments, the introduction of a UV-adsorbing moiety in N-Terminal position favors the peptide bond cleavage in this region that is normally not probable for a singly-charged peptide. This feature was probably due to the naphtalene group that increases the energy transfer from the MALDI laser to the peptide. The redistribution of the energy along the vibrational-rotational degrees of freedom of the amino acid chain has a local effect, causing the de-stabilization of the peptide bond near the modification site. Finally it results that the “early” *b* series yielding is enhanced also by the N-Terminal charge retention allowed by the dansyl moiety stabilization of the charge. This fragmentation feature leads to better complementarities between *y* and *b* series, having positive effects both on the MASCOT score, for the automatic assignation of the spectra, and also for the manual interpretation for the analysis of PTMs. The Lysine modification may also decreases the fragmentation yielding. Moreover, a control of the reaction toward a selective N-Terminal modification is still a challenging task. As perspective works, the lysine conversion to homo-arginine followed by N-Terminal dansylation will be also evaluated considering its impact both on the MS signal and on the MS<sup>2</sup> fragmentation. However the mass spectral data obtained demonstrated that the procedure set up in this work is robust for the large-scale proteomic analysis. This was confirmed by the application of the strategy to the analysis a whole *E.coli* protein extract, which showed relevant improvement in the protein identification, in terms of peptide recovery and MASCOT score.

## **4.5 References**

1. Park S.J., Song J.S., Kim H.J., *Rapid Commun. Mass Spectrom.* **2005**, 19(21):3089-96
2. Moormann M., Zahringer U., Moll H., Kaufmann R., Schmid R. and Altendorf. K., *J. Biol. Chem.* **1997**, 272 :10729
3. Vestal M.L., Campbell J.M., *Methods Enzymol.* **2005**, 402: 79- 108
4. Valero M.L., Giralt E., Andreu D., *Lett. Pept. Sci.* **1999**, 6: 109-115.
5. Pashkova A., Moskovets E., Karger B.L., *Anal Chem.* **2004**, 76(15):4550-4557
6. Krause E., Wenschuh H., Jungblut P.R., *Anal Chem.* **1999**, 71(19):4160-4165
7. Zenobi R., Knochenmuss. R., *Mass Spectrom. Rev.* **1998**, 17: 337-366.
8. Brancia F.L., Oliver S.G., Gaskell S.J., *Rapid Commun, Mass Spectrom.* **2000**, 14(21):2070-3
9. Pashkova A., Chen H.S., Rejtar T., Zang X., Giese R., Andreev V., Moskovets E., Karger B.L., *Anal Chem.* **2005**, 77(7): 2085-2096
10. Wang D., Kalb S.R., Cotter R.J., *Rapid Commun. Mass Spectrom.* **2004**, 8(1): 96-102
11. Keough T., Lacey M.P., Youngquist R.S., *Rapid Commun. Mass Spectrom.* **2000**, 14(24): 2348-2356
12. Nakagawa M., Yamagaky T., Nakinishi H., *Electrophoresis* **2000**, 21: 1651-1652
13. Nakagawa M., Nakanishi H., *Protein Pept. Lett.* **2004**, 11(1): 71-77
14. Napoli A., Aiello D., Di Donna L., Moschidis P., Sindona G., *J. Proteome Res.* **2008**, 7(7):2723-2732
15. Lin S., Yun D., Qi D., Deng C., Li Y., Zhang X.J., *Proteome Res.* **2008**; 7(3):1297-307.
16. Sun W., Gao S., Wang L., Chen Y., Wu S., Wang X., Zheng D., Gao Y., *Mol Cell Proteomics* **2006**. 5(4):769-76.
17. Pouillet P., Carpentier S., Barillot E., *Proteomics* **2007**, 7: 2553.
18. Zheng Y., Gattas-Asfura K.M., Konka V., Leblanc R.M., *Chem. Commun.* **2002**, 21: 2350.
19. Roth K.D.W., Huang Z.H., Sadagopan N., Watson J.T., *Mass Spectrom. Rev.* **1998**, 17: 255-274
20. van Dongen W.D., Ruijters H.F., Lunge H.J., Heerma W. and Haverkamp J.J., *Mass Spectrom.* **1996**, 31:1156–1162.
21. Yu W., Vath J.E., Huberty M.C, Martin S.A., *Anal. Chem.* **1993**, 65: 3015-3023
22. Renner. D., Spiteller. G., *Angew. Chem. Int. Ed Engl.* **1985**, 24: 408 – 409.

## **5. A NEW METHOD TO SELECTIVELY EVALUATE PROTEIN THIOLS OXIDATION STATE.**

### **5.1 Introduction**

Proteomics allows the study of post-translational modification state of a proteome. However, classical procedures fail to detect the oxidative products of cysteines. In the last 5 years alternative chemical labeling methods were developed to further investigate this field.

This project aims to set up a new strategy based on dansyl aziridine fluorescent reagent to monitor and characterize thiol oxidative modifications in one unique workflow from the tissue or cell to the MS identification.

Preliminary results showed that the fluorescent characteristic of dansylated proteins allowed a selective UV staining of 2DE gels. Only the species that have changed their cysteines oxidation state were differentially revealed.

Protein dansylation improves MALDI ionization yield increasing the energy transfer thanks to the 5-(dimethylamino)naphthalene moiety. Moreover, Precursor Ion Scan analysis, by using the peculiar MS<sup>2</sup> dansyl-peptides fragments, enhances the achievable dynamic range. In addition, because dansyl derivatives are cell membrane permeable, proteins can be directly labeled inside the cytoplasm giving a better picture of the oxidative cell state *in vivo*. Finally, dansyl features consent to set up the conditions for tissue histochemical staining before molecular analyses, associating proteomics data with morphological information.

#### **5.1.1 Proteomic analysis of oxidation related cysteine: state of the art**

Oxidative stress is directly related to many human diseases (19). The reaction products of oxidants with biomolecules are actually considered the best biomarker to depict a particular cellular redox state. It was demonstrated that several amino acids are modified post-translationally under oxidative stress conditions (20). However, cysteine residues are perhaps the most sensitive to the oxidation and may result in many modification levels that depend on the oxidant nature and concentration. Proteomic approach is actually the most powerful tool to depict the post-translational modification (PTMs) state of a proteome. However, many classical procedures are lacking in the detection of cysteine oxidative products. These findings result from the chemical lability of many thiol modifications as the S-nitrosilation, the susceptibility to the oxidants and reductants used in many buffers, the absence of specific antibodies useful to screen or enrich complex protein mixtures (1). In the last years many alternative chemical labeling based methods were developed in order to make possible this kind of analysis. These strategies are based on the trapping of a defined thiol oxidation state using the differential alkylation. The general approach consists in an alkylation step to block -SH- groups, followed by a selective reaction to convert the oxidized thiols in their reduced form that is successively alkylated by using a second reagent, thus allowing to detect the modified protein (2). In order to obtain a "snapshot" of thiol oxidation state *in vivo*, it is necessary to prevent un-specific air-mediated oxidations. This may be accomplished blocking the free thiols when the proteins are still in the cell using membrane permeable reagents (3). This suggestive operating fashion allows to alkylate protein in their native conformation and chemical environment, thus giving structure-function information. Indeed, thiol reactivity is

based on the chemistry of the anionic state (4), the predominant species of the dissociation equilibrium at physiological pH. In proteins the reactivity of this residue is regulated by protonation/de-protonation events, changing the local cysteine pK<sub>a</sub> by the influence of the conformation dependent micro-environment (5-7). Thus, the *in vivo* labeling may also give information about thiol reactivity and exposure. An alternative strategy consists in the cell harvesting in tri-chloro acetic acid (TCA). By using this reagent it is also possible to avoid thiol oxidation by protonation and to precipitate the protein extract. Then, protein extract is re-suspended in a solution of the alkylant in strong denaturant buffer (8). This strategy consents to have the same accessibility and reactivity toward all free thiol enhancing their recovery even losing the structural information. The further alkylation steps are pursued after a selective reduction (9-10). Thiol group may be also regenerated by the reaction of S-nitrosilated proteins with ascorbate (11). The commercial availability of a large number of thiol alkylating agents has favored the development of many labeling strategies. The most common ones are based on the thiol labeling with a fluorophore moiety in order to selectively detect oxidized protein separated by bidimensional electrophoresis (2DE) (12-14). However, in some cases the use of a bulk fluorescent tag, that un-favor peptides mass spectrometry (MS) detection, may lead to identify the oxidized protein but not to find the site of modification. An interesting strategy uses the classical <sup>14</sup>C enriched iodoacetamide for the differential alkylation (8). Radioactive labeled protein may be selectively visualized after 2DE fractionation. In addition IAM is MS compatible and since alkylation step is based on two chemical identical molecules, the 2DE co-migration of differentially alkylated proteins is improved. Other methods use a biotin or also ICAT chemistry in order to enrich the labeled peptides or proteins making also possible the gel-free analysis and quantitative estimations (15-16). It must be considered that, also in this case the presence of a bulky moiety may un-favor the peptides ionization and the eventual tag cleavage reactions, associated to various chromatography purification/enrichment steps, may be time consuming and cause of material loss. An interesting solution to these problems seems to be the HIS-TAG strategy that uses an iodoacetamide derived synthetic peptide (17). In this case the tag does not interfere with ionization propriety and it leads also to the immuno-detection because specifically recognised by an anti-body. N-Dansyl-S-nitrosohomocysteine was used as fluorescent probe to detect S-nitrosilation *in vivo* (18). In this case the cellular membrane permeability of dansyl derivatives leads to label proteins in the cytoplasm making a picture of the redox state of cysteines. However, no MS analysis or proteins identification were done.

## **5.2 Material and methods**

**Chemicals.** Bovine serum albumin (BSA), ammonium bicarbonate (AMBIC), guanidine, dithiothreitol (DTT), trypsin, iodoacetamide (IAM) were purchased from Fluka. Dansyl aziridine was purchased from Invitrogen. Tris(hydroxymethyl)aminomethane, Magnesium Chloride, trifluoroacetic acid (TFA), trichloro acetic acid (TCA), Urea, Thiourea, 3[(3 Cholamidopropyl)dimethyl ammonio)-1-propanesulfonateas] (CHAPS) well as the MALDI matrix  $\alpha$ -ciano-4-idrossicinnamic acid were purchased from Sigma. Non Detergen Sulfo-Betain (NSDB) was purchased by Merck, Agarose, Temed, Acrylamide were purchased by BioRad Acetonitrile (ACN) are HPLC grade type from Baker. Gel filtration columns PD-10, are from Amersham.

**BSA dansylation.** An aliquot of 200 µg BSA was dissolved in 198 µl of denaturing buffer (7M Urea, 2% CHAPS, 40mM Tris, pH 8.0) and it was added 2 µl (1% v:v) of 5 µg/µl solution of DAZ in ACN in a molar ratio 1:10 BSA : DAZ. The reaction was carried out under agitation for 4h at 37°C und agitation using a Bio Rad thermo block.

**Reduction and carboxamidomethylation of BSA.** BSA-DAZ was diluted in denaturation buffer (guanidine 6 M, Tris 0.2 M, EDTA 10 mM, pH 8.0). Reduction was carried out by using a 10:1 DTT: cysteine, DAZ molar ratio. After incubation at 37°C for 2 h, iodoacetamide was added to perform carboxamidomethylation using an excess of alkylating agent of 5:1 respect to the moles of thiol groups. The mixture was then incubated in the dark at room temperature for 30 min. The alkylation reaction was stopped by addition of formic acid, in order to achieve an acidic pH. The mixture was then desalted by size exclusion chromatography on a SEPHADEX G-25M column; the elution was carried out with AMBIC 50 mM and the fractions analyzed through UV spectrometry at 220 and 280 nm wavelength. Positive fractions were collected and dried.

**BSA digestion.** Protein digestion was carried out in AMBIC 50mM pH 8.0 buffer using trypsin or chymotrypsin at a 50:1 protein : enzyme mass ratio. The sample was incubated at 37°C for 16 h. Then the sample was dried.

**Microwave (MW) assisted BSA digestion.** MW digestion was carried out in the same buffer and trypsin concentration showed above. However, the reaction was driven for 2 min in a domestic Microwave (Whirpool) oven at 900W putting the tubes in a water bath.

**Bacterial strains, growth conditions and protein extract preparation.** *Escherichia coli* K12 strain was grown in aerobic conditions at 37°C in SOC medium. After 16 h, bacteria were centrifuged (5 min, 4000g, 4°C) and washed three times with 500µl of 100mM Sodium Bicarbonate 12.5 mM MgCl<sub>2</sub> pH 7.4 buffer.

**E.coli protein denaturing labeling.** *E.coli* cells were harvested in TCA by three sonication steps of 30 sec. The solution was centrifuged and the protein pellet was re-suspended in 50µl of denaturing buffer with 10% (v:v) of 5 µg/µl solution of DAZ in ACN. The mixture was reacted at 37°C for 1h. To stop the reaction 50 µl of TCA was added, dry protein pellet was re-suspended in 150 µl of TUC buffer (2M thiourea, 7M urea, CHAPS 2%, DTT 1%, Tris 40mM, NSDB 1M)

**In vivo DAZ labeling.** *E.coli* cells (0,6 O.D.<sub>600</sub>) suspended in 500µl 100mM Sodium Bicarbonate 12.5 mM MgCl<sub>2</sub> buffer pH 7,4 was incubate with 10% (v:v) of 5 µg/µl solution of DAZ in ACN at 37°C under gentle stirring. Then the cells were washed three times to eliminate the reactive and centrifuged at 4000g for 5min. The supernatant were wasted and the dry cell pellet was harvested in TUC buffer and incubated with rotator over night at 4 °C.

**2DE.** The *E.coli* protein extracts (100µg) were purified for the 2DE by the 2-D Clean-Up Kit (Amersham). The pellets were dissolved in the TUC buffer (Thiourea 2M, Urea 7M, CHAPS 2%, Tris 40 mM pH 8.8, NSDB 1M, DTT 1%) and then they were ultracentrifuged ad 70000g. The supernatant was loaded on 7 cm IPG 4-7 strips

(Amersham) as reported by the manufacturer. The iso-electrofocusing was realized using an Amersham IPG-Phore and the migration was carried out for 20h. After the first dimension the strips were re-hydrated in 3mL of Rehydration buffer (Urea 6M, 40 mM Tris pH8.8, glycerol 30%, SDS 2%) with DTT 10 mg/ml for 15 min and then in 3mL of Rehydration buffer with IAM 25mg/ml for 15 min. The strips were then deposited on a 12,5% acrylamide gel, fixing with Agarose 1%. Two SDS-PAGE were run at the same time at 50 mA constant for 1h. The gels were washed with MilliQ water (3x15min) then the fluorescence image was taken. Finally the gels were stained by the Imperial Code Coomassie (Pierce) for the time necessary to the spots detection.

**In situ protein digestion.** Protein spots that undergo to the MS analysis were excised than washed three times drying and hydrating the gel respectively with ACN and 50mM AMBIC. Protein were reduced by a solution of DTT 10 mM for 30 min at 56<sup>o</sup>C and then alkylated by a solution of IAM 55mM for 30 min at room temperature in the dark. Then, gel spots were washed by the reagents and a cold solution 1ng/ $\mu$ L of trypsin in 10mM AMBIC, was added. The tubes were incubated 2h at 4 <sup>o</sup>C then they were centrifuged and the supernatant were substituted with a fresh solution of 10mM AMBIC and incubated o.n. at 37 <sup>o</sup>C. After the digestion the tubes were centrifuged and the supernatant collected in other news tubes. After a further peptide extraction using ACN the solutions were dried by Speed-Vac and re-suspended in 10  $\mu$ L of Formic acid 1%.

**LC ESI/MS<sup>2</sup>.** The samples were loaded onto an Dionex reversed-phase precolumn cartridge (C18 PepMap 100. 15  $\times$  1 mm. 5  $\mu$ m) at 20  $\mu$ L/min with solvent A (0.1% formic acid. loading time 5 min). Peptides were then separated on a Dionex reversed-phase column (C18 PepMap 100. 150 mm  $\times$  75  $\mu$ m. 3.5  $\mu$ m). at a flow rate of 0.2  $\mu$ L/min using 0.1% formic acid. 2% ACN in water as solvent A, 0.1% and formic acid. 10% water in ACN as solvent B. The elution was accomplished by a 0-50% linear gradient of solvent B in 35 min. Mass spectra were recorded with a LTQ-FTICR (Thermo-Finnigan) mass spectrometer. Data were acquired in automatic high dynamic mode consisting of alternate acquisitions in FTMS full scan survey mode (m/z range 500-2000), 3 FTMS SIM scan mode for exact mass and charge state determination of peptide and 3 LIT MS/MS mode for the peptide sequencing

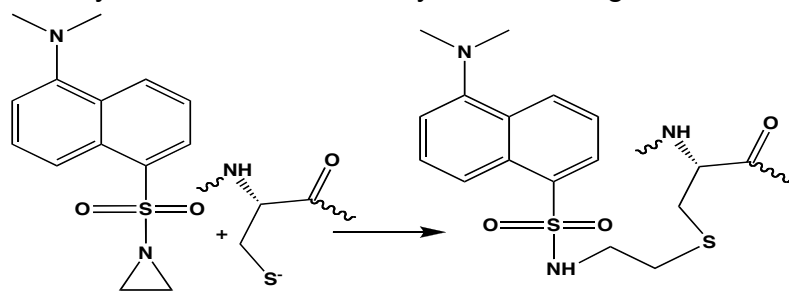
**MALDI-MS<sup>2</sup> analysis.** Peptide mixtures were diluted 10 folds in TFA 0.1% and then 0.5  $\mu$ L of the resulting solutions were charged on a 4800ABI plate and co-crystallized with 1 $\mu$ L of a solution 4mg/mL of HCCA. The spectra were automatically acquired first in MS mode than the 25 most intense peaks with a minimum signal/ratio 100 were selected as precursor for the further MS<sup>2</sup> analysis. The MS spectra were recorded using a fixed laser intensity of 2100. for 1200 shots. The fragmentation spectra were acquired using a laser at 3500. for 2400 shots. with an acceleration voltage of 2kV. CID OFF and the metastable suppressor ON.

**Protein identification.** The MS and MS<sup>2</sup> data were used for the database analysis. using MASCOT software with the following parameters: Other Mammalia and *Escherichia coli* as taxonomy respectively for the analysis of BSA and the *E.coli* protein extract. Cysteine carboxamido-methylation, Cysteine dansylation, Cysteine oxidation, Methionine oxidation were selected as variable modifications. The MS mass tolerance was 75 ppm for the MS and 0.6 Da for the MS<sup>2</sup> for the MALDI-

TOFTOF data. While for the LTQ-FTICR data 5ppm for the MS and 0,3 Da for the MS<sup>2</sup> were used

### **5.3 Result and discussion**

The biological relevance of determining protein redox behavior drives to a continuous request of new strategies and methodologies aimed to detect oxidation products and to evaluate their variations in function of different cellular events. As fully treated in the part 5.1.1, the main problem of the cysteine thiol PTMs detection is related to the chemical lability of the modifications. For this reason the best approach for this kind of study is the differential alkylation leading to “freeze” the thiol oxidation state and



**Scheme 5.1.** Thiol alkylation by Dansyl aziridine

inside the cells *in vivo* (3,18). However, many of these methods improve part of the Proteomics analysis, disadvantaging the rest of procedures. Thus, currently it is not still available a unique reagent allowing the analysis of cysteines PTMs from the tissue or cell to the MS identification. Here, the latest developments for the realization of a new Dansyl based method that should consents for the first time the unique analysis of stress oxidative Cys modifications are proposed.

**Thiol alkylation by Dansyl Aziridine.** DAZ is a fluorescent reagent to selectively label cysteine thiols showing little or no reactivity toward other weaker nucleophiles such as amines and alcohols (21). However in order to confirm by advanced MS approach the selectivity of the reaction and to test the feasibility of a differential alkylation, a standard free thiol containing protein was alkylated by using DAZ. Then the sample was reacted with IAM under reductive conditions and the sites of modification were identified by MALDI-MS<sup>2</sup> analysis. BSA was chosen as standard because it is characterized by the presence of 35 Cys, involved in 17 disulfide bonds and one free thiol. A solution 1mg/ml of BSA was reacted with DAZ in denaturing conditions as reported in Material and Methods section. The protein disulfide bridges were reduced by DTT leading to eliminate eventual DAZ excesses. Then the formed sulfhydryl groups were alkylated by iodoacetamide. In order to obtain higher sequence coverage, three aliquots of the solution were digested respectively by trypsin with classical heating, by trypsin in microwave field and by chymotrypsin. The peptides mixtures were analyzed by a MALDI-TOFTOF mass spectrometer obtaining

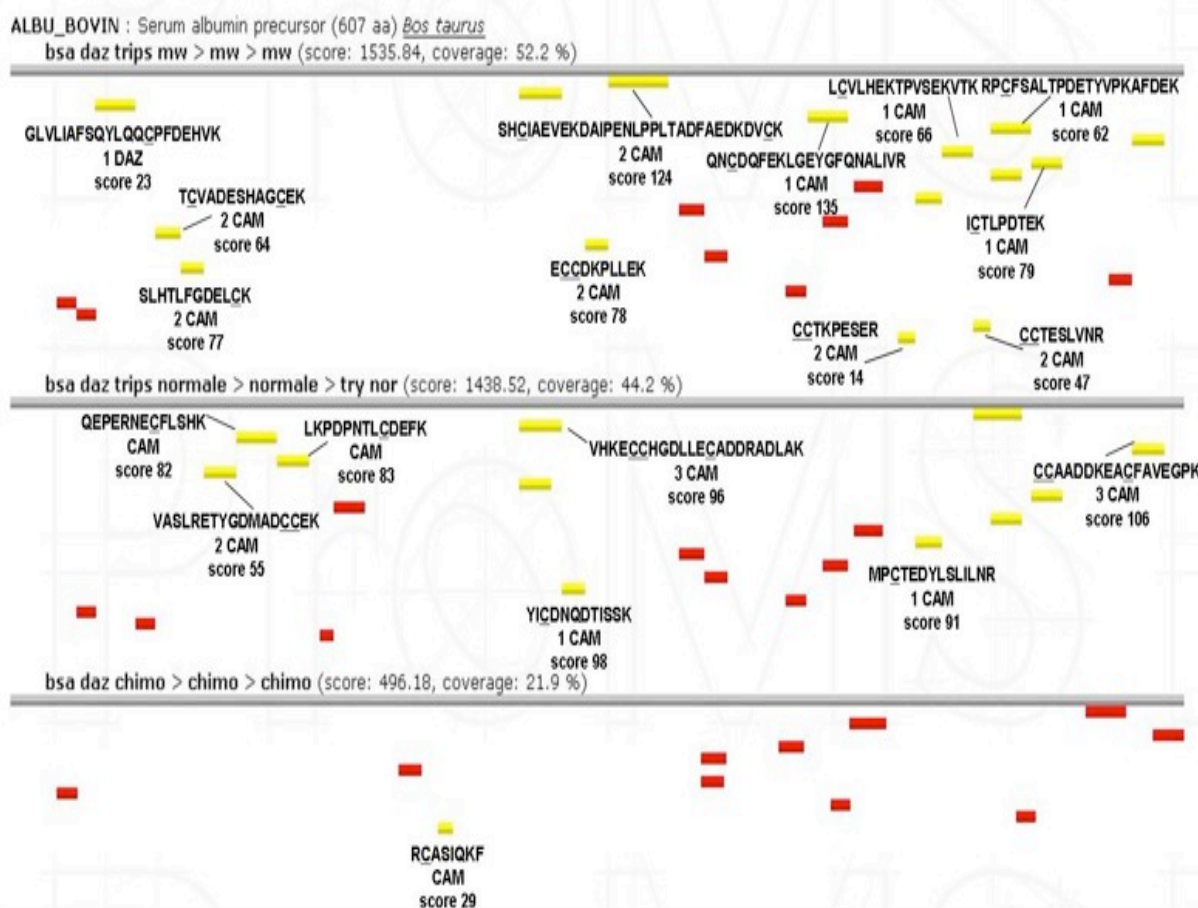


**Fig. 5.1** MyProms graphic representation of the protein coverage obtained with three different digestions.

accurate mass measurements and primary sequence data. The identifications were carried out using the flexibility of in house optimized MASCOT software to that was added in the “modification file” the value of 276 Da for the DAZ modification. In figure 5.1 are shown the results obtained by using the software MyProms (22). As showed in figure higher coverage and score resulted by MW assisted hydrolysis. By using the MS<sup>2</sup> data from the different hydrolyses, it was possible to cover 77% of the entire sequence and 100% of the cysteine residues. Moreover, the reaction conditions set up allowed the differential alkylation using DAZ. In fact, the reduced Cys58 was detected completely dansylated as indicated by the signal at m/z 2711.3 in the MS spectrum of the MW trypsin digest. This ion was further fragmented and the sequence reconstructed, confirming the detection of the peptide 45-65 (Fig. 5.1). Moreover, the dansylation of Cys58 was verified by the presence of the “y7” and “y8” fragment ions whose mass difference is 379 Da, corresponding to cysteine dansylation.

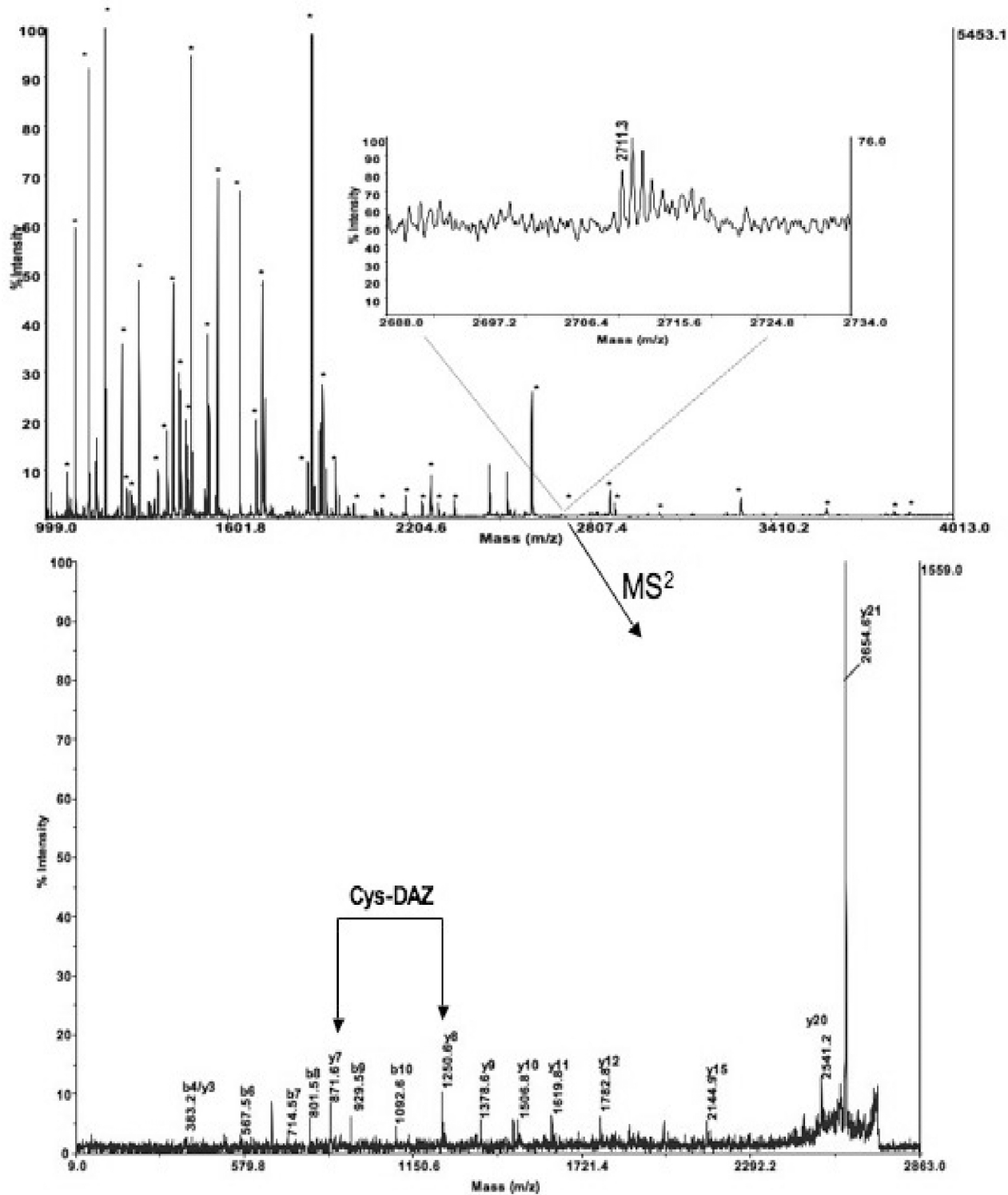


**Fig 5.2** Ms and MS<sup>2</sup> spectra of the peptide containing the BSA free thiol selectively alkylated by DAZ

All the others cysteines involved in disulfide bridges were found exclusively alkylated by IAM. Moreover, no other signals related to un-specific dansylated amino acid were found in the spectra (Fig.5.2).

**Detection of reduced cysteines in proteins fractionated by SDS PAGE.** As demonstrated in previous works, the use of Dansyl derivatives allows to perform

improved gel free strategies for PTMs identification (23-25). From the results showed

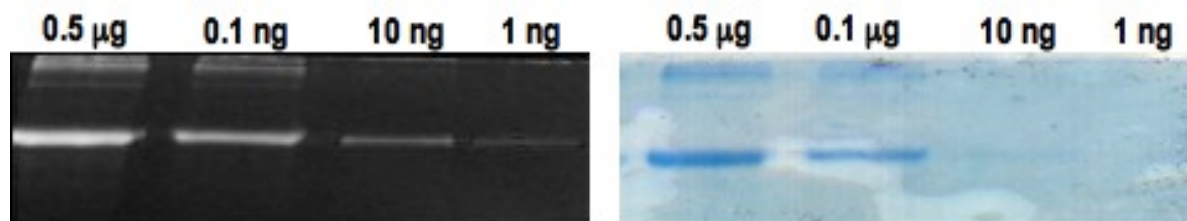


**Fig.5.3** SDS-PAGE lanes loaded with different amounts of DAZ labelled BSA. The autoradiography image shows the higher sensitivity of the fluorescence detection of free thiols

above seems that the dansyl chemistry may be useful also to study the oxidative status of protein thiols. Moreover, dansyl derivative features improve widely the proteomics analysis, in fact labeled proteins, fractionated by SDS-PAGE, may be visualized by taking advantage of its peculiar fluorescence (26). On this basis the conditions to selectively detect free thiol in proteins fractionated by electrophoresis were evaluated.

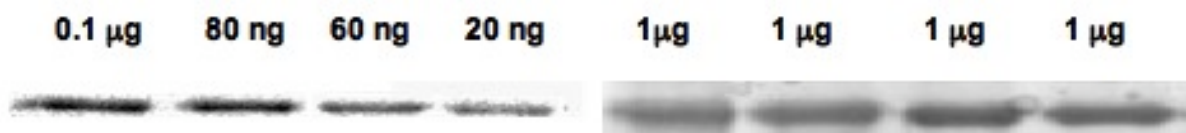


**Fig.5.4** In order to show the capacity to appreciate little difference in free thiol concentration, on a SDS-PAGE were loaded different amounts of BSA-DAZ pooled with un-labelled BSA to reach 1 µg of total protein. In order to perform a better software quantification of gel bands intensity the images were converted in negative.

The BSA free thiol was labeled with DAZ as previously described. The modified protein (BSA-DAZ) was fractionated by SDS PAGE. Respectively 0.5 µg, 100 ng, 10 ng and 1 ng of protein were charged in separated lanes. After the electrophoretic run the gel was exposed to an UV lamp and a picture was recorded. As showed in figure

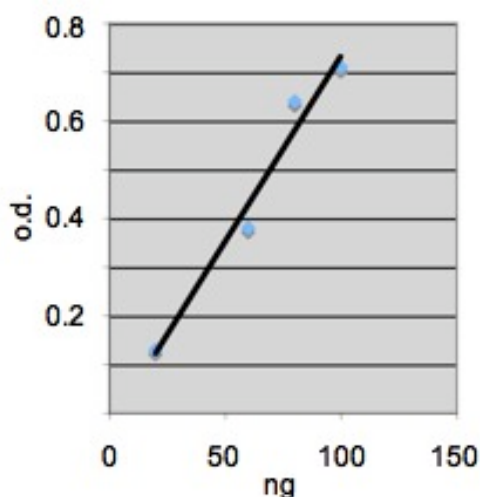


**Fig.5.5** The graphic shows the linearity between the fluorescence/Coomassie values and the theoretical protein concentration

5.3 fluorescent bands relative to the labeled BSA were visualized up to 1 ng. Then the gel was stained by a classical Coomassie dye however the bands containing 10 ng and 1 ng of protein were not visualized. Thus, by DAZ-labeling method it is possible to selectively detect free thiols containing proteins with improved sensitivity. In order to evaluate the capability to recognize the variation of thiol oxidation state and to perform semi-quantitative estimation based on the fluorescence intensity, others experiments were performed. In particular, to four aliquots containing respectively 100ng, 80ng, 60 ng and 20 ng of BSA-DAZ, an amount of BSA was added in each sample in order to obtain 1 µg protein concentration. Thus, such samples were loaded in separate gel lanes and fractionated by SDS-PAGE. The resulting gel was first visualized by fluorescence then it was stained by Coomassie (Fig.5.4). As shown in figure, it is possible to appreciate the different quantities of labelled protein by the gel autoradiography. In

contrast labelled and un-labelled protein are un-distinguishable by Coomassie

staining and the total amount of protein in all the samples is equal. Using the software "Image J" a measurement in an arbitrary scale (o.d.) of both fluorescence and Coomassie band intensities was carried out. In order to normalize the data for each sample the ratio between the value relative to the fluorescence and that relative to the Coomassie was calculated. The ratios obtained were graphically represented versus the theoretical amounts of labeled protein. It results a curve that confirms the linear relation between variation of the fluorescence intensity and the concentration (Fig.5.5). Then, the feasibility of the method to detect unknown oxidative modification of thiols was evaluated. A solution of 1mg/ml of BSA was reacted for 10 min at 37 °C with 1mM of H<sub>2</sub>O<sub>2</sub>, A similar solution of protein undergoes to the same procedure without the oxidant as control. Further the two samples were labeled with DAZ and an

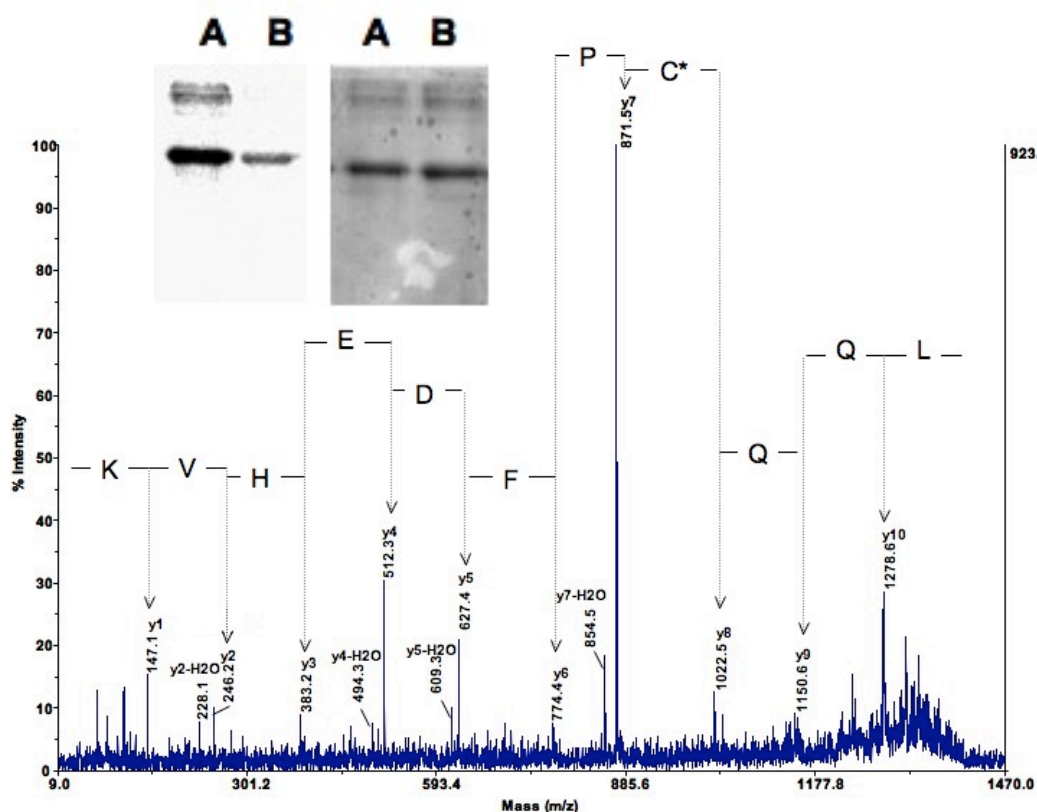


**Fig.5.6** By the use of DAZ it is possible to detect change in thiol oxidation state in protein fractionated by gel electrophoresis. MS<sup>2</sup> analysis lead to determine the modification site and the oxidation state of the cysteine thiol

aliquot of each one was fractionated by SDS-PAGE in two different lanes. The gel was first visualized using fluorescence detection then by tCoomassie staining and the images were recorded (fig 5.6).

In lane B the oxidized BSA was loaded. The corresponding fluorescent band resulted to be less intense respect to the control one in lane A. However, the Coomassie staining was able to detect the same protein quantity in both the sample meaning that the decreased fluorescence depends by the partial modification of the free thiol that is not available for the nucleophilic attack toward the aziridine. By the semi-quantitative estimation, based on the ratio of the fluorescence/Coomassie intensities, it appears that about the 40% of the protein was modified. The gel band were excised and the protein digested with trypsin. The peptide mixtures were analyzed by MALDI-TOF/TOF and the modification site was found related to the BSA free Cys that

was oxidized from sulfidric to sulfonic acid. This finding was demonstrated by the presence in the MS<sup>2</sup> spectrum (fig.5.6) of the signals related to the fragment ions “y7” and “y8”, exhibiting a mass difference of 151 Da compatible with the modification cited above. By these results it appears that by using DAZ as alkylating agent it is possible to detect selectively oxidative variations of cysteine, in protein fractionated by electrophoresis.

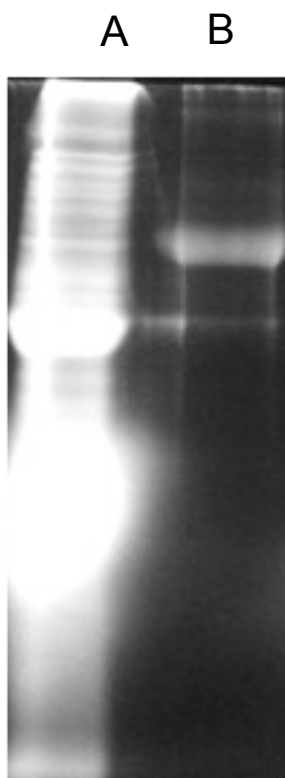


**Fig.5.7.** Selectivity trials using *E.coli* protein extracts

To confirm these data, the strategy was applied to a more complex protein mixture. *E.coli* protein extract was chosen as model. Reduced thiols were trapped by the method optimized by Leichert et al. (8), harvesting the cells in TCA. Then the first sample consisted of an *E.coli* protein extract labeled with DAZ in un-reductant denaturing conditions. The second sample was characterized by 100µg of reduced and carboxamidomethylated *E.coli* protein extract, spiked with 0,5µg of BSA. This mixture was then reacted with DAZ in un-reductant denaturing conditions. The two samples were fractionated by SDS-PAGE in two distinct lanes. By an UV lamp, the resulting gel was visualized and its image is reported in figure 5.7. In the lane A the first sample was charged, *E.coli* proteins alkylated with DAZ in non-reductant condition were visualized with intense fluorescence. The results obtained showed that the dansyl-based method is also suitable for the detection of protein containing reduced cysteines in complex mixtures. Moreover, the high percentage of free thiol in growing *E.coli* is coherent with previous data obtained by other works (8). In the lane B, where the second sample was loaded, only the band related to labelled BSA was detected while the rest of *E.coli* proteins alkylated by IAM were not fluorescent thus showing the high selectivity of DAZ alkylation at proteomic scale.

***In vivo* alkylation of protein free thiols.** Dansyl Aziridine reagent was largely used in studies related to the understanding of thiol catalytic role or to reveal protein conformational change (27-28). Moreover, the cell membrane permeability of dansyl derivative was observed (18). The reduced cysteine has many physiological functions as transduction signaling or catalytic effects that are regulated or also altered *in vivo* modulating both the redox state and the exposure of this residue. Therefore, it may be interesting evaluate the global thiol availability using DAZ to detect reduced cysteine inside the cell. In fact in this conditions the true physiological state of the protein complex networks and proteins conformation are kept, so the DAZ features may be used both to distinguish buried form exposed thiol and oxidized from reduced one. Moreover, it should be also interesting to evaluate the possibility to monitor the disulfide bonds formation in newly synthesized proteins.

In order to set up the *in vivo* alkylation conditions, 0,6 O.D.<sub>(600)</sub> of *E.coli* cells were suspended in the isotonic buffer (see Material and Methods). To keep the cell stable the alkylation was performed adding 1% (v:v) of DAZ in ACN solution and incubating at 37 °C. A time course experiment was performed; thus aliquots were taken at different time of reaction, cells was harvested and the protein extracts were analyzed by SDS-PAGE visualizing the fluorescence and then the gel was Coomassie stained.

As it results in figure 5.8 already after 30 min. of reaction the proteins resulted alkylated.

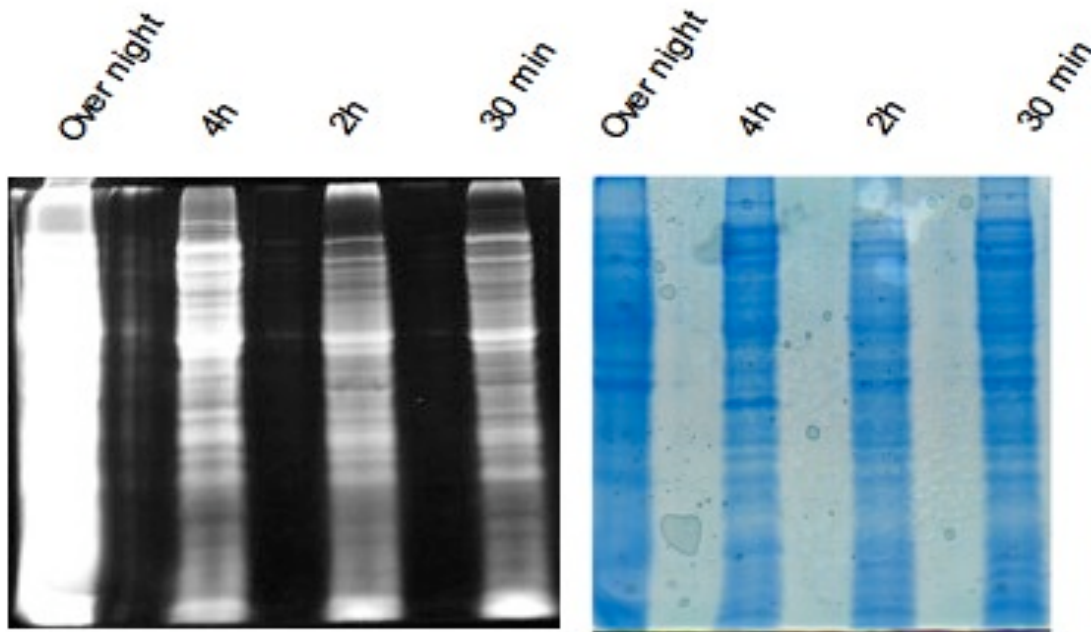


**Fig.5.8** Time course for the *in vivo* alkylation conditions setting up

However, after the over night incubation an intense fluorescence appears that is not explained by an increment of total protein concentration (fig 5.8). This could be possible due to the access to buried thiols at longer time of reaction. Thus, it is possible to modulate the labeling selectivity by choosing the time of incubation. Therefore, to have a more selective method for the further experiment DAZ incubation of the cell was driven for 30 min. The tolerance of the cells to DAZ was evaluated both by the blue trypan test and by fluorescence microscopy and flow cytometry analyses finding no toxicity.

To show the feasibility of the strategy two samples were prepared. The first consisted of *E.coli* growing cells as control and the second was represented by *E.coli* cells exposed for 10 minutes to an isotonic solution containing 1 mM H<sub>2</sub>O<sub>2</sub>. Cells were then labeled with DAZ as described above and the protein extracts were fractionated by 2DE, visualizing the resulting image first by fluorescence, then by Coomassie staining. The gel images were processed and superposed using the software "Delta 2D" developed by Decodon. Briefly, the software discharge for each image all the color information, keeping just the green channel for the Coomassie staining image and the red channel for that relative to the fluorescence. Thus, when the images are superposed the spots appear yellow whose tonality allows the software to make quantitative estimation, calculating the ratio from the intensity of the two different detections. However, also if the fluorescence intensity is given only by the reduced proteins and the Coomassie intensity is related to the total proteins amount, the ratio between the two measures may not be converted in an absolute percentage of reduced/oxidized forms, because the two detections have different sensitivity. However, in this mode it is possible to normalize the measure and to compare different analysis.

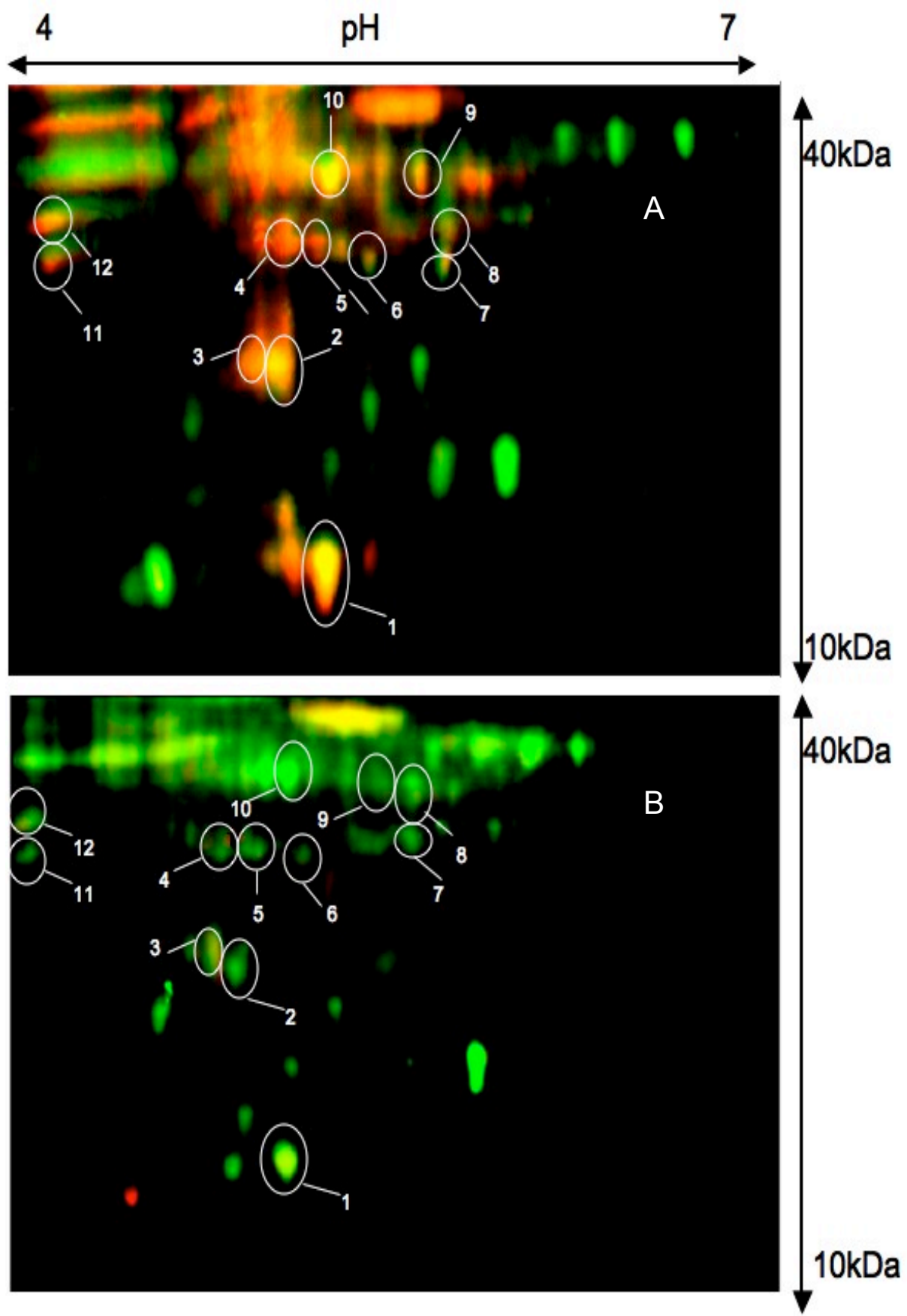


**Fig.5.9** 2DE of *in vivo* DAZ-alkylated free thiol protein in two different oxidative cell states.

Figure 5.9 showed the image resulting by the superposition of the Coomassie and the fluorescence 2DE visualization, related to *in vivo* alkylated *E.coli* proteins. In the control sample (figure 5.9A), many spots appear as combination of red and green component confirming that during the normal growth the greater part of proteins are in their reduced form (8). Figure 5.9B reports the image related to the oxidized cells. It is evident that large part of the spots is green thus suggesting that the fluorescence is strongly decreased due to cysteines oxidation. In addition, changes in the protein expression are observed. This event could be rationalized by considering the cells response to the oxidative stress. In particular the attention was focused on 12 spots that were quantified by “Delta 2D”, then they were excised, digested by trypsin and analyzed by LC-MS<sup>2</sup>. The semi-quantitative approach allows the estimation of the oxidation levels for the proteins identified from the examined spots (Tab. 5.1). This is realized calculating for each spot the ratio between fluorescent and Coomassie intensities obtaining a “Q” value. By the comparison of the Q values obtained from the control (Qcon) and oxidized (Qox) samples the extent of cysteine modifications may be estimated.

Spot number	Protein name	Signle-Acc. Number	Qcon	Qox
1	Autonomus glycy radical factor	GRCA-A8A391	1.2	0.6
2	Alkyl hydroperoxidase reductase sub.C	AHPC-P0AE08	1.2	0.5
3	Inorganic pyrophosfatase	IPYR-P0A7A9	1.2	0.8
4	Phosphoribosyl-aminoimidazole-succino carboxi amide syntetase	PUR7-A7ZPS1	3.1	1.0
5	2-deoxy-D-gluconate-3-dehydrogenase	KDUD-P37769	1.2	0.5
6	Ribose-5-phosphate isomerase A	RPIA-P0A7Z0	1.3	0.9
7	KHG/KDPG aldolase	ALKH-P0A955	1.7	0.3
8	Adenylate kinase	KAD-P699441	1.0	0.6
9	6-phosphofructokinase isozyme 1	K6PF1-P0A796	1.5	0.8
10	Elongation factor Ts	EFTS-P0A6P1	1.5	0.3
11	Triosphosphate isomerase	TPIS-P0A858	1.7	0.9
12	30S ribosomal protein S2	RS2-P0A7V0	2.1	0.9

**Table 5.1**

It is very interesting underline than many identified proteins are known to be regulated by their thiol oxidation state. For example AhpC has been demonstrated to be a peroxiredoxine that plays the role of H<sub>2</sub>O<sub>2</sub> scavenger by the oxidation of cysteines 46 and 165 (29). IPYR was found S-Glutathionylated in human peripheral blood mononuclear cells and its activity is regulated by glutathione in *Streptococcus faecalis* and it is S-cysteinylated in *Bacillus Subtilis* (30-32). PUR7 and K6PF1 were found sensitive to the thiol oxidation also in *Bacillus Subtilis* after treatment with diamide (12). Ribose-5-phosphate isomerase was already suggested to be redox-regulated in photosynthetic organisms. This hypothesis was reinforced by the evedence that was found S-Thiolated in *Chlamydomonas reinhardtii* (33). The Elongation factor Ts activity is regulated by the correct oxidation of the Cys22 (34) and its oligomer Elongation factor Tu was already demonstrated thiol-sensitive to the H<sub>2</sub>O<sub>2</sub> stress in *E. coli* (15). The TPIS cysteines oxidation was demonstrated play important roles in different organisms. In the chicken the Cys126 oxidation leads to discriminate three isoforms and the accumulation of the higer oxidized one is accumulated during aging (35). The oxidation of the same residue in Rabbit and yeast causes the inactivation of the protein (36).

The MS analysis let us to identify the proteins that undergo to the change of thiol oxidation state, but also to localize the site of modification. However, the experiment here reported has just the aim to show the ability to *in vivo* detect thiol modifications by using the fluorescence features of a dansyl derivative by 2DE. Even if image analysis coupled to the MS analysis leads to recognize the oxidized protein, almost in all the cases it is not simple to attribute what and how many a cysteine residue has contributed to the observed decreased fluorescence. This because *in vivo* protein thiols are mainly in a percentage of reduced/oxidized forms also in stress oxidative conditions. Thus from this scenario, it is generated a pool of peptides whose cysteines are modified in different extents by each reactive used. Therefore, it results that, except the case of quantitative modification, it is not possible to know what cysteine has changed its oxidation state if isotopically enriched reagents are not used, as done by Leichert et al. with their Oxycat strategy (15). For the identified protein no spectra of cysteine higher oxide were found, that is in contrast to the results obtained with the standard protein where a sulfonation was detected. This result is in agreement with other data, where it is affirmed that the irreversible sulfonic acid formation is strongly avoided *in vivo* by the ROS scavenger (37).

## **5.4 Conclusion**

This chapter showed the preliminary results for the optimization of a unique strategy aimed to study the stress oxidative related cysteine PTMs, using Dansyl derivatives. From the preliminary results obtained it appears that the fluorescent thiol reactive Dansyl Aziridine (DAZ) may be used for the specific alkylation of thiols without secondary reactions involving other amino acid. Dansylated proteins fractionated by electrophoresis may be visualized selectively by fluorescence with sensitivity comparable to the silver staining. By using this kind of gel visualization it is possible to detect change in the oxidation state of thiols. DAZ may be used to differentially label thiols both in protein extracts in denaturing buffer and *in vivo* by using dansyl derivatives cell permeability. By using specific image software, it was demonstrated possible to generate redox maps of 2DE fractionated proteins using the double visualization fluorescence/Coomassie, making also possible semi-quantitative estimation between different cellular states. Mass spectrometry also benefits of the dansyl labeling. In fact dansylation of no-basic amino acid improve the MALDI ionization as demonstrated in the chapter 4. Moreover the “Bidimensional Tandem MS” analysis in PIS/MS<sup>3</sup> mode may enhance the sensitivity toward labelled peptides. However the procedures optimized is still to be improved. Optimization of 2DE fractionation is necessary, in addition reproducibility between *in vivo* and *in vitro* alkylations have not been explored yet. Moreover, the differential alkylation using different thiol reactive dansyl derivatives as Dansyl iodoacetamide has to be verified.

### **5.4.1 Perspectives**

The methods already set up may be part of a wider strategy aimed to monitor cysteines redox changes starting from tissues or cell populations using the Dansyl derivatives features in each analytical step. The study may start from the cells that may be labelled *in vivo* as showed above. Different oxidative stressed cell populations may be fractionated by flow cytometry (38) discriminating the different fluorescence intensity. In fact oxidized cells labelled with DAZ are less fluorescent by the un-reactivity of oxidized cysteines. By this analysis it will be possible both to

make a snapshot of different cell populations and to separate them for the further differential analysis. The study may also start by tissues in fact different methods were proposed in the past for the histochemical detection using dansyl derivatives (39-42). The modern technique as the laser capture (43) or micro-dissection may be applied to recover the interesting tissue slices for the further analysis. This kind of the analysis leads to enrich with morphological information the Proteomic data. Cells or tissues may be then homogenized and the extracted proteins may undergo to more specific PTMs detection by differential alkylation followed by 2DE fractionation and selective visualization as showed above. The use of Dansyl derivatives allows also to overcome 2DE classical limits by the possibility to perform parallel or alternative gel free approach by RIGhT strategy. Also the quantitative aspects may be explored. In fact fluorescence intensity may be used for semi-quantitative estimation in several analytical steps. In future the synthesis of isotopically enriched dansyl derivatives may also allow the MS quantitation approach, leading to set up the first strategy capable to localize un-ambiguously the modified cysteines in protein fractionated by 2DE.

## **5.5 References**

- 1) Eaton P., *Free Rad.Biol.Med.* **2005**, 40, 1889-1899
- 2) Schilling B., Yoo C.B., Collins C.J., Gibson B.W. *Int. J. Mass Spec.* **2004**, 236 117–127
- 3) Zander T., Phadke N.D. and Bardwell J.C., *Methods Enzymol.* **1998**, 290: 59–74.
- 4) Jocelyn P.C. , *London, New York: Academic Press* **1972**.
- 5) Gonzales-Segura L., Velasco-Garcia R., Munoz-Clares R.A., *Biochem J.* **2002**, 361: 577-585
- 6) Munoz-Clares R.A., Gonzales-Segura L., Mujica-Jimenez C., Contreras-Diaz L., *Chem. Biol. Int.* **2003**, 143-144: 129-137
- 7) Bakardjieva A., Crichton R.R., *Biochem J.* **1974**,143(3):599-606
- 8) Leichert L.I., Jakob U., *PLoS Biol2: e333* **2004**
- 9) Poole L. B., Ellis H. R., *Methods Enzymol.* **2002**, 348:122–136.
- 10)Ellis H. R., Poole, L. B., *Biochemistry* **1997**, 36 (48):15013–15018;
- 11)Sun J., Steenbergen C., Murphy E., *Antiox Redox Signal* **2006**, 8: 1693-1705
- 12)Hochgrafe F., Mostertz J., Albrecht D., Hecker M., *Mol. Microbiol.* **2005**, 58:409-425.
- 13)Han P., Zhou X., Huang B., Zhang X., Chen C., *Anal. Biochem.* **2008**, 377(2):150-155.
- 14)Sethuraman M., McComb M.E., Huang H., Huang S., Heibeck T., Costello C.E., Cohen R.A., *J. Proteome Res.* **2004**, 3(6):1228-33.
- 15)Leichert L.I., Gehrke F., Gudiseva H.V., Blackwell T., Allbert M., Walker A.K., Strahler J.R., Andrews P.C., Jakob U., *Proc. Natl. Acad. Sci. U S A.* **2008** 105(24):8197-202
- 16)Forrester M.T., Foster M.W., Stamler J.S., *Biol Chem.* **2007**, 282(19):13977-83.
- 17)Camerini S., Polci M.L., Restuccia U., Usuelli V., Malgaroli A., Bachi A., *J. Proteome Res.* **2007**,(8):3224-31.
- 18)Ramachandran N., Jacob S., Zielinski B., Curatola G., Mazzanti L., Mutus B., *Biochim. Biophys. Acta.* **1999**, 1430(1):149-54
- 19)Stadtman E.R., Ann. N.Y., *Acad. Sci.* **2001**, 928: 22
- 20)Gianazza E., Crawford J., Miller I., *Amino Acids.* **2007**, 33(1):51-56.
- 21)Scouten W.H., Lubcher R., Baughman W., *Biochem. Biophys. Acta* **1974**, 336 421-426
- 22)Pouillet P., Carpentier S., Barillot E., *Proteomics* **2007**, 7: 2553.
- 23)Amoresano A., Monti G., Cirulli C., Marino G., *Rapid Commun. Mass Spectrom.* **2006**, 20(9):1400-4
- 24).Amoresano A., Chiappetta G., Pucci P., D'Ischia M., Marino G., *Anal. Chem.* **2007**, 79(5):2109-2117
- 25)Cirulli C., Marino G., Amoresano A., *Rapid Commun. Mass Spectrom.* **2007**, 21(14):2389-97
- 26)Hsi K.L., O'Neill S.A., Dupont D.R. and Yuan P.M., *Anal. Biochem*, **1998**, 258: 38-47.
- 27)Broo K., Wei J., Marshall D., Brown F., Smith T.J., Johnson J.E., Schneemann A., Siuzdak G., *Proc. Natl. Acad. Sci. U S A* **2001**, 98(5):2274-2277.
- 28)Zhao X., Kobayashi T., Gryczynski Z., Gryczynski I., Lakowicz J., Wade R., Collins J.H., *Biochim Biophys Acta.* **2000**, 1479(1-2):247-54
- 29)Yamamoto Y., Ritz D., Planson A.G., Jonsson T.J., Faulkner M.J., Boyd D.; Beckwith J., Poole L.B., *Molecular cell.* **2008**, 29(1): 36-45
- 30)Fratelli M., Gianazza E. and Ghezzi P., *Expert Rev. Proteomics* **2004**, 1: 365–376

- 31) Lahti R. and Suonpaa M., *J. Gen. Microbiol.* **1982**, 128: 1023–1026n
- 32) Hochgräfe F., Mostertz J., Pöther D.C., Becher D., Helmann J.D., Hecker M., *J. Biol. Chem.* **2007**, 282(36):25981-25985
- 33) Michelet L., Zaffagnini M., Vanacker H., Le Maréchal P., Marchand C., Schroda M., Lemaire S.D., Decottignies P., *J. Biol. Chem.* **2008**, 283(31):21571-21578.
- 34) Hwang Y.W., Sanchez A., Hwang M.C., Miller D.L., *Arch. Biochem. Biophys.* **1997**, 348(1):157-162
- 35) Gracy K.N., Tang C.Y., Yüksel K.U., Gracy R.W., *Mech. Ageing Dev.* **1990**, 56(2):179-86
- 36) Zubillaga R.A., Pérez-Montfort R., Gómez-Puyou A., *Arch. Biochem. Biophys.* **1994**, 313(2):328-336
- 37) Poole L.B., Nelson K.J., *Curr. Op Chem Biol.* **2008**, 12: 18-24
- 38) Czechowska K., Johnson D.R., van der Meer J.R., *Curr. Opin. Microbiol.* **2008**, 11(3):205-212
- 39) Weber P., Harrison F.W., Hof L. *Histochemistry* **1975**, 45: 271-277
- 40) Marks R., Black D., Hamami I., Caunt A., Marshall R.J., Br. J., *Dermatol.* **1984**, 265-270
- 41) Takahashi M., Black D., Hughes B., Marks R., *Clin. Exp. Dermatol.* **1987**, 12: 246-249
- 42) Braga-Vilela A.S., de Campos Vidal B., *Acta Histochem.* **2006**, 108(2):125-32.
- 43) Mustafa D., Kros J.M., Luider T., *Methods Mol. Biol.* **2008**, 428:159-78



## **INDEX A: table of abbreviations**

**ACN:** acetonitrile  
**AMBIC:** ammonium hydrogen carbonate  
**BSA -DAZ:** dansyl aziridine modified albumin serum bovine  
**BSA:** bovine serum albumin  
**CHAPS:** 3[(3 Cholamidopropyl)dimethyl ammonio)-1-propanesulfonateas]  
**CHCA:** alpha-cyano-4-hydroxycinnamic acid  
**CID:** collision induced dissociation  
**DAZ:** dansyl aziridine  
**DC:** direct current  
**DNS:** dansyl  
**DNSCI:** dansyl chloride  
**DTT:** dithiothreitol  
**ESI:** Electrospray Ionisation  
**FTICR:** Fourier transform ion cyclotron resonance  
**IAM:** iodoacetamide  
**ICAT:** isotope coded affinity tag  
**IEF:** Iso-Electric Focusing  
**IT:** ion trap  
**iTRAQ:** Isobaric Tag for Relative and Absolute Quantification  
**LC:** liquid chromatography  
**LIT:** linear ion trap  
**m/z:** mass-to-charge ratio  
**MALDI:** Matrix-Assisted Laser Desorption/Ionisation  
**MRM:** multiple reaction monitoring  
**MS:** mass spectrometry  
**MW:** microwave  
**N-BSA:** nitrated bovine serum albumin  
**NH<sub>2</sub>-Tyr:** 3-amino tyrosine  
**NL:** neutral loss  
**NO<sub>2</sub>Tyr:** 3-nitrotyrosine  
**NSDB:** Non Detergen Sulfo-Betain  
**PIS:** precursor ion scan  
**PMF:** Peptide Mass Fingerprinting  
**PSD:** Post Source Decay  
**PTMs:** post translational modifications  
**Q:** quadrupole  
**QqQ:** triple quadrupole  
**RF:** radio frequency  
**RIGhT:** reporter ion generating tag  
**RNS:** reactive nitrogen species  
**ROS:** reactive oxygen species  
**RP:** reverse phase  
**S/N:** signal to noise ratio  
**SCX:** strong cationic exchange  
**SDS:** Sodium Dodecyl Sulphate

## INDEX B

### Pubblications

1) Amoresano A., Chiappetta G., Pucci P., D'ischia M., Marino G., Bidimensional Tandem Mass Spectrometry for Selective Identification of Nitration Sites in Proteins. *Anal.Chem* 2007; 79, 21091

2) Cirulli C., Chiappetta G., Marino G., Mauri P., and Amoresano A., Identification of free phosphopeptides in different biological fluids by a mass spectrometry approach , *Anal. Bioanal. Chem.* 2008; 392, 147-159

3) Chiappetta G., Corbo C., Palmese A., Marino G., Amoresano A., Quantitative identification of protein nitration sites *Proteomics.* 2008 in Press

### Congress communications

1) *Dansyl chemistry in Proteomics: back to the future*, Amoresano A., Cirulli C., Chiappetta G., Marino G., Itpa 2006, Pisa.

2) *A novel method to selectively detect, identify and quantify post translational modifications by MS/MS/MS fragmentation*, Chiappetta G., Corbo C., Marino G. and Amoresano A, Itpa 2007, Acitrezza (Ct)

3) *Quantitative analysis of nitrated proteins probed by iTRAQ reagents*, Corbo C., Chiappetta G., Amoresano A., Marino G., XX Congresso Nazionale di Chimica Analitica, Viterbo 2007

4) *New Applications of iTRAQ in Protein chemistry and Proteomic*, Palmese A., Chiappetta G., Corbo C., Marino G., and Amoresano A., Itpa 2008, Fasano (Ba), Italia

5) *An approach to whole blood serum Proteomics using flow field-flow fractionation with multiangle laser scattering detection and nano-chip ion trap mass spectrometry*, Zattoni A., Rambaldi D.C, Reschiglian P., Amoresano A., Chiappetta G., Marino G., Itpa 2008, Fasano (Ba), Italia

6) *A new strategy for selective detection of thiols oxidative modifications in vivo*, Chiappetta G., Verdier Y., Senechal H, Sutra J.P., Amoresano A., Marino G., Rossier J., Vinh J., SFEAP 2008, Tours, France